

# **Molecular Mechanisms Controlling Guided Germ Cell Migration in Zebrafish**

**PhD Thesis**

in partial fulfilment of the requirements  
for the degree “Doctor of Philosophy (PhD)”  
in the Molecular Biology Program  
at the Georg August University Göttingen,  
Faculty of Biology

**submitted by**

Bijan Boldajipour

**born in**

Bremen, Germany

**June 2009**

**PhD Thesis Committee**

**Prof. Dr. Erez Raz (Supervisor)**

Institute of Cell Biology, Westfälische-Wilhelms-Universität Münster  
Von-Esmarch-Str. 56, 48149 Münster

**Prof. Dr. Ivo Feußner**

Department of Plant Biochemistry, Georg-August-Universität Münster  
Justus-von-Liebig-Weg 11, 37077 Göttingen

**Prof. Dr. Thomas Pieler**

Department of Developmental Biochemistry, Georg-August-Universität Göttingen,  
Justus-von-Liebig-Weg 11, 37077 Göttingen

Success is a science; if you have the conditions, you get the result.

*Oscar Wilde*

Success is a lousy teacher. It seduces smart people into thinking they can't lose.

*Bill Gates*

Success is getting what you want. Happiness is wanting what you get.

*Dale Carnegie*

**Affidavit**

I hereby declare that this thesis has been written independently and without any other aids than quoted.

## List of Publications

Boldajipour and Raz. What is left behind--quality control in germ cell migration. *Sci STKE* **2007**, pe16.

Kedde, Strasser, Boldajipour, Vrielink, Slanchev, Sage et al. RNA-binding protein Dnd1 inhibits microRNA access to target mRNA. *Cell* **131**, 1273-1286.

Boldajipour, Mahabaleshwar, Kardash, Reichman-Fried, Blaser, Minina et al. Control of chemokine-guided cell migration by ligand sequestration. *Cell* **132**, 463-473 (2008).

Mahabaleshwar, Boldajipour, and Raz. Killing the messenger: The role of CXCR7 in regulating primordial germ cell migration. *Cell adhesion & migration* **2**, 69-70 (2008).



## Table of Contents

<b>Figures</b>	<b>IV</b>
<b>Tables</b>	<b>V</b>
<b>Acknowledgements</b>	<b>VI</b>
<b>Abstract</b>	<b>VII</b>
<b>Abbreviations</b>	<b>VIII</b>
<b>1. Introduction</b>	<b>1</b>
<b>1.1. General aspects of directional cell migration</b>	<b>1</b>
1.1.1. Prokaryotic directional migration	1
1.1.2. Cell migration of unicellular eukaryotes	2
1.1.3. Cell migration in multicellular organisms and the role of ECM	2
1.1.4. Zebrafish as a model system to study directed cell migration	3
<b>1.2. Chemokines</b>	<b>3</b>
1.2.1. Chemokine nomenclature and structure	4
1.2.2. Chemokine receptors and their signaling pathways	5
1.2.3. Control of cell migration by CXCL12 and its receptors	7
1.2.4. Regulation of chemokine signaling levels	8
1.2.5. Integration of multiple signals into directional migration	9
<b>1.3. Primordial germ cell migration</b>	<b>9</b>
1.3.1. PGC migration in <i>Drosophila</i>	10
1.3.2. PGC migration in chicken	12
1.3.3. PGC migration in mouse	12
1.3.4. PGC migration in zebrafish	14
1.3.5. Zebrafish PGC migration as a tool to study chemokine signaling	16
1.3.6. Aim of the thesis	17
<b>2. Materials and Methods</b>	<b>18</b>
<b>2.1. Materials</b>	<b>18</b>
2.1.1. Laboratory equipment and materials	18
2.1.2. Buffer compositions	22
<b>2.2. Molecular Cloning</b>	<b>23</b>
2.2.1. cDNA synthesis	23
2.2.2. Polymerase chain reaction (PCR)	23
2.2.3. DNA gel electrophoresis	23
2.2.4. Expression clones	23
2.2.5. Bacterial DNA amplification	24
2.2.6. <i>In vitro</i> mRNA and antisense probe synthesis	24

<b>2.3.</b>	<b><i>Zebrafish work</i></b>	<b>24</b>
2.3.1.	Injections	25
2.3.2.	Morpholino-mediated gene knockdown	25
2.3.3.	Cell transplantations	25
2.3.4.	Heparin-bead implantations	25
2.3.5.	<i>In vivo</i> calcium measurements	26
2.3.6.	Whole-mount immunostaining	26
2.3.7.	Whole-mount <i>in situ</i> hybridization	26
<b>2.4.</b>	<b><i>Recombinant chemokine production</i></b>	<b>26</b>
2.4.1.	Bacterial cultures	26
2.4.2.	SDS polyacrylamide gel electrophoresis (SDS-PAGE)	27
2.4.3.	Chemokine purification and modification	27
<b>2.5.</b>	<b><i>In vitro chemokine biochemistry</i></b>	<b>28</b>
2.5.1.	NMR spectroscopy and analytical ultracentrifugation	28
2.5.2.	Chemokine-ECM interaction studies	28
<b>2.6.</b>	<b><i>Cell culture</i></b>	<b>29</b>
2.6.1.	General handling	29
2.6.2.	Transfection	29
2.6.3.	Generation of stable lines	29
2.6.4.	Generation of conditioned media	30
2.6.5.	<i>In vitro</i> transwell migration assays	30
<b>2.7.</b>	<b><i>Microscopy</i></b>	<b>30</b>
2.7.1.	Epifluorescence microscopy	30
2.7.2.	Confocal microscopy	31
2.7.3.	Image processing	31
<b>3.</b>	<b>Results</b>	<b>32</b>
<b>3.1.</b>	<b><i>CXCR7 controls PGC migration by CXCL12 sequestration</i></b>	<b>32</b>
3.1.1.	Expression of the second CXCL12 receptor CXCR7 during zebrafish development	32
3.1.2.	CXCR7 function is required for PGC migration	33
3.1.3.	PGC migration depends on CXCR7 function in somatic cells	37
3.1.4.	CXCR7 is a constitutively cycling chemokine receptor that binds and internalizes CXCL12a	37
3.1.5.	CXCR7-mediated internalization directs CXCL12a for lysosomal degradation	39
3.1.6.	CXCR7 function is required for the establishment of PGC polarity	41
3.1.7.	CXCR7 function does not require the activation of major secondary signaling pathways	42
3.1.8.	Localized CXCR7 expression shapes chemotactic CXCL12a gradients	45
3.1.9.	Summary	46



<b>3.2.</b>	<b><i>Differential recognition of two chemokine ligands in zebrafish PGC migration</i></b>	<b>47</b>
3.2.1.	Zebrafish PGCs are responsive to two CXCL12 ligands	47
3.2.2.	Comparative expression analysis of CXCL12 paralogs during early zebrafish development	48
3.2.3.	CXCL12a is a more potent ligand than CXCL12b	48
3.2.4.	A single amino acid determines the chemotactic activity of the zebrafish CXCL12 paralogs	51
3.2.5.	Expression and purification of recombinant zebrafish chemokines	53
3.2.6.	Structure determination of CXCL12a and CXCL12b indicates oligomerization of the chemokine	56
3.2.7.	Zebrafish CXCL12 exhibits very high affinity to GAGs	58
3.2.8.	Diffusion of the zebrafish CXCL12 paralogs <i>in vivo</i>	59
3.2.9.	Measuring CXCR4 binding and activation	60
3.2.10.	Enhanced internalization of CXCL12a by CXCR7 <i>in vivo</i>	61
3.2.11.	Summary	61
<b>4.</b>	<b>Discussion</b>	<b>64</b>
<b>4.1.</b>	<b><i>CXCR7 functions as a decoy receptor in cell migration</i></b>	<b>64</b>
4.1.1.	CXCR7 controls PGC migration by CXCL12a sequestration	64
4.1.2.	CXCR7 function in the regulation of inflammatory responses	65
4.1.3.	CXCR7 – professional decoy or signaling receptor?	66
<b>4.2.</b>	<b><i>Differential recognition of two CXCL12 paralogs in PGC migration</i></b>	<b>68</b>
4.2.1.	PGCs distinguish between two CXCL12 paralogs	68
4.2.2.	Structural implications of the 30's loop for the function of CXCL12	68
4.2.3.	CXCL12-GAG interactions in PGC guidance	69
4.2.4.	Zebrafish embryonic development is an accessible system to study chemokine ligand-receptor networks	70
<b>5.</b>	<b>Summary and Conclusions</b>	<b>71</b>
<b>6.</b>	<b>Bibliography</b>	<b>72</b>
<b>7.</b>	<b>Appendix</b>	<b>87</b>
<b>7.1.</b>	<b><i>Declaration of author contributions</i></b>	<b>87</b>
<b>7.2.</b>	<b><i>List of constructs</i></b>	<b>87</b>
<b>7.3.</b>	<b><i>List of morpholinos and primers</i></b>	<b>89</b>
<b>8.</b>	<b>Curriculum Vitae</b>	<b>90</b>

## Figures

Figure 1.	Structures of CXC chemokines.	5
Figure 2.	Chemokine receptor signaling pathways.	6
Figure 3.	Hallmarks of PGC migration in <i>Drosophila</i> .	11
Figure 4.	Hallmarks of PGC migration in chicken.	12
Figure 5.	Hallmarks of PGC migration in mouse.	13
Figure 6.	Hallmarks of PGC migration in zebrafish.	15
Figure 7.	Expression pattern of <i>cxcr7</i> .	32
Figure 8.	CXCR7 is essential for normal PGC migration and required in the somatic environment of the embryo.	34
Figure 9.	Morpholino-mediated knockdown of <i>cxcr7</i> and rescue of <i>cxcr7</i> morphants by <i>cxcr7</i> mRNA injection.	35
Figure 10.	CXCR7 promotes the internalization of CXCL12a.	36
Figure 11.	CXCL12a accumulates in lysosomes upon CXCR7-mediated internalization.	38
Figure 12.	Cells expressing CXCR7 reduce extracellular CXCL12a levels <i>in vitro</i> .	40
Figure 13.	CXCR7 controls PGC polarity by regulating CXCL12 levels.	41
Figure 14.	CXCR7 does not activate major secondary pathways downstream to chemokine signaling.	43
Figure 15.	CXCR7 affects directionality of germ cell migration <i>in vivo</i> .	44
Figure 16.	CXCL12b can function as a guidance cue for PGCs, but is not essential for normal PGC migration.	47
Figure 17.	Comparative expression analysis of the zebrafish <i>cxcl12</i> paralogs.	49
Figure 18.	CXCL12a is a more potent chemoattractant for PGCs compared to CXCL12b.	50
Figure 19.	The chemotactic activity of zebrafish CXCL12 is defined by amino acid position 33.	52
Figure 20.	Chemokine purification strategies.	54
Figure 21.	Delivery of recombinant CXCL12 into zebrafish embryos by implantation of heparin-coated microspheres.	55
Figure 22.	Properties of recombinant zebrafish CXCL12 protein.	56
Figure 23.	Illustration of the SPR principle.	57
Figure 24.	Increased chemotactic activity of CXCL12b S33N does not depend on GAG affinity.	57
Figure 25.	Accumulation of CXCL12-EGFP protein on cell membranes.	59
Figure 26.	Diffusion of CXCL12a-EGFP is not detectable by <i>in vivo</i> microscopy.	60
Figure 27.	Migration of NIH/3T3-CXCR4b cells towards CXCL12a-conditioned medium <i>in vitro</i> .	61
Figure 28.	Reduced internalization of CXCL12b by CXCR7 <i>in vivo</i> .	62
Figure 29.	A model for the role of CXCR7 in PGC migration.	65

## Tables

Table 1.	List of reagents, chemicals, kits, equipment, and software used in this work.	18
Table 2.	Composition of buffers used in this work.	22
Table 3.	List and description of constructs used in this work.	87
Table 4.	List of morpholinos and primers used in this work.	89

## **Acknowledgements**

I would like to thank my family for their trust in me, continuous support, and encouragement. Without you I would not be where I am today.

I also owe lots of 'thank you' to all my friends that endured my moods, both good and bad, throughout these years. Life would be quite sad without you.

I am in special debt to my colleagues, as considerable part of my work and also this thesis would not exist without their contribution. A detailed list of contributions can be found in the Appendix.

I would also like to thank Kate and Shanti for spending their free time on proofreading this thesis.

Finally, I would like to thank Prof. Raz for his support and supervision.

## Abstract

During zebrafish embryonic development, primordial germ cells (PGCs) migrate through the developing embryo towards the developing gonad, where they will differentiate into sperm and egg. During their migration, these cells are guided by the chemokine CXCL12a and its receptor CXCR4b. Dynamic *cxc12a* expression lays out a chemotactic path, and germ cells remain in immediate proximity to cells secreting the chemokine. This implies that the protein level is highest at the site of mRNA expression, yet little is known about the molecular mechanisms controlling the distribution of this chemoattractant *in vivo*. This work demonstrates that the activity of a second CXCL12a receptor, CXCR7, is crucial for proper migration of PGCs toward their targets. It is shown that CXCR7 is expressed in the somatic environment rather than within migrating PGCs. Upon loss of CXCR7 function, PGCs exhibit a phenotype that signifies defects in CXCL12a gradient formation, as the cells fail to polarize effectively and to migrate toward their targets. Indeed, somatic cells expressing CXCR7 show enhanced internalization of the chemokine suggesting that CXCR7 acts as a decoy for CXCL12a; thus, allowing the dynamic changes in the transcription of *cxc12a* to be mirrored by similar dynamics at the protein level.

In addition to guidance by CXCL12a, a second paralog of CXCL12 termed CXCL12b is expressed during zebrafish development. This chemokine is not required for germ cell migration towards the gonads, but is capable of attracting germ cells *in vivo*. Although being expressed during the time of germ cell migration, CXCL12b expression is ignored by the migrating germ cells as long as CXCL12a is present. This work sets out to identify the mechanism that germ cells employ to differentiate between these very similar ligands and identified an amino acid in the 30's loop of the chemokines being responsible for the differential chemotactic activity. To this end, recombinant production of the zebrafish chemokines is established and protein structure, receptor binding *in vivo*, and glycosaminoglycan binding *in vitro* investigated. Although experiments are still in progress, it appears that the single amino acid controls receptor binding and activation, whereas binding to glycosaminoglycans is not affected.

## Abbreviations

BSA	bovine serum albumin
cAMP	cyclic adenosine-5'-monophosphate
cDNA	complementary DNA
CV	column volumes
DAG	diacylglycerol
DNA	deoxyribonucleic acid
ECM	extracellular matrix
EDTA	ethylenediaminetetraacetic acid
FBS	fetal bovine serum
G-protein	GTP-binding protein
GAG	glycosaminoglycan
GPCR	G-protein coupled receptor
GRK	G-protein coupled receptor kinase
GTP	guanosine-5'-triphosphate
HMGCoAr	3-hydroxy-3-methyl-glutaryl-coenzyme A reductase
hpf	hours postfertilization
IP <sub>3</sub>	inositol 1,4,5-triphosphate
IPTG	Isopropyl-β-D-thiogalactopyranosid
mRNA	messenger ribonucleic acid
ORF	open reading frame
PCR	polymerase chain reaction
PGC	primordial germ cell
PH-domain	Pleckstrin homology domain
PI3K	phosphatidylinositol-3-kinase
PIP <sub>2</sub>	phosphatidylinositol-4,5-bisphosphate
PIP <sub>3</sub>	phosphatidyl-(3,4,5)-trisphosphate
PLC	phospholipase C
PTEN	phosphatase and tensin homolog
RNA	ribonucleic acid
SDS-PAGE	sodium dodecyl sulfate-polyacrylamide gel electrophoresis
SEM	standard error of the mean
SPR	surface plasmon resonance
UTR	untranslated region
WHIM syndrome	wart, hypogammaglobulinemia, infection, and myelokathexis syndrome

## 1. Introduction

Development of a highly organized multi-cellular organism from a single cell requires at least three major processes: proliferation, differentiation, and change of cell positions relative to each other. Gastrulation and organogenesis of a vertebrate organism primarily depend on complex movements of cells and tissues, and attracting and repelling cues tightly coordinate these movements<sup>1-13</sup>. Deregulation of cell migration results in a number of pathological conditions that ultimately may cause the death of the organism<sup>14-24</sup>. Mechanistic principles involved in directing migration of a cell from its origin during embryogenesis towards the final position in an adult organism set the stage for this work.

### 1.1. General aspects of directional cell migration

#### 1.1.1. Prokaryotic directional migration

Directional cell migration is an ancient feature of life as it is also found in the majority of prokaryotes<sup>25-28</sup>. It provides a relatively simple mechanism to adapt to environmental changes by relocating a cell to a more supportive environment, defined by factors such as nutrients, temperature, pH, osmolarity, or light. For example, instead of changing their metabolism after a drop in their preferred nutrient supply, bacteria simply change their location to where the nutrient is still abundant.

The bacterial chemotaxis system of *Escherichia coli* has been studied in great detail<sup>26,29-34</sup>. Bacteria move by the rotation of flagella - when rotating in a coordinated fashion the flagella movement propels cells forward, whereas uncoordinated rotation causes the cell to tumble on the spot. The direction of rotation is determined by intracellular motor proteins and is reverted in regular intervals<sup>27</sup>. This causes bacteria to perform a so-called random walk - a meandering path of migration created by alternating phases of migration and tumbling, with a new random direction of migration after each tumbling event<sup>30</sup>. In order to migrate directionally, bacteria employ receptors on one tip of the bacterial cell to probe the environment for ligands (e.g. sugars or ions) or physical parameters (e.g. osmolarity or light)<sup>28,32</sup>. These receptors signal to the intracellular chemotaxis machinery and either prolong or reduce the time interval of the rotational switch. Only when a bacterial cell is migrating towards an attractant source the receptors prolong the time of directional migration towards the attractant source, otherwise the migration interval remains short. With time, this leads to an accumulation of cells at the source of their attractant or to an avoidance of a repellent<sup>27</sup>.

Due to their small cell size prokaryotes cannot sense the gradient of diffusible molecules along the cell length but instead have to measure the change of environmental factor concentrations over time. The nature of the bacterial random walk causes the cells to frequently migrate away from the attractant for a short time and thus is a fairly inefficient way to find the source of an attractant. In comparison, eukaryotic cells have significantly increased their efficiency of migration. The enlarged cell size now enables a

cell to sense a chemotactic gradient along the cell perimeter in order to define the direction of the guidance cue before it initiates the active migration<sup>8,35,36</sup>.

### 1.1.2. Cell migration of unicellular eukaryotes

There are many well-studied cell migration processes in eukaryotic species during various phases of their lifetime. For example, studies of the migration of the slime mould *Dictyostelium discoideum* have delivered a lot of insight on directional migration principles<sup>37-39</sup>. This example introduces two major concepts of guided cell migration, where first, a diffusible signaling molecule is forming a gradient that encodes the direction of migration<sup>40-42</sup>, and second, receptors on the cell interpret this gradient and accordingly polarize the activity of the intracellular signaling components to remodel the cell's cytoskeleton for migration<sup>35,43-45</sup>. At appropriate environmental conditions *Dictyostelium* exists as individual undifferentiated cells that migrate randomly in order to find nutrient sources<sup>10</sup>. The cells of this organism express a G-protein coupled receptor (GPCR) that senses cyclic adenosine monophosphate (cAMP). Upon starvation, some cells begin to secrete cAMP. Neighboring cells interpret the establishing gradient of cAMP, polarize accordingly, and begin to migrate towards the starving cell<sup>46-48</sup>. Once many cells have swarmed in they form a fruiting body in which some cells will form long-lived spores that create a new generation once nutrient levels are favorable again. Thus the ability of a chemoattractant to elicit a response in its target cell not only depends on its ability to bind and activate its receptor, but also on the robust formation and interpretation of the extracellular gradient<sup>42</sup>.

### 1.1.3. Cell migration in multicellular organisms and the role of ECM

Although research on migrating unicellular organisms such as *Dictyostelium* has given a lot of insight into cell migration processes these model systems lack an important aspect of cell migration in the higher eukaryotes: in complex tissues and organs cells encounter many different cell types and signals at the same time<sup>49-51</sup>. Although *Dictyostelium* can assemble into multicellular structures, these are not comparable to the highly developed tissues found in vertebrate animals. Here a multitude of cells and different tissue types have assembled to form functional organs. In addition to cells, the extracellular matrix (ECM), a large repertoire of extracellular proteins and sugar chains to which cells adhere, provides three-dimensional structure and support to these organs<sup>52,53</sup>. The ECM proteins are often modified with glycosaminoglycans (GAG), highly charged, and crosslinked, either directly through chemical modifications or by linker proteins<sup>54</sup>. Depending on composition of GAGs, types of modifications and the presence of linker proteins, unique ECM properties and functions are established, thereby characterizing the function of the tissues<sup>55,56</sup>.



The ECM adds another level of complexity to directional cell migration in higher eukaryotes<sup>57</sup>. A dense ECM, for example, can act as a physical guide for cells; a less dense ECM can provide a permissive track in an otherwise tightly packed and thus impenetrable environment<sup>58,59</sup>. The ECM also binds or scavenges signaling molecules<sup>55</sup>. Many signaling molecules found in higher vertebrates have GAG-binding properties, which affect the free diffusion of the molecules and thus the shape of the extracellular gradient<sup>60,61</sup>. For example, a high affinity to GAGs can immobilize a signaling molecule and create a very short but steep gradient, whereas little GAG interaction allows development of a long-distance but shallow gradient<sup>62</sup>.

In addition, extracellular enzymes deposited in the ECM process the secreted signaling molecules<sup>63-66</sup>. These modifications can have numerous effects on extracellular availability, receptor affinity, or activation<sup>67</sup>. Therefore, robust and precise directional migration is a combination of several molecular mechanisms to enhance, reduce, or even antagonize a chemoattractant ability to elicit a response in its target cell.

#### **1.1.4. Zebrafish as a model system to study directed cell migration**

As noted before, a lot of knowledge about the principles of guided cell migration has been acquired from the migration of individual cells in culture, such as *Dictyostelium*. Cultured mammalian cell lines, or primary immune cells such as neutrophils, also serve well to study cell migration processes<sup>68-70</sup>. However, these systems lack the three-dimensional migratory environment that cells are exposed to in a multicellular organism (e.g. other cell types, complex ECM, multiple signaling molecules)<sup>50,71,72</sup>. Thus, although three-dimensional culturing methods are now available, the *in vitro* technology will always be a simplification of the *in vivo* reality.

A good model system to study cell migration *in vivo* is the embryonic development of zebrafish (*Danio rerio*)<sup>73</sup>. This tropical fresh water fish is a member of the teleost fish. The zebrafish has become an important model system for comparative biology<sup>74-77</sup>. The extrauterine development of a translucent embryo and the ease of genetic manipulation by microinjection of DNA<sup>78-81</sup>, *in vitro* transcribed mRNA, and antisense oligonucleotides for gene knockdown<sup>82,83</sup> allow the investigation of cell migration processes using fluorescence microscopy techniques at high temporal and spatial resolution.

### **1.2. Chemokines**

Belonging to the group of cytokines, chemokines (chemotactic cytokines) represent one of the most important families of chemotactic molecules<sup>84,85</sup>. Initially found to be important chemoattractants for lymphocytes<sup>86</sup>, today it has been acknowledged that chemokines have numerous functions in development<sup>87-89</sup>, homeostasis<sup>72,90</sup>, and disease<sup>22,91,92</sup>.

### 1.2.1. Chemokine nomenclature and structure

Chemokines are small secreted cytokines with a mass between seven and 12 kDa and are grouped according to the number and spacing of conserved cysteine residues<sup>85</sup>. Besides the conserved cysteines all chemokines share a certain degree of sequence similarity (about 20-50%) and usually have a high net positive charge. Chemokine genes have evolved only in vertebrate species, and many of them are found clustered on the chromosomes<sup>76,77</sup>.

As of today, four chemokine groups have been described<sup>76,77</sup>. The CC chemokine ligands (CCLs) compose the largest family with currently more than twenty members (variable numbers between humans and mice, as well as between different mouse strains) and are characterized by two neighboring cysteines that are involved in overlapping disulphide bridges: an N-terminal cysteine forms a bridge with the third cysteine, whereas the neighboring second cysteine bridges with the fourth cysteine located in the C-terminal region of the protein (Figure 1). For the CXC chemokine ligand group (CXCLs) 15 murine and 17 human members are known, and they differ from the CC chemokines as here the second and the third cysteine are separated by a single amino acid. The class of C chemokine ligands (XCLs) contains two members in humans and one in mice. This group is special as these chemokines have only one cystine bridge in contrast to the other groups. The CX3C chemokine ligand group (CX3CLs) consists of a single chemokine, as known today, which differs from all chemokines by having three amino acids separating the cystine bridges and an exceptional size of 90 kDa. This chemokine is tethered to the membrane of certain cells by a large mucin-like structure that can be cleaved in order to release a soluble chemokine<sup>76,77</sup>.

Chemokines exhibit a characteristic tertiary structure, in which an unstructured N-terminus, a beta-sheet consisting of three antiparallel beta-strands, and a C-terminal helix form a greek key motif<sup>93</sup> (Figure 1). The cystine bridges are formed between the N-terminus and the  $\beta$ -sheet, thereby creating a long N-loop. The unstructured N-terminus and N-loop contain amino acids responsible for receptor activation<sup>94-96</sup>, whereas the antiparallel  $\beta$ -sheet and the C-terminal helix is mostly involved in binding of the extracellular matrix through heparin-binding motifs<sup>97-99</sup>. The 30's loop connecting the first and second beta strand is a highly flexible region that cooperates with N-terminus and N-loop in receptor binding (Baysal 2001, Crump 1999, Clark-Lewis 1994).

The positive charge of chemokines and intrinsic glycosaminoglycan (GAG)-binding motifs create a very high affinity to many ECM components, thereby effectively immobilizing and concentrating chemokines<sup>100,101</sup>. The interaction with ECM components is not required for receptor activation but has been shown to be crucial for chemokine function *in vivo*<sup>102,103</sup>. Chemokines are also found in various oligomerization states that are highly dependent on protein concentration, pH, salts, and ECM components<sup>104</sup>. The binding to heparin for example promotes oligomerization for many chemokines, and the oligomerization state has been implied in a modulation of chemokine receptor activation<sup>105-108</sup>.

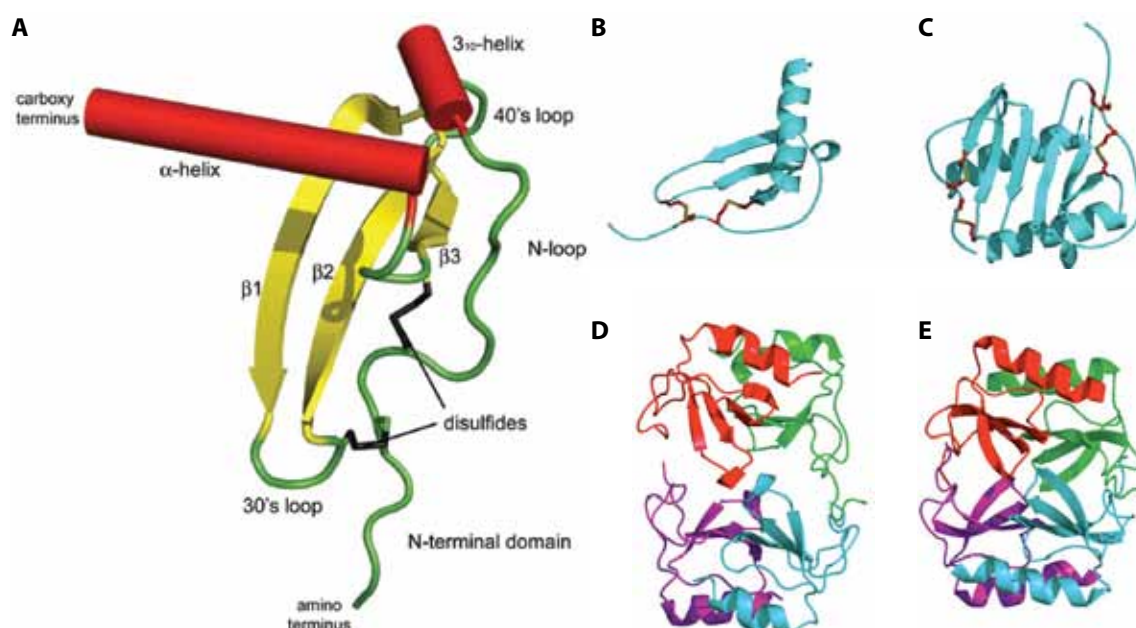


**Figure 1. Structures of CXC chemokines.**

Monomeric structures are given at the example of (A) CXCL12 and (B) CXCL8. (C) shows a dimer of CXCL8. (D-E) Tetramers of CXCL10 (D) and CXCL4 (E). The structures are adapted from <sup>101</sup> (A) and <sup>93</sup> (B-E).

Chemokines can also be found as heterodimers of two different chemokines<sup>109,110</sup>; the relevance of this heterodimer state for directional migration is not properly understood.

### 1.2.2. Chemokine receptors and their signaling pathways

Chemokines exert their biological function by activating a panel of 18 chemokine receptors known today (in mouse and human)<sup>75</sup>. According to the type of ligand these receptors bind they are classified as CC chemokine receptors (CCRs), CXC chemokine receptors (CXCRs), XC chemokine receptors (XCRs), or CX3C chemokine receptors (CX3CRs). All chemokine receptors are GPCRs, and may have broad ligand specificities<sup>85</sup>. For example, the chemokine receptor CCR1 can bind seven different CC chemokines, whereas CCR7 can only bind CCL19 and CCL21. However, these ligands are also recognized by CCR11, thereby establishing a complicated signaling network<sup>111</sup>. It is believed that chemokine receptors function as homodimers<sup>112,113</sup>, but similar to chemokine ligands, heterodimerization of receptors has also been observed<sup>114-116</sup>.

As depicted in Figure 2, once bound by their respective ligand(s), chemokine receptors activate specific heterotrimeric GTP-binding proteins (G-proteins) that are proteins associated to the receptor's intracellular loops<sup>16,117</sup>. The activation of G-causes their disassembly into a G $\alpha$  and a G $\beta\gamma$ -subunits, which both can activate numerous signaling pathways, depending on the combination of G $\alpha$  and G $\beta\gamma$  used by the GPCRs<sup>118,119</sup>. Often, chemokine receptor activation triggers an increase of intracellular calcium levels through the activation of phospholipase C (PLC) that cleaves phosphatidylinositol-4,5-

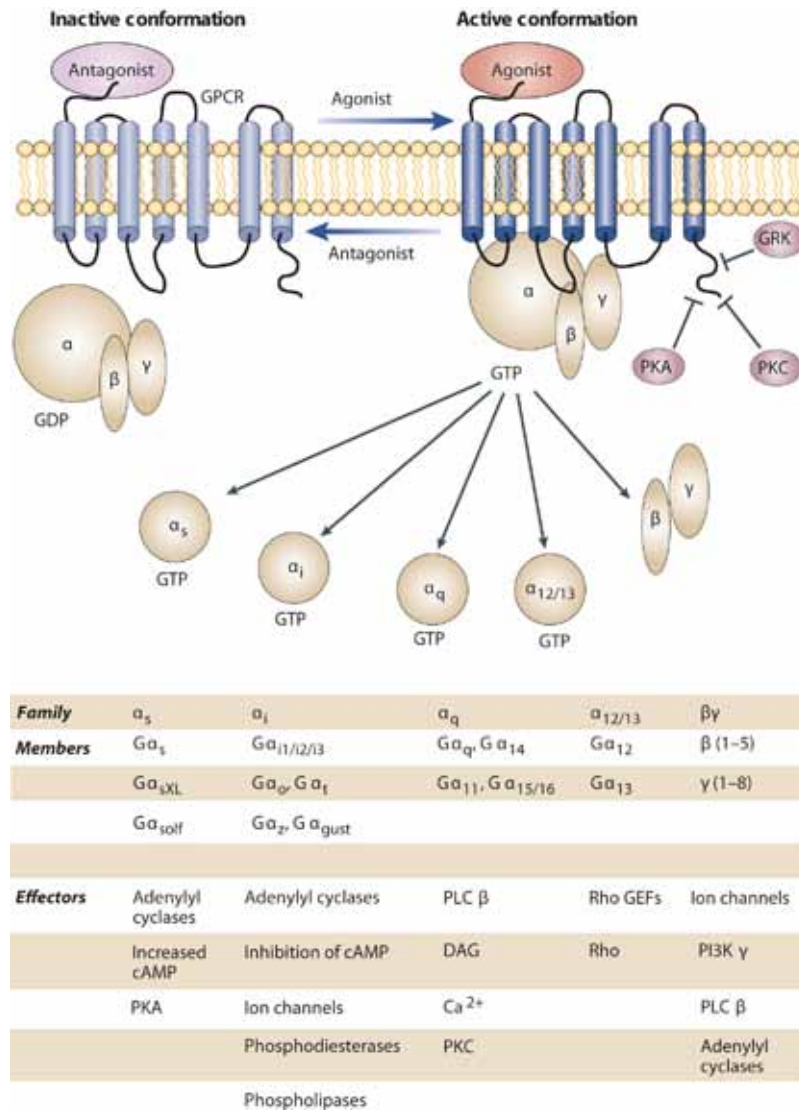


### Figure 2. Chemokine receptor signaling pathways.

Upon agonist binding, chemokine receptors adopt a different conformation that allows interaction with heterotrimeric G proteins. Depending on the type of G proteins a receptor interacts with, different downstream signaling cascades are activated. The members of the different G protein families and their downstream effectors are listed. PI3K $\gamma$ , phosphatidylinositol 3-kinase  $\gamma$ ; Rho GEFs, guanine nucleotide-exchange factors for Rho-like GTPases. Adapted from <sup>118</sup>.

bisphosphate (PIP<sub>2</sub>) into the second messengers diacylglycerol (DAG) and inositol 1,4,5-triphosphate (IP<sub>3</sub>)<sup>118,120,121</sup>. These second messengers in turn activate calcium channels leading to the increase of intracellular calcium<sup>122</sup>. Released calcium ions may act as activators of many calcium-dependent remodeling processes of the cytoskeleton and many other processes<sup>123,124</sup>.

Chemokine receptors have also been shown to activate the phosphatidylinositol-3-kinase (PI3K) pathway<sup>125</sup>. PI3K is involved in many directional migration processes by creating an intracellular gradient of phosphatidyl-3,4,5-trisphosphate (PIP<sub>3</sub>)<sup>126</sup>. PIP<sub>3</sub> is not only an important activator of the Akt/protein kinase B (Akt/PKB) pathway, but also many cytoskeletal components have PIP<sub>3</sub>-binding Pleckstrin homology domains (PH-

domains) that bind to PIP3 and therefore can be localized specifically by PI3K activity<sup>125</sup>. In *Dictyostelium* and neutrophils, efficient cell migration is dependent on the concerted action of PI3K and the PIP3 phosphatase PTEN (phosphatase and tensin homolog)<sup>127,128</sup>. Along with other signaling pathways, the PIP3 gradient created by PI3K/PTEN facilitate directional motility of these cells<sup>129,130</sup>. PI3K has also been identified as a promigratory effector in tumor-cell migration<sup>131,132</sup>.

Other signaling molecules important in cell migration, besides calcium and PIP3, are small Rho GTPases<sup>133,134</sup>. These small G-proteins are important regulators of the actin cytoskeleton and are crucial for cell migration<sup>135-137</sup>. It has been shown that G protein coupled receptors exert their function through the Rho GTPase family members Rac, RhoA, and Cdc42<sup>117,138</sup>, therefore offering another pathway to control directional migration.

### 1.2.3. Control of cell migration by CXCL12 and its receptors

Important regulators of cell migration are the chemokine CXCL12 and its receptors CXCR4 and CXCR7. CXCL12 was initially identified as a B-cell proliferation and recruitment factor secreted by cells in murine bone marrow (deriving its original name stromal cell-derived factor 1, SDF-1, which is still widely used in the literature)<sup>139-141</sup>. It was found later, that the coreceptor for HIV entry into T cells, LESTR/Fusin, was actually the receptor for CXCL12, and subsequently renamed as CXCR4<sup>142,143</sup>.

Since their discovery, CXCL12 and CXCR4 functions have gained a lot of attention in numerous processes besides HIV entry and their activity in B cell development and maturation in the bone marrow. For example, CXCL12 and CXCR4 are also important for T cell entry into lymph nodes and clinical symptoms of the WHIM syndrome are associated with mutations in the C-terminal domain of CXCR4<sup>144,145</sup>. Apart from that, CXCR4 expression is upregulated in many malignant tumors and believed to be associated with an increase in metastatic capacity<sup>146,147</sup>. CXCL12-expressing fibroblasts in the tumor enhance angiogenesis and growth rate of breast tumors by mobilization and attraction of endothelial progenitor cells from the bone marrow<sup>148,149</sup>. In addition, this chemokine-receptor pair is also involved in many developmental processes. Important examples include integrin activation necessary for the coupled migration of mesoderm and endoderm during gastrulation<sup>13,150</sup>, vascularization<sup>89,151</sup>, neuronal migration<sup>152,153</sup>, and migration of primordial germ cells<sup>154-157</sup>.

CXCL12 and CXCR4 have been considered special within the chemokine family. In contrast to all other chemokines, *cxcl12* is not found in a chemokine gene cluster but is separated from the other chemokines. It has the highest conservation amongst species and because of the almost equal relation to both CC- and CXC-chemokines it was considered to be the closest to an ancestral chemokine<sup>75,76</sup>. Finally, CXCL12 and CXCR4 shared a monogamous relationship, as they did not bind to any other receptors or ligands and knockout mice display similar lethal phenotypes. This exclusive monogamous inter-

action between CXCL12 and CXCR4 has been overthrown by the recent discovery of the chemokine receptor CXCR7 that binds CXCL11 and CXCL12 with high affinity<sup>158,159</sup>. However, canonical chemokine signaling could not be shown convincingly. Furthermore, CXCR7-deficient mice die during development from different defects than the CXCR4/CXCL12 counterparts<sup>160</sup>, and therefore, the function of this receptor in CXCL12-regulated processes remains unclear.

#### 1.2.4. Regulation of chemokine signaling levels

High signaling levels or persistent stimulation require that signaling intensity be reduced in order to prevent excessive stimulation and deregulated responses. For this purposes mechanisms regulating ligand and receptor have evolved. For example, chemokines are subject to various post-translational modifications: metalloproteases on the surface of cells, in the extracellular environment and the blood stream modulate lifetime and signaling ability of chemokines<sup>63,66</sup>. Recently, citrullination (conversion of arginine to citrulline by deamination) of chemokines has been described as an effective means of chemokine inactivation<sup>64,161</sup>. In turn, binding of chemokines by auxiliary factors or proteoglycans can activate or deactivate them by the induction of structural changes, protect these from modification, or induce the latter<sup>66,100</sup>.

On the side of the receptor, mechanisms have evolved to adapt the receptor response to high signaling levels. G-protein coupled receptor kinases (GRKs) phosphorylate the intracellular C-terminus of activated receptors that is often rich in serine residues.  $\beta$ -arrestins bind those phosphoserines and thereby block the binding and activation of new heterotrimeric G-proteins. Sustained receptor phosphorylation marks the receptor for internalization and degradation<sup>162,163</sup>. The clinical symptoms of the previously mentioned WHIM syndrome are often associated with C-terminal truncations of CXCR4 that prevent phosphorylation<sup>145,164</sup>. These receptor mutants display a lack of desensitization and internalization in response to CXCL12<sup>165</sup>. The increased signaling of the receptor has further been shown to reduce the accuracy of directional migration *in vivo*, highlighting the importance of the dynamic receptor modulation for cell migration<sup>166</sup>.

Chemokine receptor internalization has gained more attention with the discovery of chemokine decoy receptors. These receptors bind chemokines with high affinity, but instead of creating a signaling response, they internalize their ligand and direct it for degradation<sup>92,167</sup>. An example is D6, a receptor that balances the immune response in mice after acute infection<sup>168</sup>. D6 removes inflammatory chemokines, thereby shortening the time of inflammation. Loss of D6 in turn causes massive inflammation, which leads to severe tissue damage<sup>169,170</sup>. Decoy receptors have also been implied to mediate transcytosis and subsequent presentation of chemokines to the blood stream by endothelial cells, thereby allowing an immune defense to take place<sup>171,172</sup>. Not all decoy receptors are silent. When required some chemokine receptors can switch from a signaling to a

decoy mode – these part-time decoys provide yet another possibility to fine-tune cellular responses to chemokine signaling<sup>167</sup>.

### 1.2.5. Integration of multiple signals into directional migration

During their migration, cells encounter many signaling molecules - possibly encoding for conflicting information. Therefore, mechanisms for the integration of multiple signals have evolved that provide cells with means to distinguish important from at that moment dispensable, or even misleading guidance cues<sup>173-175</sup>. For fighting bacterial infections, neutrophils leave the bloodstream close to the site of infection, and then migrate to bacteria causing the infection. Chemokines produced by blood vessel endothelial cells, macrophages, and dendritic cells instruct neutrophils to extravasate from the blood stream and to migrate towards the site of inflammation<sup>176</sup>. At the same time, the innate immune system and bacteria themselves produce small molecules that also activate neutrophil GPCRs and serve as potent chemoattractants<sup>177</sup>. At this timepoint, signals from the inflamed tissue and the bacteria create opposing chemoattractant gradients, yet neutrophils preferentially migrate towards the bacteria<sup>177</sup>. A recent study now shows that chemoattractants of the bacteria and the intermediary chemokines of the inflamed tissue utilize two different receptor pathways to direct the cells towards their respective target<sup>128</sup>. When both pathways are activated, the bacterial signaling pathway becomes dominant by inhibiting the intracellular signaling downstream to the intermediary chemokines, a process called orthogonal receptor crosstalk<sup>178,179</sup>.

Orthogonal receptor crosstalk may also be used to activate an otherwise dormant signaling pathway<sup>180</sup>. Naive T cells are circulating in the blood stream and enter lymph nodes in regular intervals, where they encounter the presented antigens of the peripheral tissues. Major signals to induce T cells to enter the lymphatic system are the activation of CCR7 by its ligands CCL19 and CCL21, and CXCL12-mediated activation of CXCR4<sup>72</sup>. A recent study has now shown that activation of CXCR4 by CXCL12 allows cells to respond to normally ineffective levels of CCL19/CCL21 by enhancing CCR7 signaling. Crosstalk of chemokine receptors with other receptor signaling pathways has also been described. For example, CXCR4 was shown to interact with signaling pathways of tyrosine kinase receptors<sup>181</sup> and the T cell receptor<sup>182-184</sup>. Thus, orthogonal signaling between chemokine receptors presents a likely mechanism to integrate multiple chemokine signals into a common cellular response.

## 1.3. Primordial germ cell migration

This work focuses on mechanisms that control directional migration of primordial germ cells (PGCs). PGCs are the earliest progenitors of the gametes that will form sperm and egg<sup>185,186</sup>. Specification of PGCs differs between species and is carried out either by the deposition of maternal determinants (*C. elegans*, *Drosophila*, *Xenopus*, zebrafish, chicken) or through inductive signals from neighboring cells (Urodele amphibians,

mammals)<sup>186,187</sup>. In either case, a distinct transcription profile is established that distinguishes PGCs from surrounding somatic cells<sup>188-191</sup>. The specification from the somatic cell lineages occurs early during development, at a distant location to where gonads will eventually form<sup>186</sup>. This requires PGCs to migrate through a developing embryo to the gonadal precursors where they can complete their developmental program and differentiate into the germ cell stem cells. Depending on the species, PGCs take different routes through a developing embryo<sup>185</sup>.

### 1.3.1. PGC migration in *Drosophila*

In *Drosophila*, PGCs are excluded from the syncytial embryo as a tightly packed cluster of immotile pole cells at the posterior pole and are passively carried into the posterior midgut by gastrulation movements<sup>192,193</sup> (Figure 3A-B). Once inside the midgut, the PGCs individualize and migrate through the midgut epithelium and migrate on the midgut towards the mesoderm (Figure 3C-D). For this purpose, the GPCR Tre1 polarizes cell-cell adhesion by redistributing E-cadherin and Rho GTPase activity towards the rear of the cell<sup>194,195</sup>. The directional signal for the epithelial transmigration is dependent on the function of two lipid phosphate phosphatases called Wunen and Wunen2<sup>196-198</sup>. *Wunen/wunen2* expression is found in tissues flanking the migratory route of PGCs: the ventral midgut, the central nervous system that overlies the mesoderm, and the ectoderm that flanks the mesoderm laterally. In flies deficient for *wunen/wunen2* PGCs migrate randomly into tissues they would normally avoid and overexpression of these genes in the mesoderm repels PGCs from their target<sup>196,197,199</sup>. Phospholipids known to control the migration of lymphocytes and heart precursors in vertebrates are hydrolyzed by Wunen/Wunen2 activity *in vitro*, and the hydrolyzed product is taken up into the cells<sup>200-202</sup>. In *Drosophila*, these lipids might serve a similar purpose - however the *in vivo* substrate for Wunen/Wunen2 has not yet been identified and no homologs to the phospholipid-sensing GPCRs of vertebrates have been found in *Drosophila*. Interestingly, it was found that although somatic expression of *wunen/wunen2* repels PGCs, Wunen/Wunen2 activity is required within PGCs for their survival<sup>199,200,203</sup>. Localized degradation of this cue therefore creates an inverse survival-promoting gradient<sup>196,197,199,200,203</sup>. However, it remains unclear how the product of Wunen/Wunen2 activity mediates survival and how this survival signal is also translated into directional migration.

In addition to the directional signal generated by Wunen/Wunen2, expression of the fly homolog of 3-hydroxy-3-methyl-glutaryl-coenzyme A reductase (HMGCoAr) attracts PGCs towards the lateral mesoderm and the gonadal<sup>204</sup> (Figure 3E-F). Genetic analysis has found that among the many enzymatic pathways served by HMGCoAr, geranylation of a yet unknown protein mediates the attraction of PGCs towards the gonadal mesoderm<sup>192</sup>. Once PGCs have arrived in the gonadal mesoderm, they become immotile, align with somatic gonadal precursor cells, and together they finally coalesce into the gonad<sup>205</sup> (Figure 3G-H). The signal for the PGCs to stop migration is unknown,



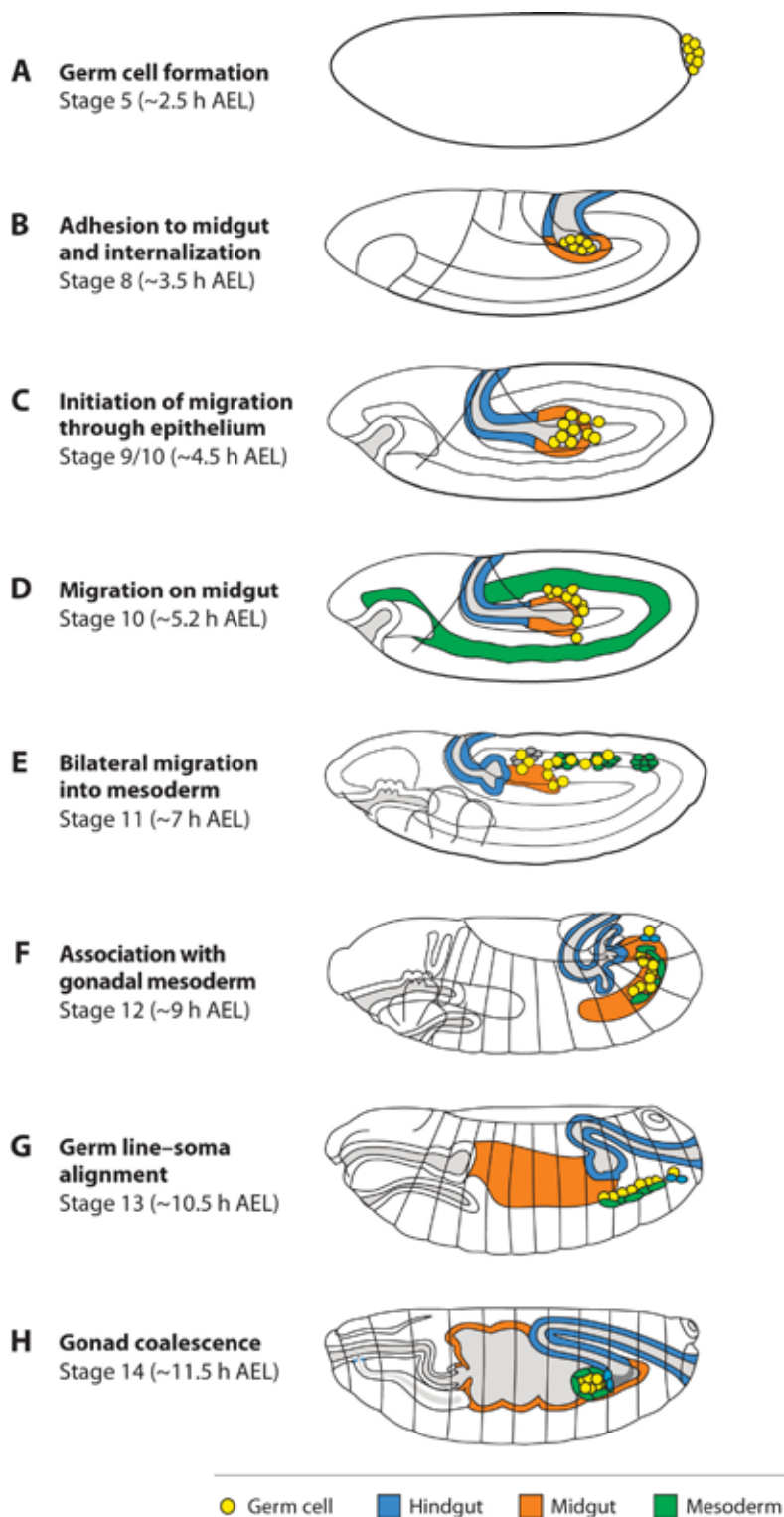


**Figure 3. Hallmarks of PGC migration in *Drosophila*.**

(A-B) Germ cells are formed at the posterior pole of the embryo and are internalized by midgut epithelium during gastrulation movements. (C) At stages 9/10 germ cells migrate out of the midgut. (D) Germ cells have moved to the dorsal surface of the midgut by late stage 10. (E) At stage 11, germ cells migrate bilaterally to reach the gonadal mesoderm from the dorsal surface of the midgut. (F-H) Germ cells associate, align, and coalesce with the gonadal mesoderm to form the gonad at stage 14. AEL stands for after egg laying at 25°C. Adapted from <sup>185</sup>.

but somatic gonadal precursors express high levels of HMGC $\alpha$ , and it is postulated that high levels of the unknown attractant might be the reason for loss of motility<sup>204</sup>.

### 1.3.2. PGC migration in chicken

Chicken PGCs are specified in the epiblast in the center of the area pellucida from where they are translocated by morphogenetic movements towards the anterior extraembryonic region<sup>206,207</sup> (Figure 4, left panel). In this region, they incorporate into extraembryonic vascular vessels and circulate in the blood stream (Figure 4, middle panel). At a later time in development, PGCs extravasate from the blood stream and migrate towards the developing gonads (Figure 4, right panel). Strikingly, the guidance of chicken PGCs to leave the blood stream and migrate towards the developing gonads was found to be the chemokine CXCL12<sup>208</sup>. As CXCL12 is involved in the extravasation of leukocytes from the bloodstream to sites of infection<sup>209,210</sup>, chicken PGCs might recapitulate these steps of rolling, tethering, and extravasation during their migration to gonadal precursor cells.

### 1.3.3. PGC migration in mouse

Mouse PGCs are specified in the posterior primitive streak from where they disperse into the posterior embryonic endoderm that will later become the hindgut<sup>212,213</sup> (Figure 4A). Similar to *Drosophila* PGC migration, mouse PGCs migrate along the hindgut until they cross the hindgut epithelium dorsally and split into two clusters that then orient towards the developing gonads (Figure 5B-C). The migration of PGCs within the hindgut and

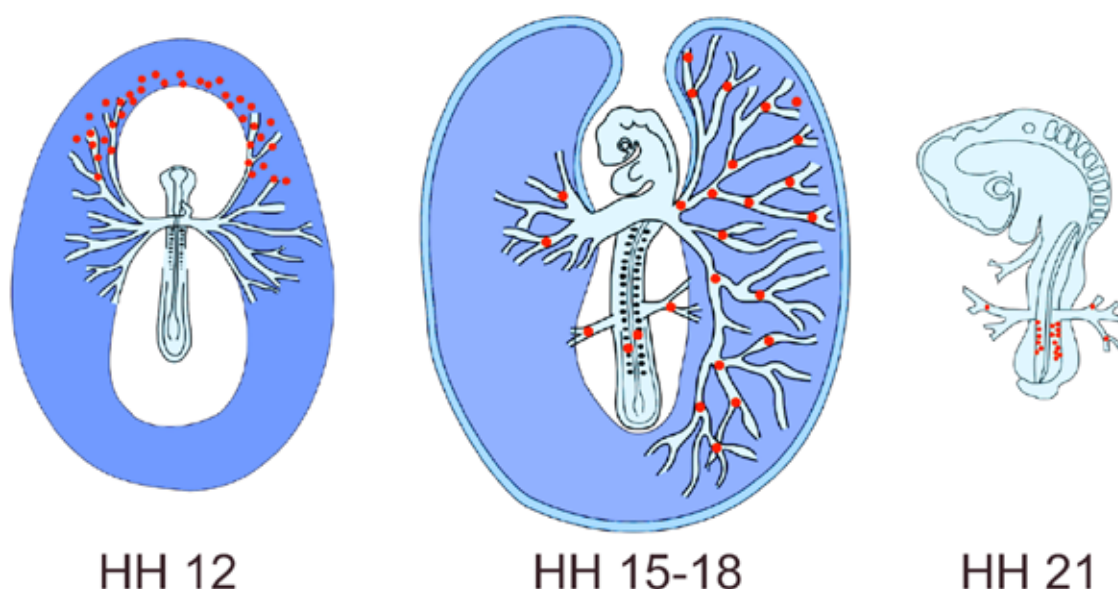


**Figure 4. Hallmarks of PGC migration in chicken.**

At HH 12, PGCs (red dots) are located in the anterior extraembryonic tissues and are taken up by the forming vascular system. During HH 15-18, the cells are passively circulating in the blood stream. At HH 21, PGCs have extravasated the vascular network and migrated towards the developing gonads. HH stages according to <sup>211</sup>.

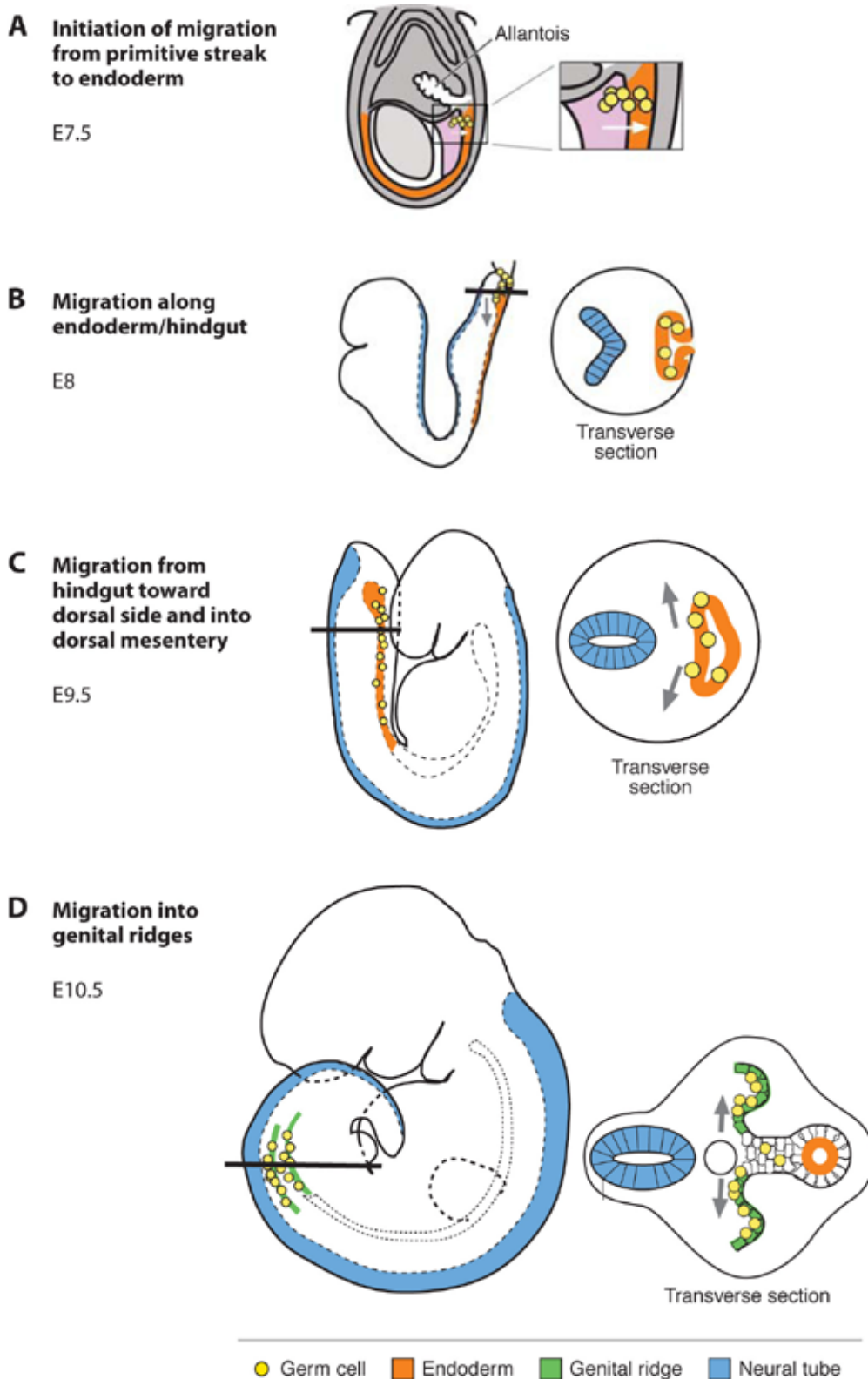


**Figure 5. Hallmarks of PGC migration in mouse.**

(A) Germ cells (yellow) are specified in the primitive streak. At E7.5, they initiate their migration to the endoderm (orange). An enlargement of the boxed area is shown to the right. In (B-D) a transverse section (straight black line) is shown to the right of each panel. (B) At E8, germ cells migrate along the hindgut. (C) At E9.5, germ cells leave the hindgut toward the dorsal body wall. (D) By E10.5, germ cells reach the genital ridges (green) to form the gonad; germ cells remaining in the hindgut and the midline will be lost. The time of onset of each step is indicated at the top left of each panel. E stands for embryonic day. Adapted from <sup>185</sup>.

the exit from that area is controlled by the tyrosine kinase receptor c-Kit and its ligand Steel<sup>214-217</sup>. Steel promotes the survival and proliferation of PGCs and is initially uniformly expressed within hindgut and surrounding tissues. Gradual downregulation of *steel* in the midline and hindgut forces PGCs to exit the hindgut, cells that have remained die by apoptosis<sup>214</sup>. This early control of PGC migration by the usage of a survival factor is very similar to the regulation of *Drosophila* PGC migration by Wunen/Wunen2<sup>218</sup>. After PGCs have left the hindgut they are targeted to the gonadal precursors by high expression of the chemokine CXCL12 in mesenchymal and gonadal precursor cells<sup>154,155</sup> (Figure 5D). Thus, PGC migration in chicken and mouse share a common guidance mechanism.

### 1.3.4. PGC migration in zebrafish

Zebrafish PGCs are specified by inheritance of maternal determinants that localize to the cleavage planes of the first four blastomeres<sup>219</sup>. These determinants (called germ plasm in zebrafish) are thereby incorporated into four evenly spaced cell clusters along the periphery of the embryonic disc. Initially immotile, these cells initiate their migratory program with the onset of zygotic transcription around 3.5 hours postfertilization (hpf) and soon begin to follow a canonical migration track that is highly reproducible<sup>220,221</sup>. With the beginning of epiboly (the covering of the large yolk ball by embryonic tissues) around 4 hpf, the four clusters begin to migrate dorsally in a deep cell layer between the endo- and mesoderm, but avoid the dorsal shield, the zebrafish organizer (Figure 5A-B). By the time epiboly has completed around 10 hpf, more dorsal clusters have positioned in the middle of the embryo in lateral stripes perpendicular to the midline (Figure 6C). Due to convergence movements, originally more ventral clusters are now trailing behind as posterior clusters and migrate towards the more anterior clusters. With the beginning of somitogenesis, the anterior stripes have formed clusters parallel to the midline that now begin to move anteriorly on the lateral mesoderm where they congregate with the posterior clusters and gonadal precursor cells at the end of the first day of development<sup>36,221</sup> (Figure 6D-E).

The reproducible pattern of PGC migration in zebrafish hinted towards a mechanism that collects PGCs from all parts of the embryo and then guides them towards their final position in the larvae. Genetic screens identified fish homologs of the chemokine CXCL12 and its receptor CXCR4 as required for migration of PGCs<sup>156,157</sup>. Indeed, expression of the fish chemokine CXCL12a by the somatic mesoderm predicts the migratory route of PGCs that express the fish chemokine receptor CXCR4b<sup>156</sup>. At the beginning of their migration the four PGC clusters move anterior on a ring of mesodermal cells expressing CXCL12a that are excluded from the dorsal shield. Lack of CXCL12a expression in the organizer causes PGC clusters born in this area to relocate towards ventral *cxcl12a* expression sites. Morphogenetic movements cause the *cxcl12a* transcription domain to enclose the posterior half of the embryo and an increase of *cxcl12a* expression from posterior to anterior is detectable. PGC clusters continuously move towards the site

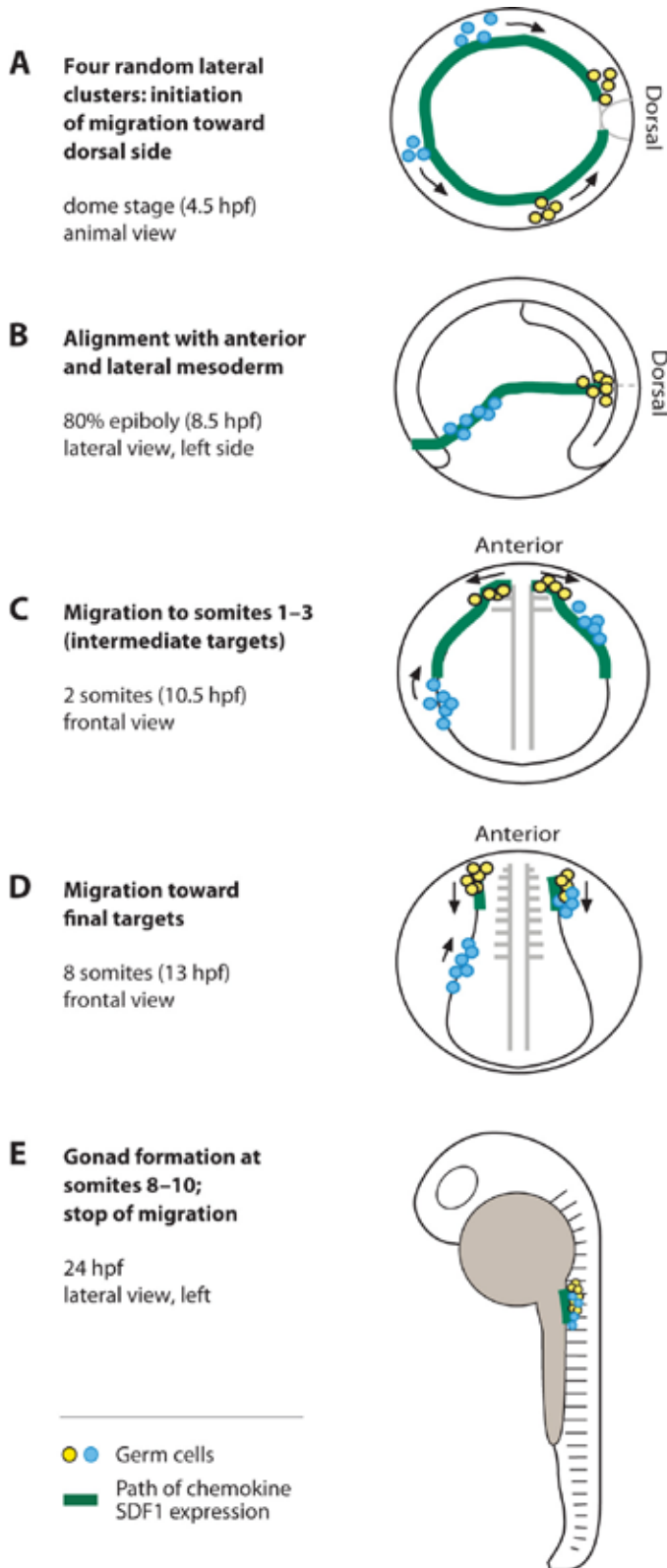


**Figure 6. Hallmarks of PGC migration in zebrafish.**

(A) At dome stage, germ cells (blue and yellow) are found in four clusters and begin migrating towards the dorsal side of the embryo.

(B) At 80% epiboly, germ cells are found aligning with the anterior and lateral mesoderm.

(C) By the two-somite stage, the anterior cluster of germ cells (yellow) migrates close to somites 1-3, which act as intermediate targets. The trailing posterior cluster (blue) is migrating anteriorly on the lateral plate mesoderm.

(D) At 8-10 somites, the anterior cluster moves posterior towards the developing gonad, towards the trailing cluster.

(E) By 24 hpf, germ cells coalesce with their somatic counterparts to form the gonads. The time of onset of each step and the perspective of the view shown are indicated to the left of each panel. hpf represents the hour post fertilization at 29°C. Adapted from<sup>185</sup>.

of highest *cxcl12a* expression located in the middle of the embryo and eventually merge into the two lateral clusters at the position of the future gonads<sup>36,156</sup>.

Unlike in *Drosophila* and mouse PGC migration, a mechanism to guide zebrafish PGC migration by repellent cues or the regulation of survival has not been found<sup>222,223</sup>, and CXCL12/CXCR4 signaling is not required for survival and proliferation of PGCs during the first day of development<sup>156</sup>. The experimental accessibility of PGC migration in zebrafish therefore offers a unique possibility to investigate CXCL12-dependent migratory processes in an *in vivo* context.

### 1.3.5. Zebrafish PGC migration as a tool to study chemokine signaling

Due to genome duplication in the speciation of the teleost fish, the zebrafish genome contains many gene duplicates<sup>74,224</sup>. Often, the existence of these paralogs complicate studies on these genes as there might be a considerable redundancy and compensation of genetic function<sup>225,226</sup>. The genome duplications had an enormous impact on the number of chemokine genes<sup>76,77</sup>. Numbers given in the literature are very variable, the most recent study has identified more than 100 chemokine genes in the zebrafish genome and also introduced a new class of CX chemokines<sup>77</sup>. Many of the identified genes display developmentally regulated expression that could hint towards potential roles in the embryonic development.

Despite the increased complexity, this situation offers a unique possibility to study chemokine signaling in the context of highly regulated developmental processes. For example, the chemokine *cxcl12* and its receptor *cxcr4* each have two paralogs in zebrafish: *cxcl12a* and *cxcl12b*, *cxcr4a* and *cxcr4b*<sup>227,228</sup>. Whereas *cxcl12* or *cxcr4* knockouts in mammals are embryonically lethal<sup>188,143,229,230</sup>, fish with null-mutations or morpholino anti-sense oligonucleotide-mediated gene knockdown of either paralog are viable and fertile with developmental defects that are distinct from each other<sup>13,156,157,228,231</sup>. This raises the possibility that these paralogs have evolved to divide the original function of the ancestral gene. Accordingly, the fish paralog CXCL12a is predominantly found to interact with the receptor CXCR4b in the guidance of migratory cells and neurons<sup>153,156,157</sup>, whereas CXCL12b and CXCR4a mostly have been implied in processes involving transcriptional gene regulation in proliferation, tissue morphogenesis and regeneration<sup>13,232</sup>.

With respect to PGC migration the idea of a divergent evolution of the chemokine genes also holds true, as only the paralogs *cxcr4b* and *cxcl12a* have been reported being of functional relevance<sup>156,157</sup>. In agreement, only expression of *cxcr4b* but not *cxcr4a* is detectable in these cells, and the expression of *cxcl12a* but not *cxcl12b* correlates with the positioning of the PGCs at 24 hpf<sup>156</sup>. Nevertheless, interactions of the receptors with both ligands are likely to occur, as the ligands are highly similar (85% identity and 97% similarity on the amino acid level, Figure 16), and expressed simultaneously during

development<sup>156,233</sup>. The control of PGC migration during zebrafish development by two chemokine genes thus offers a unique possibility to study integration of two signals into a cellular response in an easily accessible *in vivo* system.

The zebrafish genome also contains homologs to CXCR7, the recently identified second receptor to CXCL12 (see section 1.2.3). The expression and function of this receptor during early zebrafish development is yet to be determined, specifically in the context of CXCL12-guided PGC migration.

### **1.3.6. Aim of the thesis**

Structural intricacies of chemokines and their receptors allow the existence of complex regulatory networks. Ligand regulation, receptor crosstalk and the possibility of heteromerization of chemokine receptors and ligands results in a myriad of possible pathway interactions and fine-tuning mechanisms, yet the biological significance of these have not been confirmed to satisfaction. Furthermore, there is still little data as to how the individual chemokine receptors distinguish between their multiple ligands. The chemokine-directed migration of zebrafish PGCs offers an easily accessible system to study these mechanisms *in vivo*. In this work we will study zebrafish homologs of CXCL12 and its receptors to identify general regulatory principles that might be recognized in many other cell migration processes controlled by mammalian counterparts. At first, the function of the recently deorphanized CXCL12-receptor CXCR7 in PGC migration will be investigated. Then, we will aim to understand how PGCs differentiate between the two CXCL12 ligands present during embryonic development.

## 2. Materials and Methods

### 2.1. Materials

#### 2.1.1. Laboratory equipment and materials

**Table 1. List of reagents, chemicals, kits, equipment, and software used in this work.**

Given are names, manufacturers, and where available, ordering numbers for material used.

<b>Chemicals, reagents, media</b>	
Acrylamide Rotiphorese A 30%	Roth (3037.1)
Agarose SeaKem LE (for electrophoresis)	Lonza (50004)
Agarose UltraPure (for microscopy)	Invitrogen (15510-027)
Ambion Nuclease-free Water (not DEPC-treated)	Applied Biosystems (AM9932)
Amine Coupling Kit	GE Healthcare (BR-1000-50)
Ampicillin	Gerbu (1046)
Buffer components (molecular biology grade)	AppliChem, Merck, Roth, Sigma, Roche
CM4 Sensorchip	GE Healthcare (BR-1005-39)
Complete Protease Inhibitor Cocktail	Roche (1183614001)
Biotinylated heparin, 12 kDa	gift from H. Lortat-Jacob, IBS Grenoble, France
Biotinylated heparan sulfate, 6 kDa	gift from H. Lortat-Jacob, IBS Grenoble, France
DIG RNA Labelling Mix	Roche (11277073910)
Dextran Alexa568	Invitrogen (D-22912)
Dextran Oregon Green BAPTA-1	Invitrogen (O-6798)
DMEM, stable glutamine	PAA (E15-883)
DNA Oligonucleotides	Eurofins/MWG
Dow Corning High-Vacuum Grease	Fisher Scientific (14-635-5D)
Enzyme-free dissociation buffer (PBS-based)	Invitrogen (13151-014)
Fetal Bovine Serum, heat inactivated	PAA(A15-104)
Fluorescein RNA Labelling Mix	Rocher (11685619910)
Heparin	Sigma (H3393)



Kanamycin	Gerbu (1091)
LB medium powder	AppliChem (A0954)
Lipfectamine 2000	Invitrogen (11668019)
MaXtract High Density	Qiagen (129056)
Morpholino antisense oligonucleotides	Gene Tools
N,N'-Methylen-bis-acrylamid	Roth (7867.1)
Nucleo Bond PC 20	Macherey-Nagel (740571)
NucleoSpin Extract II	Macherey-Nagel (740609)
PageBlue Protein Staining Solution	Fermentas (R0571)
PBS, without Ca and Mg	PAA (H15-002)
Penicillin/Streptomycin	Invitrogen (15140163)
Plasmid Midi Kit	Qiagen (12143)
Poly-D-Lysine	BD Bioscience (354210)
Pyrex Cloning Cylinders	Fisher Scientific (09-552-21)
SeeBlue Plus2 Prestained Standard	Invitrogen (LC5925)
Torula RNA	Sigma (R6625)
TRIZOL	Invitrogen (15596026)
<b>Enzymes and Proteins</b>	
Ambion mMessage Machine SP6	Applied Biosystems (AM1340)
Ambion mMessage Machine T3	Applied Biosystems (AM1348)
Factor Xa	NEB (P8010)
Omniscript RT	Qiagen (205111)
Pfu Methionine Aminopeptidase	Sigma (M6435)
Phusion HF	NEB (F-531)
Protease K	Sigma (P8811)
Restriction enzymes	Fermentas, New England Biolabs
sheep anti-digoxigenin antibody (alkaline phosphatase-conjugate)	Roche (11093274910)
sheep anti-fluorescein antibody (alkaline phosphatase-conjugate)	Roche (11426338910)
SP6 RNA Polymerase	Roche (10810274001)
Streptavidin	AppliChem (A1495)
T3 RNA Polymerase	Roche (11031163001)

T4 DNA Ligase	Invitrogen (15224-017)
T7 RNA Polymerase	Roche (10881767001)
Trypsin/EDTA	PAA (L11-004)

### Bacterial and eukaryotic cells

TOP 10F' (cloning bacteria)	Invitrogen (C303003)
BL21 (DE3) (expression bacteria)	Merck Biosciences (70235)
HEK293 (mammalian cell line)	DSMZ (ACC 305)
HEK293T (mammalian cell line)	DSMZ (ACC 635)
NIH/3T3 (mammalian cell line)	DSMZ (ACC 59)

### Laboratory equipment

Agarose gel electrophoresis chambers	VWR International
Biacore 3000	GE Healthcare
CellTram Vario Oil	Eppendorf (5176000.033)
Centrifuge RC 5Cplus	Heraeus
Eppendorf Research Micropipettors	Eppendorf
Glass capillaries TW-100-4	World Precision Instruments
Laminar flow hoods	BDK
Microcentrifuge tubes	STARLAB
Microinjector pump 6-15	JUN-AIR
Microinjector PV 820	World Precision Instruments
Micromanipulator M3301	World Precision Instruments
Mircopipet tips	STARLAB
Needle puller PN-30	Narishige
pH meter SevenEasy	Mettler Toledo
Plastic dishes	Greiner Bio-One
Poly-D-Lysin coated cell culture plates and flasks	Greiner Bio-One
SDS-PAGE Protean Mini III	Bio-Rad
Reaction tubes	Greiner Bio-One
Serological pipettes	VWR international
Sonicator UP200s	Dr. Hielscher
Table-top microcentrifuge 5417R	Eppendorf
Table-top centrifuge primo R	Heraeus
ThinCert cell culture inserts (8µm pore size)	Greiner Bio-One (662638)

Cell culture dishes and plates	Greiner Bio-One
Water desalting system	Millipore
<b>Protein purification equipment</b>	
Affinity chromatography column	GE Healthcare (17-0406-01)
HiTrap Heparin HP	
Affinity chromatography medium	Sigma (H5263)
Heparin acrylic beads	
Empty chromatography column HR 16/10	GE Healthcare
Disposable columns 25ml	VWR International
Ion exchange chromatography medium	GE Healthcare (17-0944-01)
Source 15S	
Metal chelate chromatography medium	Qiagen (30210)
NiNTA agarose	
Peristaltic pump P-1	GE Healthcare (18-1110-91)
Peristaltic pump ISM726	Ismatec
Size exclusion chromatography column Superdex75 10/300 GL	GE Healthcare (17-5174-01)
<b>Microscopy equipment</b>	
Confocal microscope TCS SL	Leica
10x air objective, 40x and 63x water lens objectives, Laser lines 458, 488, 514, 546 nm	
Epifluorescence microscope Axioplan2	Zeiss
5x, 10x, and 20x air objectives, 40x and 63x water lens objectives, Diagnostic Instruments RTSlider color camera, Diagnostic Instruments Spot RT SE monochrome camera, HBO 100 UV light source	
Epifluorescence microscope Imager.Z1	Zeiss
5x, 10x, and 20x air objectives, 40x and 63x water lens objectives, Photometrics CoolSnap ES2 monochrome camera, Märzhäuser/Wetzlar Scan 100x80 motorized table, Ludl MAC500 filter wheel, EXFO X-Cite 120 UV light source	
Epifluorescence microscope Imager.M1	Zeiss
5x, and 10x air objectives, 40x and 63x water lens objectives, Diagnostics Instruments Spot XPlorer monochrome camera, Märzhäuser/Wetzlar Scan 100x80 motorized table, HXP-120 120 UV light source	
UV Stereomicroscope MZFLIII	Leica
UV Stereomicroscope MZ16F	Leica
Stereomicroscope MZ75	Leica

**Software**

Biacore3000 Control	GE Healthcare
Bia Evaluation 4.1	GE Healthcare
ImageJ	National Institutes of Health
Illustrator CS3	Adobe
Leica TCS SL	Leica
MetaMorph	Molecular Devices
Photoshop CS3	Adobe

**2.1.2. Buffer compositions****Table 2. Composition of buffers used in this work.**

All buffers were made in Millipore water. Buffers used in protein purification, SDS-PAGE and Surface Plasmon Resonance experiments were sterile filtered and degassed extensively. Danieau stock medium was sterile filtered. LB medium and TAE stock medium was autoclaved.

<b>Buffer A</b>	50 mM Tris, pH 8.0
<b>Buffer AU</b>	50 mM Tris, pH 8.0 2M Urea
<b>Buffer AUX</b>	50 mM Tris, pH 8.0 2M Urea 2% (v/v) Triton X-100
<b>Buffer B</b>	50 mM Tris, pH 7.5
<b>Buffer GF</b>	20 mM sodium phosphate, pH 6.0 150 mM NaCl
<b>Buffer R</b>	50 mM Tris, pH 7.5 6M guanidine hydrochloride 20 mM DTT
<b>Danieaus</b>	150 mM HEPES, pH 7.6 1.74M NaCl 21 mM KCl 12 mM MgSO <sub>4</sub> • 7 H <sub>2</sub> O 18 mM Ca(NO <sub>3</sub> ) <sub>2</sub> • 4 H <sub>2</sub> O
<b>Egg water</b>	0.03% (w/v) sea salt 0.002% (w/v) methylene blue
<b>HBS-EP</b>	10 mM HEPES, pH 7.4 150 mM NaCl 3 mM EDTA 0.005% (v/v) P-20
<b>HBS-P</b>	10 mM HEPES, pH 7.4 150 mM NaCl 0.005% (v/v) P-20

<b>Hybridization buffer</b>	9 mM citric acid monohydrate, pH 6.0 132.5 mM disodium citrate dihydrate 4.375% (w/v) NaCl 0.05% (w/v) torula yeast RNA 0.005% (w/v) heparin 0.1% (v/v) Tween-20 50% (v/v) formamide, deionized
<b>LB</b>	0.5% (w/v) yeast extract 1% (w/v) tryptone 0.5% (w/v) NaCl
<b>PAGE resolving gel</b>	0.357 mM bis-Tris, pH 6.5 8% (v/v) acrylamide/bisacrylamide (30%:2%) 0.6% (v/v) APS 0.2% (v/v) TEMED
<b>PAGE stacking gel</b>	0.357 mM bis-Tris, pH 6.5 4% (v/v) acrylamide/bisacrylamide (30%:2%) 0.05% (w/v) bromophenol blue 0.6% (v/v) APS 0.4% (v/v) TEMED
<b>TAE</b>	40 mM Tris-acetate, pH 8.0 1 mM EDTA

## 2.2. Molecular Cloning

### 2.2.1. cDNA synthesis

Total RNA was isolated from embryos of various stages or cell cultures using TRIZOL reagent according to the manual. RNA was resuspended in RNase-free water and complementary DNA (cDNA) was synthesized immediately using the Omniscript RT kit with poly-dT primers according to the manual. cDNA was stored at -20 °C.

### 2.2.2. Polymerase chain reaction (PCR)

DNA amplification using PCR was performed using Phusion HF DNA polymerase according to the manual. The PCR was either cleaned directly or after gel electrophoresis using NucleoSpin Extract II.

### 2.2.3. DNA gel electrophoresis

DNA was resuspended in loading buffer (Fermentas) and loaded onto agarose gels of the required percentage for analysis. If required, the DNA was excised from the gel using clean scalpels and isolated using NucleoSpin Extract II.

### 2.2.4. Expression clones

Expression clones were generated using standard molecular biology techniques. For *in vitro* transcription, the gene of interest was introduced into vectors based on the pBlue-

script or pSP64TS backbone containing the SP6 or T3 promoters with either the *nanos1* 3' untranslated region (UTR) (for PGC-specific expression) or the *Xenopus globin* 3' and 5' UTRs (for uniform expression). For subcloning or antisense probe generation the gene was introduced into pCR-TOPOII (Invitrogen). For mammalian expression, the open reading frames of interest were introduced into pcDNA3.1 (Invitrogen). For bacterial expression, open reading frames were introduced into vectors of the pET expression series (Novagen). The constructs used in this work are listed in the appendix.

### **2.2.5. Bacterial DNA amplification**

The *E.coli* TOP 10 F' strain was used for DNA amplification. Electrocompetent bacteria were electroporated with DNA or ligation mixtures and grown on LB agar plates with appropriate antibiotics at 37°C over night. Colonies were transferred to 2 ml LB cultures with antibiotics and grown over night. DNA was isolated using the NucleoBond PC 20 kit, clonal identity was confirmed using restriction digests and sequencing in case the clone had been generated by PCR. From correct clones, 50 ml cultures were inoculated and the DNA isolated using Plasmid Midi kits. Bacterial solutions containing 10% glycerol were stored at -80°C.

### **2.2.6. In vitro mRNA and antisense probe synthesis**

*In vitro* mRNA synthesis and purification was performed using the mMessage Machine Kit, according to the manual. The mRNA was extracted using phenol-chloroform extraction with the MaxTract High Density columns, according to the protocol. Precipitated mRNA was resuspended in 10 mM Hepes pH 7.4 and stored at -80°C.

*In vitro* antisense probe synthesis was performed using SP6, T3, or T7 RNA polymerases according to the manuals. Antisense probes were precipitated by adding 0.5 volumes 7.8M ammonium acetate and 3 volumes pure ethanol, followed by incubation for 40 minutes at room temperature. RNA was pelleted in a table-top centrifuge for 40 minutes at 20000g; the pellet was washed with 70% ethanol twice, air-dried, and resuspended in 25 µl RNase-free water. The RNA concentration was measured in a spectrophotometer before addition of 80 µl hybridization buffer. The integrity of the RNA was assessed using agarose gel electrophoresis. The RNA was stored at -20°C. A list of antisense probes used in this work can be found in the appendix.

## **2.3. Zebrafish work**

Zebrafish strains were kept in accordance with local regulations under permanent fresh water flow conditions at 28°C ambient temperature. Fish of the AB and AB/TL strains were used as wild-type fish. Furthermore, fish of the *spadetail* (*spt*) mutant<sup>234</sup> were used to study PGC migration in embryos with abnormal somatic development. Fish with a Tol-*kop*-EGFP-F-*nanos*<sup>124</sup> or a similar Tol-*kop*-DsRedEx-*nanos* transgene were used to label PGCs in attraction experiments.

### 2.3.1. Injections

Embryos were obtained from natural spawning and transferred to agarose ramps filled with 0.3x Danieaus buffer with penicillin/streptomycin. Genetic manipulations were performed by injection of antisense oligonucleotides or *in vitro* transcribed mRNA into the yolk of a one cell-stage embryo using glass capillaries. mRNA and morpholinos are distributed to all cells of the embryo by cytoplasmic flow. A list of used constructs and morpholinos can be found in the appendix. Embryos with mosaic expression patterns were generated by injection into the blastomeres of later cell stages (four to 16 cell-stage). Embryos were raised in Danieaus with antibiotics for microscopy analysis or in egg water containing methylene blue for all other purposes.

### 2.3.2. Morpholino-mediated gene knockdown

Antisense morpholino oligonucleotides were designed against the start codon of the gene of interest, according to the recommendations of the manufacturer. A morpholino with irrelevant sequence was used as control. In embryos injected with morpholino oligonucleotides the morpholino binds to complementary sequences of mRNA and thereby blocks its translation<sup>82,235</sup>. The sequences of all morpholinos and concentrations used in this work can be found in the appendix.

### 2.3.3. Cell transplantations

Host and donor embryos were raised to the appropriate age (for PGC transplantations 3.5 hpf for both, for PGC attraction experiments 3.5 hpf for a donor embryo and 5.5 hpf for a host embryo) and dechorionated manually using watchmaker's forceps in agarose coated plastic dishes. The embryos were mounted in agarose ramps and cells were transferred directly from a single donor to one or several host embryos using a glass capillary with an opening of 1-2 cell diameters. For PGC transplantations, about 20 cells were taken from superficial layers of the epiblast margin and transferred into random locations of the host embryo. For PGC attraction experiments 20 to 50 cells were taken from random locations of the donor embryo and transferred into apical positions of the host embryo. Treated embryos were incubated in 0.3x Danieaus until microscopy analysis.

### 2.3.4. Heparin-bead implantations

Heparin-coated acrylic beads were washed in 70% ethanol for sanitization, and then washed three times in PBS. 15  $\mu$ l of microsphere suspension was incubated with 5  $\mu$ g/ml CXCL12a, CXCL12b, CXCL12b S33N, or buffer alone for one hour at 4°C. Beads were washed in PBS, and implanted into 6 hpf *Tol-kop-EGFP-nanos* embryos, injected with CXCL12a and CXCL12b morpholino. PGC migration was followed using time-lapse brightfield and epifluorescence microscopy.

### 2.3.5. *In vivo* calcium measurements

Calcium measurements were performed as described in reference <sup>124</sup>. Embryos were injected with morpholinos, *Vasa-DsRedEx-nanos* mRNA to label PGC granules, and the calcium sensitive dye Dextran Oregon Green BAPTA-1. Between 9 and 12 hpf, migrating PGCs were imaged along with surrounding somatic cells by confocal microscopy. To determine the calcium levels of somatic cells, regions of interest were selected in cytosol and nucleus. The fluorescence intensity  $F$  of these regions was calculated using the Leica TCS SL software, and the ratio of  $F_{\text{cytosol}}/F_{\text{nucleus}/2}$  was derived. The signal intensity of the nucleus was chosen as an internal standard, allowing the comparison among different experiments and developmental stages.

### 2.3.6. Whole-mount immunostaining

Embryos were fixed over night in 4% PFA in PBS at 4°C. Embryos were washed three times in PBS containing 0.2% Tween-20 (PBT). In some cases, embryos were either washed five times with methanol and incubated at -20°C over night, or incubated in acetone at -20°C for seven minutes before continuing. Embryos were blocked in PBT containing 5% BSA, and 10% goat serum for one hour at room temperature. Primary antibody was added at varying dilutions and embryos were incubated at 4°C over night. Embryos were washed with six washes of PBT within three hours, before addition of varying dilutions of labelled secondary antibody in PBT containing 5% BSA and 10% goat serum. Embryos were incubated for one hour at room temperature or over night at 4°C. Secondary antibody was removed by washing with PBT over several hours. Embryos were stored at 4°C until they were analyzed by confocal microscopy.

### 2.3.7. Whole-mount *in situ* hybridization

mRNA transcripts were detected using whole-mount *in situ* hybridization (ISH). For a detailed description of the method and reagents see the published protocol<sup>236</sup>. For comparative ISH, antisense probes of identical length were used at equal concentrations throughout all experiments. A list of used probes can be found in the appendix.

## 2.4. Recombinant chemokine production

### 2.4.1. Bacterial cultures

Expression bacteria were transformed with expression vectors and plated on LB plates containing 1.5% agar with appropriate antibiotics (100µg/ml ampicillin or 30µg/ml kanamycin). 2-3 colonies were transferred to 25 ml LB with antibiotics (concentrations as above) and incubated in a shaker at 37°C at 300 revolutions per minute (rpm) over night. In the morning prewarmed 1 l LB cultures with antibiotics were inoculated with 5 ml of the overnight culture. Bacterial growth was monitored by measuring the optical density at 600 nm (OD600). Protein expression was induced at an OD600 of 0.6 – 0.8 by addition of Isopropyl-β-D-thiogalactopyranosid (IPTG) to a final concentration of 1 mM. Cultures



were incubated for 6 hours at 37°C with 300 rpm. Bacteria were centrifuged at 5000g for 10 minutes. Bacterial pellets were stored at 20°C until further use. 1 ml samples corresponding to 0.1% of total culture volume were taken before induction and after induction.

#### **2.4.2. SDS polyacrylamide gel electrophoresis (SDS-PAGE)**

SDS-PAGE was performed according to the manual of the NuPage electrophoresis system (Invitrogen) using self-made bis-Tris gels (see buffer compositions). 8% Gels were poured in 0.75 or 1.5 mm Protean III mini gel gaskets with 4% stacking gels and stored at 4°C until usage. Protein samples were prepared in LDS sample buffer (Invitrogen) and heated to 70°C for 5 minutes immediately prior to loading. Gels were run at 150-200 V until the buffer front had reached the lower of the gel. SeeBlue Plus2 Prestained Marker served as molecular weight estimate. Gels were stained using PageBlue Protein Staining Solution.

#### **2.4.3. Chemokine purification and modification**

Bacterial pellets were resuspended in buffer A containing Complete protease inhibitor cocktail and lysed by sonification for 5-10 minutes at medium amplitude and frequency. Chemokine-containing inclusion bodies were prepared by centrifugation at 20000g for 10 minutes. The supernatant was kept for analysis and the inclusion bodies were likewise washed in buffers AUX, AU, and again in A. Samples of the lysed bacteria, all supernatants, and inclusion bodies resuspended in the final wash were taken for SDS-PAGE analysis, sample size corresponded to 0.1% of the total volume. After the last wash, inclusion bodies were stored at -20°C until refolding.

The inclusion bodies were resuspended in 25 ml buffer R and linearized by heating to 50°C for 10 minutes. Protein solutions were cleared by centrifugation at 20000g for 10 minutes. The protein was refolded by drop-wise dilution into 275 ml of ice-cold, rapidly spinning buffer B containing protease inhibitors. The protein solution was incubated with light mixing at 4°C over night. The solution was cleared from improperly folded protein by centrifugation at 20000g for 10 minutes at 4°C, diluted further to 600 ml using ice-cold buffer B and spun again at 20000g for 10 minutes at 4°C. Samples corresponding to 0.1% total amount were analyzed in SDS-PAGE. Guanidine-containing samples were precipitated by addition of trichloroacetic acid to a final concentration of 10%, incubation on ice for 20 minutes and centrifugation at 20000g for 15 minutes at 4°C. Protein pellets were washed twice in pure acetone, air dried, and resuspended in LDS sample buffer.

The protein solution was loaded on a 5ml Source 15S ion exchange column equilibrated in buffer B. Column loading was performed over night at a maximum flow rate of 0.5 ml per minute at 4°C. Unbound protein was washed from the column using two column volumes (CV) buffer B. Bound protein was eluted from the column using a linear gradient of 20 CV against buffer B containing 1M NaCl. The column was washed in buffer B with 1M NaCl for 5 CV and then equilibrated with buffer B alone for 5 CV. Between runs with different chemokines the column was cleaned in place according to the manual.

Fractions containing the chemokine were assessed by SDS-PAGE (sample size 0.5% of total volume). Relevant fractions were pooled diafiltrated to buffer GF and loaded on a pre-equilibrated heparin affinity column at a flow rate of 0.5 ml per minute. The chemokines were eluted from the column as described for the ion exchange column, with a linear gradient of 20 CV against buffer GF containing 2 M NaCl as the end point. Relevant fractions were identified by SDS-PAGE. Only the chemokines eluting in a sharp peak were considered for further purification.

Relevant fractions were pooled, concentrated, and loaded on a Superdex 75 size exclusion column equilibrated in buffer GF. In some cases a Superose 12 column was used. Chemokine-containing fractions were determined by SDS-PAGE. Relevant fractions were pooled and the protein concentration determined by measurement of the optical density at 260 nm. The identity of the protein was confirmed by mass spectrometry fingerprinting performed by the Integrated Functional Genomics (IFG) core facility of the Interdisziplinäres Zentrum für Klinische Forschung Münster (IZKF). Formation of the cystin bridges was confirmed by loss of 4 Dalton from the theoretical protein mass. The protein solutions were stored at -20°C.

## **2.5. *In vitro* chemokine biochemistry**

### **2.5.1. NMR spectroscopy and analytical ultracentrifugation**

Cedric Laguri at the Institut de Biologie Structurale, Grenoble, France, performed production of <sup>13</sup>C- and <sup>15</sup>N-labeled chemokines, NMR spectroscopy and analytical ultracentrifugation. All analysis was performed in buffer GF.

### **2.5.2. Chemokine-ECM interaction studies**

Binding studies of chemokines to ECM components were performed on a Biacore 3000 system equipped with a CM4 sensorchip. The sensorchip was coated with 2500 to 2800 response units (RU) streptavidin (50 µg/ml in HBS-P) using the Amine Coupling Kit, at a flow rate of 5 µl per minute. Biotinylated heparan sulfate fragments (gift of Hugues Lortat-Jacob, Institut de Biologie Structurale, Grenoble, France) were dissolved in HBS-P buffer containing 0.3M NaCl to a final concentration of 10 µg/ml and injected using 10 µl pulses at a flow rate of 5 µl per minute until 30 RU were reached.

Chemokines were dissolved in buffer HBS-EP in varying concentrations and injected to the flow cells at a rate of 50 µl per minute for 5 minutes. The injection phase was followed by a dissociation phase of 10 minutes at 50 µl per minute, and a regeneration phase of 2 minutes at 50 µl per minutes of HBS-P containing 2M NaCl. Kinetic data was extracted from the binding and dissociation phases using the BiaEval software.  $K_d$  values were derived from the steady state by plotting the response against the concentration of the chemokine. The  $K_d$  values were then obtained by fitting using the BiaEval software.

## **2.6. Cell culture**

### **2.6.1. General handling**

Cell cultures were generally handled under sterile conditions in a laminar flow hood. Cell lines were grown in 10 cm cell culture dishes containing DMEM with 10% fetal bovine serum (FBS) and penicillin/streptomycin (PS) (DMEM/FCS/PC). Stable cell lines containing the neomycin resistance gene were grown in DMEM/FCS/PS containing G418 (0.5 mg/ml) as selection marker. Culture dishes were incubated in humidity controlled incubators at 37°C and 5% CO<sub>2</sub>.

For general passaging, cells were grown to 80% confluency. Medium and Trypsin/EDTA solution was prewarmed to room temperature. Cells were washed twice in 10 ml PBS and detached in 1 ml Trypsin/EDTA. Trypsin/EDTA was inactivated by dilution with 9 ml medium and cells were centrifuged at 300g for 5 minutes at room temperature. The cell pellet was resuspended in 3ml medium and diluted to new cell culture dishes at an appropriate density. For cell counting, 10 µl of a freshly resuspended cell suspension was counted in a hemocytometer.

Frozen cell stocks were prepared by resuspending the detached cells in freezing medium (DMEM containing 20% FCS and 10% DMSO) to a cell density of one million cells per ml. 1 ml aliquots were transferred to cryotubes and frozen at a cooling rate of one degree per minute to 80°C over night. Finally, cell tubes were stored permanently in the vapor phase of liquid nitrogen.

For thawing, frozen cells were transferred quickly to a 37°C waterbath until the ice clump detached from the cryotube wall. The cell clump was quickly diluted into a prepared cell culture dish containing appropriate medium and incubated over night before the medium was changed again.

### **2.6.2. Transfection**

Cells were transfected with DNA using Lipofectamine 2000 according to the manual. In a few cases cells numbers and DNA amount were adjusted to reduce cell death. Transfection medium was replaced on the next day of transfection, cells were assayed for transgene expression 48 hours after transfection.

### **2.6.3. Generation of stable lines**

Cells were transfected as described before and split 1:15 on the day after transfection to several 10 cm dishes. The following day the cells were transferred to medium containing G418 at a final concentration of 0.5 mg/ml. Medium was exchanged on a daily basis to remove dead cells until G418-resistant colonies emerged four to seven days after the addition of selection medium. Colonies were washed in PBS and isolated using sterile cloning cylinders submerged in sterilized vacuum grease. Cells were detached by addi-

tion of Trypsin/EDTA to the cylinders and the colonies were transferred to 6 well plates in which they were grown for determination of transgene expression.

#### **2.6.4. Generation of conditioned media**

HEK293T cells were transfected with the plasmids of interest using Lipofectamine 2000 in 10cm dishes. Cells were grown for two days and starved overnight in 2ml DMEM containing 0/2% (w/v) BSA. Medium was collected and either frozen at -20°C or used immediately.

#### **2.6.5. *In vitro* transwell migration assays**

NIH/3T3 mouse fibroblasts transiently expressing zebrafish CXCR4b were assayed two days after transfection. Cells were starved over night in DMEM containing 0.2% (w/v) BSA (DMEM/BSA) and were harvested using enzyme-free dissociation buffer. Cells were resuspended in DMEM/BSA at a density of 10<sup>6</sup> cells per milliliter. CXCL12a-conditioned medium was prepared as described above, conditioned medium from HEK293T cells transfected with pEGFP vector served as negative controls. 24-well plates were filled with 600 µl pure conditioned media or dilutions with DMEM/BSA. DMEM with 10% FCS served as positive control. Thincert transwell inserts with 8 µm pores were loaded with 200 µl of cell suspension, submerged into test medium, and incubated at 37°C and 5% CO<sub>2</sub> for 4 hours. The medium of the insert and the lower well were removed and the well was washed once with PBS. 200µl Trypsin/EDTA was added to the lower cell and cells were detached for 5 minutes at 37°C with sporadic agitation to the filter. The inserts were discarded and the cells in the lower well were resuspended and added to 1.5 ml reaction tubes containing 300 µl DMEM/FCS/PS. The wells were washed with another 500 µl DMEM/FCS/PS, which was added to the reaction tubes. The cells were harvested by centrifugation at 300g for 5 minutes, resuspended in 50 µl DMEM/FCS/PS, and counted using a hemocytometer.

## **2.7. Microscopy**

### **2.7.1. Epifluorescence microscopy**

Time-lapse microscopy was performed on Zeiss epifluorescence microscopes at ambient temperatures of 28°C. Embryos were mounted in 1.5% agarose ramps with 0.3x Danieaus/PS. For high magnification movies images were every 10 seconds using 40x or 63x water lens objectives and assembled into movie stacks using the MetaMorph or ImageJ software. For low magnification movies images were acquired every minute using a 10x air lens objective. In cases when low magnification movies were acquired with several focus planes on multiple stage positions, a frame rate of once per minute was not feasible. The images were then acquired at the shortest interval possible.

### **2.7.2. Confocal microscopy**

Confocal microscopy was performed on Leica confocal microscope at ambient temperatures of 28°C. Embryos were mounted in 1.5% agarose ramps with 0.3x Danieaus/PS. The Leica TCS SL was operated with a 40x water lens and images were acquired with an increased pinhole diameter.

### **2.7.3. Image processing**

Images were processed using MetaMorph, Leica TCS SL, ImageJ, and Adobe Photoshop CS2/CS3 software suites. Images were assembled using Adobe Illustrator CS2/CS3.

### 3. Results

#### 3.1. CXCR7 controls PGC migration by CXCL12 sequestration

##### 3.1.1. Expression of the second CXCL12 receptor CXCR7 during zebrafish development

CXCR7 had recently been identified as a receptor for CXCL12, yet its function was still under debate (see section 1.2.3). To test whether the recently deorphanized CXCL12 receptor CXCR7 could have an influence on PGC migration in zebrafish, we performed *in situ* hybridization in order to detect the expression of this gene during development. We amplified the *cxc7* open reading frame (ORF) from total mid-somitogenesis cDNA by PCR (see section 2.2) and cloned it into the pCR-TOPOII vector for the synthesis of an antisense probe.

Weak and uniform *cxc7* expression was first observed with the beginning of zygotic transcription around 3.3 hpf (Figure 7A-D, I). The absence of maternally provided

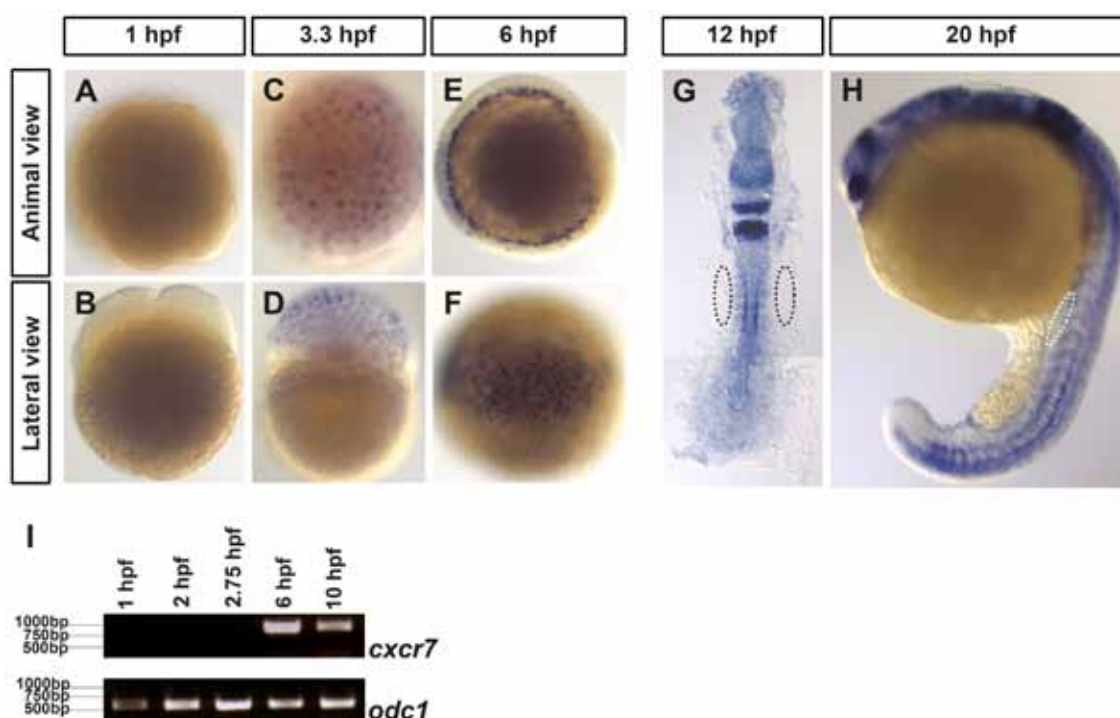


**Figure 7. Expression pattern of *cxc7*.**

(A–H) Distribution of *cxc7* mRNA in wild-type embryos during the first 20 hr of development. *In situ* hybridization using a *cxc7*-specific probe shows no staining in four-cell stage embryos (A and B), weak uniform expression at 3.3 hpf (C and D), and enhanced *cxc7* expression in a ring of deep cells at 6 hpf (E and F). At later stages of development (G and H), uniform *cxc7* expression with enhanced expression in mesoderm derivatives and in the nervous system is detected, but no expression is observed at the region where the PGCs are located (encircled domains). (I) Absence of maternally provided *cxc7* mRNA as determined by RT-PCR at the indicated stages. Control reactions are presented in which primers specific for the maternally provided ornithine decarboxylase1 (*odc1*) mRNA were used.

mRNA was confirmed by RT-PCR on total cDNA of 1 hpf and 2 hpf embryos (Figure 7I). At 6 hpf, *cxcr7* mRNA was detected in a broad ring of deep cells (Figure 7E-F). Between 8 and 10 hpf, *cxcr7* mRNA was uniformly expressed at low levels (data not shown). At 12 hpf, *cxcr7* expression was weakly expressed throughout the embryo, with more specific expression at the midline borders of the somites and two strong expression domains at the head-trunk border (Figure 7G). At 24 hpf *cxcr7* transcription was found in the nervous system, eyes and weakly in somite muscles (Figure 7H). In contrast to *cxcr4b* expression that could readily be detected in migratory PGCs<sup>156</sup>, we failed to detect PGC-specific *cxcr7* expression during later developmental stages (positions of PGCs are outlined by dotted circles). *Cxcr7* thus showed a dynamic expression throughout the first day of development, yet the possibility that PGCs expressed the receptor during at the onset of zygotic transcription could not be excluded.

### 3.1.2. CXCR7 function is required for PGC migration

To investigate whether CXCR7 played a role in PGC migration, we knocked down CXCR7 function using a morpholino antisense oligonucleotide (see section 2.3.2 and Appendix) and found that PGCs did not arrive at the position of the developing gonads at 24 hpf (Figure 8A-F). Instead, PGCs were scattered throughout the embryo, which was reminiscent of PGC migration defects in CXCR4b knocked-down embryos (morphants). To test the efficacy of *cxcr7* gene knockdown, we coinjected CXCR7-EGFP-*globin* mRNA with either CXCR7 or control morpholino. A successful knockdown of *cxcr7* mRNA translation should thus prevent expression of the CXCR7-EGFP fusion protein encoded by CXCR7-EGFP-*globin* mRNA. While control embryos exhibited uniform fluorescence of CXCR7-EGFP, we did not observe EGFP-fluorescence in embryos coinjected with CXCR7 morpholino (Figure 9A). To rule out that CXCR7 knockdown disturbed PGC migration by interfering with normal *cxcl12a* expression, we stained for the germ cell-specific marker *nanos1* and *cxcl12a* in *in situ* hybridization. Normal *cxcl12a* expression in CXCR7 morphant embryos thus suggested that the observed failure of PGCs to migrate towards their target was likely to be a direct effect on cell motility (Figure 8G-H). Furthermore, PGC specification and proliferation were also unaffected, as indicated by PGC numbers (Figure 8I), maintenance of specific PGC characteristics, such as expression and protection of the PGC-specific *nanos1* mRNA (Figure 8A-H), and correct localization of the germ plasm component Vasa to germ cell granules (Figure 8D-F).

To exclude that unspecific targets of the used morpholino caused the PGC migration defect, we coinjected CXCR7 morpholino with CXCR7-*globin* mRNA. The mRNA carried mutations in the morpholino-binding site that conferred resistance to morpholino-mediated knockdown. Indeed, uniform expression of CXCR7 from this mRNA was able to restore PGC migration, confirming that the migration defect was caused by specific knockdown of CXCR7 (Figure 8J-L). Interestingly, germ cell-specific expression of CXCR7 was not able to restore PGC migration to the same extent as uniform expression of CXCR7 (data not shown). This finding, in combination with the apparent lack of *cxcr7*

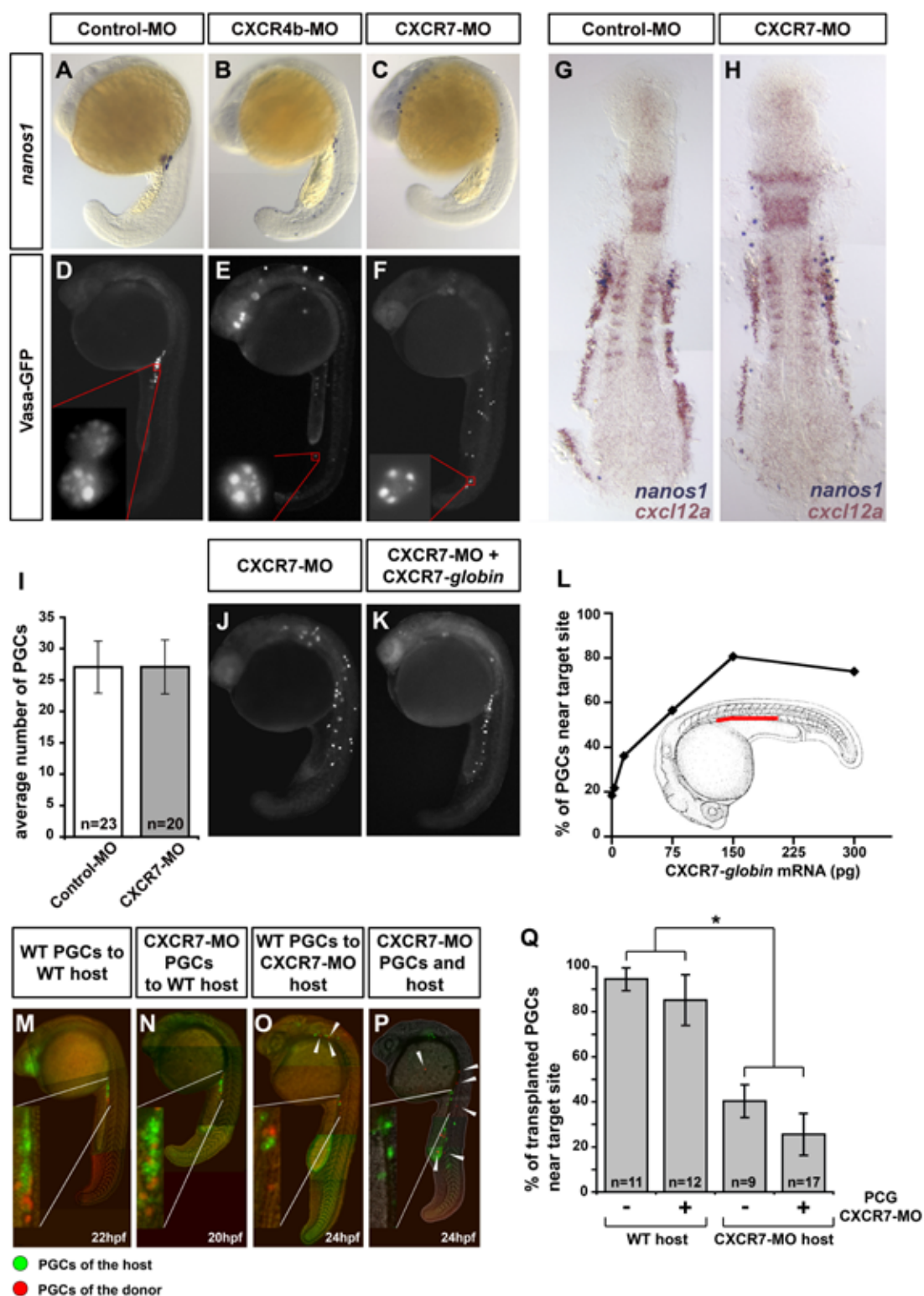


**Figure 8. CXCR7 is essential for normal PGC migration and required in the somatic environment of the embryo.**

(A-C) Reduction of CXCR7 activity leads to aberrant PGC migration as demonstrated by *in situ* hybridization using a germ cell-specific *nanos1* probe. PGCs in control embryos cluster at the region where the gonad develops after 20 hours of development (A). Similar to reduction of CXCR4b activity (B), knockdown of CXCR7 results in a pronounced germ cell migration defect (C). (D-F) CXCR7 knockdown does not affect PGC specification. Low-magnification fluorescence images of 22hpf embryos injected with Vasa-GFP-*nanos* mRNA. Germ-cell specific mRNA protection



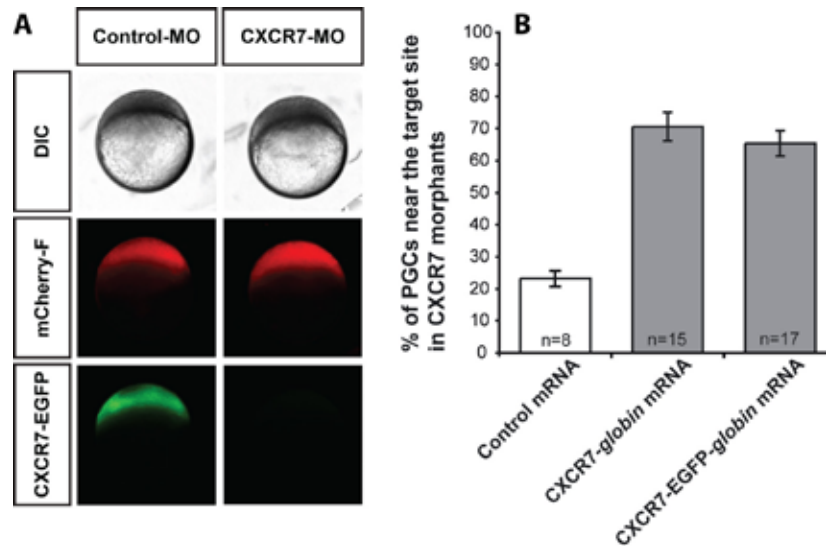


**Figure 9. Morpholino-mediated knockdown of *cxcr7* and rescue of *cxcr7* morphants by *cxcr7* mRNA injection.**

(A) Low magnification DIC and epifluorescence images of 4 hpf embryos coinjected with morpholino-sensitive CXCR7-EGFP-*globin* mRNA and either control (left panel) or CXCR7 morpholino (right panel). Expression of mCherry-F-*globin* mRNA serves as control.

(B) A graph showing the rescue of CXCR7 morpholino treatment by injection of morpholino-resistant CXCR7-EGFP-*globin* mRNA in comparison with equimolar amounts of morpholino-resistant CXCR7-*globin* or control mRNA.

tion and proper localization of the Vasa-GFP fusion protein to germinal granules is observed in embryos injected with control morpholino (D), CXCR4b morpholino (E) and CXCR7 morpholino (F).

(G-H) General embryonic patterning and expression of the guidance cue *cxcl12a* are not affected by CXCR7 knockdown. Two-color *in situ* hybridization using *nanos1* (blue) and *cxcl12a* probes (red) of embryos injected with control (G) or CXCR7 (H) morpholino.

(I) CXCR7 knockdown does not affect PGC number as counted at 12hpf. n signifies the number of embryos examined. Error bars represent standard error of the mean (SEM).

(J-L) The effect of CXCR7 morpholino on PGC migration is reversed by CXCR7 expression in a dose-dependent manner. Low magnification images of 20 hpf embryos coinjected with GFP-*nanos* mRNA. The severe migration phenotype induced by the CXCR7 antisense oligonucleotide (J) is reversed by injection of morpholino-resistant CXCR7-*globin* mRNA (K). A graph demonstrating the dose-dependent rescue of the CXCR7 morpholino-induced phenotype by global expression of CXCR7 (L). For all injections the total amount of injected mRNA was kept constant (300 pg) by addition of control mRNA (mCherry-F-*globin* mRNA). The red bar in the cartoon spans the area that was considered as the correct target for the migrating PGCs.

(M-Q) Germ cell migration depends on the activity of CXCR7 in somatic tissues. Transgenic germ cells expressing DsRedExpress (red) were transplanted into transgenic embryos with PGCs expressing EGFP-F (green). Control morpholino-treated germ cells arrived at the region of the gonad in control hosts (M). PGCs from CXCR7-depleted donor embryos also migrate properly to the gonad (N), but a large proportion of wild-type and CXCR7-depleted PGCs does not arrive at the correct target in CXCR7-depleted host embryos (O and P, arrowheads). (Q) A graph showing the percent of transplanted germ cells reaching their target after the first day of development. Germ cells in CXCR7-depleted hosts embryos show a significant reduction of migration fidelity as compared to PGCs in wild-type hosts ( $p < 0.001$ , t-test, marked with an asterisk). PGCs deficient for CXCR7 do not show a significant difference in arriving at the target as compared to control PGCs ( $p > 0.17$ , t-test). n signifies number of embryos examined. Error bars represent SEM.

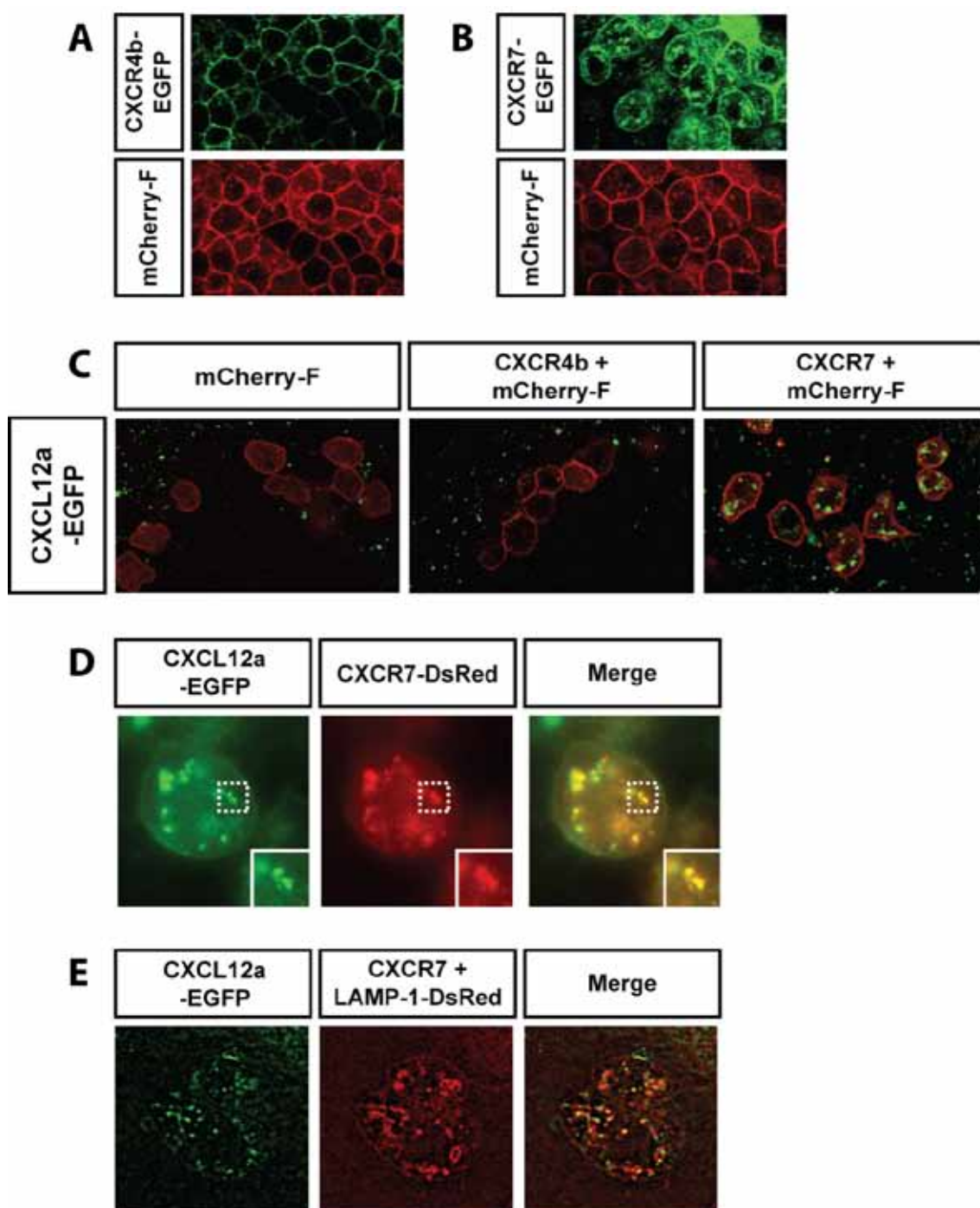


**Figure 10. CXCR7 promotes the internalization of CXCL12a.**

(A-B) Subcellular localization of CXCR4b and CXCR7 (green) in somatic cells of 4 hpf embryos injected with CXCR4-EGFP-*globin* or CXCR7-EGFP-*globin* and mCherry-F-*globin* mRNA. (A) CXCR4b (green) is predominantly found on the membrane of cells (red label of farnesylated mCherry), while CXCR7 (green) is found on the plasma membrane and in intracellular vesicles (B).

(C) CXCL12a is internalized by CXCR7-expressing cells. Somatic cells of 4 hpf embryos injected with CXCR7-*globin*, CXCR4b-*globin*, or control mRNA and mCherry-F-*globin*, were transplanted into 6 hpf host embryos injected with CXCL12a-EGFP-*globin* mRNA. Confocal images were taken 1 hour after transplantation. Transplanted cells (red) expressing either control protein or CXCR4b

expression within PGCs hinted towards the possibility that CXCR7 might not function within PGCs, but rather in somatic cells surrounding them.

### 3.1.3. PGC migration depends on CXCR7 function in somatic cells

To investigate the idea that CXCR7 function might not be required in PGCs but instead in somatic tissues, we created embryos with a chimeric germ line by transplanting PGCs from 4 hpf donor into 4 hpf host embryos (Figure 8M-Q). By injection of CXCR7 morpholino into donors or hosts, we were able to create embryos in which CXCR7 was knocked down specifically in transplanted PGCs, somatic cells of the host, or both. If CXCR7 were required exclusively within PGCs, CXCR7 morpholino-treated donor PGCs should not be able to migrate towards the gonads in control morpholino-injected hosts. On the other hand, if CXCR7 function were required in somatic cells surrounding PGCs, control morpholino-treated PGCs would not be able to find the gonads in CXCR7-treated host embryos. We used transgenic embryos with PGC-specific expression of membrane-localized EGFP (host) or DsRed (donor) to distinguish between transplanted and host PGCs, the latter serve as an internal control for the efficacy of CXCR7 knockdown. Embryos were grown to 24 hpf and the PGC migration defect of the host and donor-derived PGCs was determined. Whereas loss of CXCR7 function in transplanted PGCs did not affect their migration (Figure 8N, Q), CXCR7 deficiency within surrounding somatic tissues had a deleterious effect on PGC migration (Figure 8O-Q). This confirmed our notion that PGC migration was dependent on a chemokine receptor that was functioning outside of the migrating cells.

### 3.1.4. CXCR7 is a constitutively cycling chemokine receptor that binds and internalizes CXCL12a

To gain insight into the possible mechanisms employed by CXCR7 to control PGC migration, we determined the localization of CXCR7 in somatic cells by expressing CXCR7-EGFP fusion protein in these cells. To confirm that this receptor-fluorophore fusion is a fully functional protein, we coinjected wild-type embryos with CXCR7 morpholino and morpholino-resistant CXCR7-EGFP-globin mRNA. We found that the fusion protein was

---

(left and middle panel, respectively) do not show uptake of CXCL12a (green). In contrast, cells expressing CXCR7 showed intracellular accumulations of CXCL12a protein (right panel).

(D) CXCL12a (green) and CXCR7 (red) colocalize in vesicular structures. Somatic cells of 4 hpf embryos injected with CXCR7-mDsRed-*globin* were transplanted into 6 hpf host embryos injected with CXCL12a-EGFP-*globin mRNA*. Epifluorescence images were taken 1 hour after transplantation. The inset shows a magnification of the dotted box.

(E) CXCL12a (green) accumulates in lysosomes (red) upon CXCR7-mediated internalization. Somatic cells of 4 hpf embryos injected with CXCR7-*globin* and LAMP1-mDsRed-*globin mRNA* were transplanted into 6 hpf host embryos injected with CXCL12a-EGFP-*globin mRNA*. Deconvoluted images were taken 1 hour after transplantation.

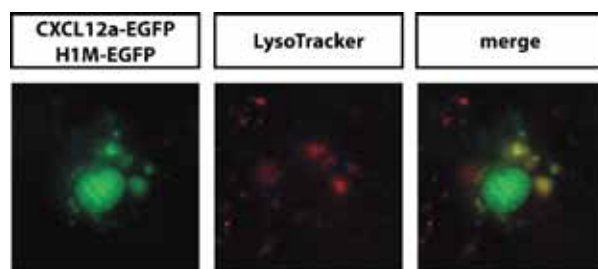


**Figure 11. CXCL12a accumulates in lysosomes upon CXCR7-mediated internalization.**

Somatic cells of 4 hpf embryos injected with *CXCR7-globin* and *H1M-GFP-globin*, were transplanted into 6 hpf host embryos injected with *CXCL12a-EGFP-globin* mRNA. Lysosomal labeling was obtained by incubation of the embryos in 0.3x Danieau's buffer containing 70  $\mu$ M LysoTracker (Invitrogen), starting 1 hour prior to transplantation. Epifluorescent images were taken 1 hour after transplantation; transplanted cells were identified by H1M-GFP-positive nuclei (green).

able to rescue the PGC migration defect caused by CXCR7 morpholino injection to a similar extent as the untagged receptor (Figure 9B). We thus expressed CXCR7-EGFP along with the plasma membrane marker farnesylated mCherry in somatic cells, and detected its localization in 4 hpf embryos. In contrast to CXCR4-EGFP that localized to the plasma membrane (Figure 10A), CXCR7-EGFP was found in quickly moving intracellular vesicles and on the plasma membrane (Figure 10B). Interestingly, we detected a drastic decrease of CXCR7-EGFP localization to the membrane in older stages, and were not able to detect any EGFP fluorescence after 9 hpf.

Mammalian CXCR7 was reported to have a very high affinity to CXCL12<sup>158</sup>, and the apparent high rate of receptor internalization and turnover of the zebrafish CXCR7 led us to believe that there could be a considerable amount of cointernalization and degradation of CXCL12a. To detect CXCL12a protein *in vivo*, we generated a C-terminal fusion of CXCL12a to EGFP. The functionality of CXCL12a-EGFP was confirmed in transplantation experiments in which cells expressing this protein were able to attract PGCs in CXCL12-deficient embryos (Figure 26). We then determined whether CXCR7 is able to bind and internalize CXCL12 *in vivo*. For this purpose, we transplanted cells from embryos coexpressing CXCR7 or CXCR4 with farnesylated mCherry as a cell tracer into embryos uniformly expressing CXCL12a-EGFP, and investigated the distribution of CXCL12a protein 30 minutes after transplantation.

We found that CXCR7-overexpressing cells accumulated large amounts of CXCL12a in intracellular vesicles (Figure 10C, right panel). However, we were not able to detect any CXCL12a uptake by cells expressing CXCR4 or farnesylated mCherry alone (Figure 10C, middle and left panel, respectively). We furthermore asked whether CXCR7 is directly involved in the internalization of CXCL12a. To this end, we repeated the experiment with cells that expressed a C-terminal fusion of CXCR7 to the red fluorescent mDsRed protein. We detected strict colocalization of both molecules in individual intracellular vesicles (Figure 10D). We therefore concluded that there was constant internalization of CXCL12a by somatic cells expressing CXCR7.

### 3.1.5. CXCR7-mediated internalization directs CXCL12a for lysosomal degradation

Internalization of CXCL12a might be followed by transcytosis, a mechanism found to be required for the diffusion and cellular presentation of other chemokines *in vivo*<sup>237</sup>. This way, CXCR7 function would be the key to set up the gradient of CXCL12a in developing zebrafish embryos. Alternatively, CXCR7 might direct CXCL12a to degradation, thereby continuously reducing the extracellular availability of free chemokine. In such a case, a good portion of internalized CXCL12a should localize to vesicles positive for lysosomal markers, such as the lysosomal-associated membrane protein 1 (LAMP-1). To test this, we transplanted cells expressing CXCR7 and a fusion of LAMP-1 to mCherry into CXCL12a-EGFP expressing embryos, and indeed found a considerable accumulation of CXCL12a in LAMP-1-mCherry labelled lysosomes (Figure 10E). We also used the commercially available LysoTracker reagent to label lysosomes during our experiments. Lysosomal labeling with LysoTracker was not as effective as the LAMP-1-mCherry fusion protein, yet we were able to confirm that CXCR7-mediated uptake directs CXCL12a to lysosomal degradation (Figure 11).

Since we detected apparent targeting of CXCL12a to lysosomes after CXCR7-mediated uptake, we investigated whether this degradation could affect the availability of extracellular CXCL12a. CXCR4b is internalized upon sustained high CXCL12a levels<sup>166</sup>, and thus can be used as a probe for extracellular CXCL12a levels. We first addressed this point *in vitro*, and produced CXCL12a-conditioned medium by transfecting human embryonic kidney cells (HEK293) with expression plasmids coding for CXCL12a (Figure 12A). We then created reporter cells by expressing CXCR4-Ypet (a yellow-fluorescent protein fusion) in HEK293 cells. In agreement with the published data<sup>166</sup>, incubation of the CXCR4-EGFP reporter cells with CXCL12a-conditioned medium induced internalization of the receptor. We reasoned that incubating the CXCL12a-conditioned medium with HEK293 cells expressing CXCR7 would remove a considerable portion of CXCL12a from the medium. This reduction of CXCL12a levels should then manifest in reduced receptor internalization in the CXCR4 reporter cells. Indeed, HEK293 cells expressing CXCR7 reduced the ability of CXCL12a-conditioned medium to induce CXCR4 internalization (Figure 12B-E). Specifically, pretreatment of the conditioned medium with cells expressing CXCR7 drastically reduced the internalization of CXCR4b in the reporter cells (56.3% of cells showed internalization, compared to medium pretreated with cells transfected with empty expression vectors, Figure 12D). On the other hand, pretreatment of the medium with cells expressing CXCR4b only mildly reduced CXCR4b internalization (87.5% as compared to control, Figure 12C).

In a similar manner, we tested the effect of CXCR7 expression on extracellular CXCL12a levels *in vivo*. We directed expression of CXCR4b-EGFP to PGCs, and investigated the localization of the fusion protein upon CXCR7 knockdown (Figure 12F). In line with the *in vitro* approach, we observed a strong reduction of CXCR4b localization to the plasma membrane in *cxcr7* morphants. Furthermore, the internalization of CXCR4b was

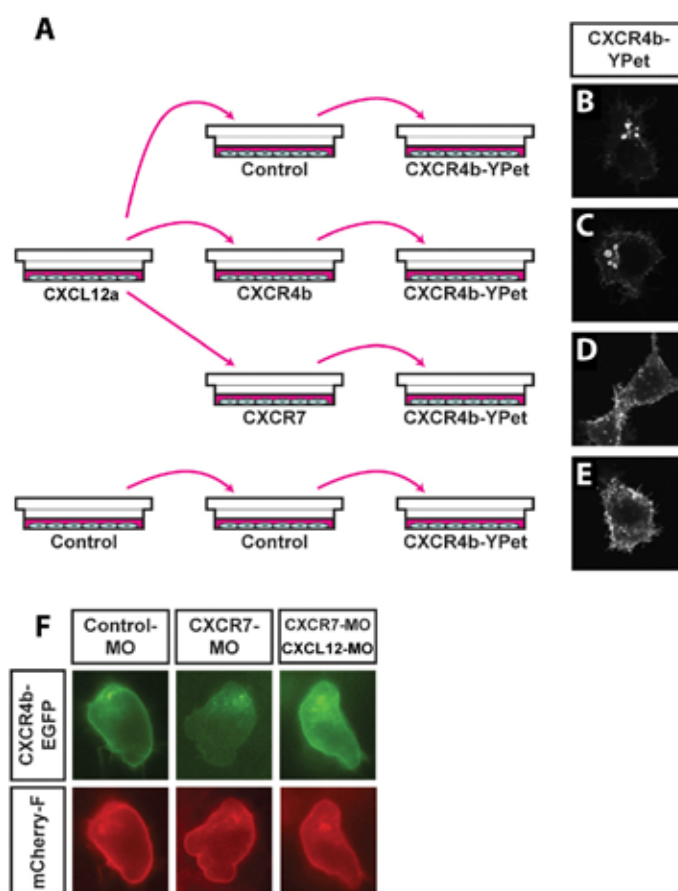


**Figure 12. Cells expressing CXCR7 reduce extracellular CXCL12a levels *in vitro*.**

(A-E) CXCR7-expressing cells reduce extracellular CXCL12a levels *in vitro*. (A) Graphic illustration of the experiments designed to examine the depletion of CXCL12a from conditioned medium by CXCR7-expressing cells, *in vitro*. See text for detailed description. (B) Strong CXCR4b internalization is observed in cells exposed to medium treated with control cells. (C) Medium depleted by CXCR4b-expressing cells induced CXCR4b internalization in 87.5% of all reporter cells, compared to control. CXCR4b internalization was only observed in 56.3% of cells exposed to medium depleted by CXCR7-expressing cells (D), while medium from cells transfected with empty expression vector did not induce CXCR4b internalization (E).

(F) CXCR7 knockdown increases extracellular CXCL12a levels *in vivo* as judged by internalization of CXCR4b in germ cells. Epifluorescence images of PGCs in 10 hpf wild-type embryos coinjected with CXCR4-EGFP-*nanos*, mCherry-F-*nanos*, and different morpholinos. In control embryos (left panel), CXCR4b (green) localizes to the plasma membrane of PGCs (red). CXCR7 knockdown leads to a reduction of CXCR4b on the membrane (middle panel). Membrane localization of CXCR4b in CXCR7 morphants is restored when CXCL12 is knocked down (right panel).

reversed by simultaneous knockdown of CXCL12a. This not only confirmed that CXCR7 effectively reduced extracellular CXCL12a levels, but also suggested that the effect of CXCR7 knockdown on PGC migration was CXCL12a mediated.

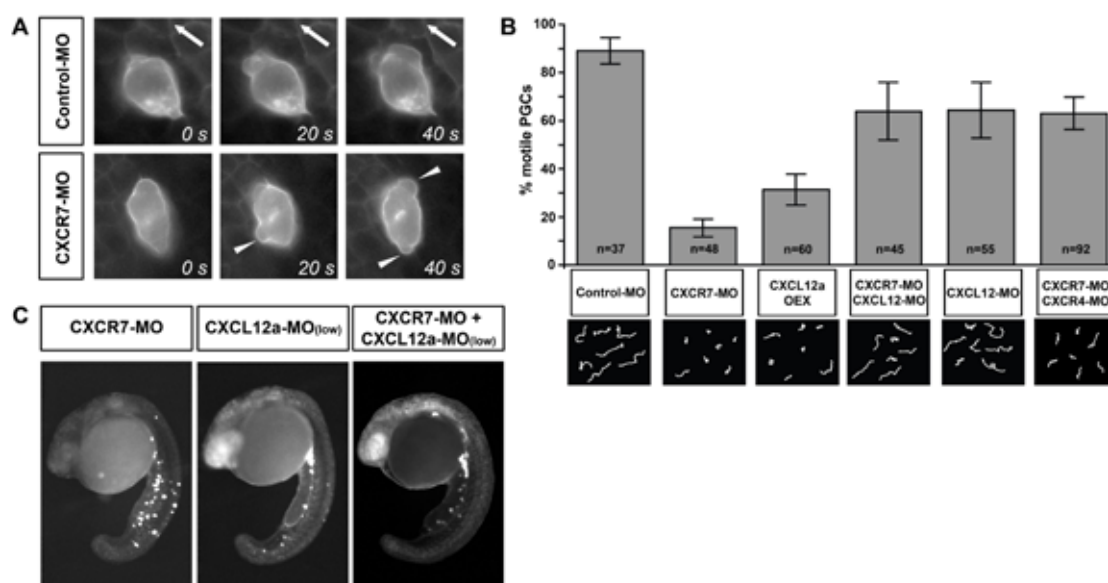


**Figure 13. CXCR7 controls PGC polarity by regulating CXCL12 levels.**

(A) CXCR7 knockdown reduces the polarity of migrating germ cells. Transgenic embryos with EGFP-F expressing germ cells were injected with control or CXCR7 morpholino. Snapshots of time-lapse movies of migrating wild-type PGCs show a typical polarization of the cells with protrusions at the leading edge in the direction of migration (upper panel, arrows). PGCs in CXCR7-depleted embryos exhibit reduced polarity with protrusions extended in opposite directions (lower panel, arrowheads).

(B) CXCR7 depletion reduces the motility of PGCs in a CXCL12a-dependent manner. Germ cell migration was followed transgenic embryos with EGFP-F expressing PGCs between 8 and 10 hpf by time-lapse microscopy. PGCs were scored for high motility in various CXCR4, CXCR7 and CXCL12 expression conditions. Examples for migration paths of germ cells are shown and represent 70 minutes of migration. PGCs in CXCR7 morphants exhibit low motility with short tracks that are reminiscent of PGCs migrating in embryos with high uniform CXCL12a expression (CXCL12a-OEX). Removal of CXCL12a and CXCL12b in CXCR7-depleted embryos restores PGC motility to a level that is identical to that in CXCL12-depleted embryos. Similarly, knocking down CXCR4 restores PGC motility in CXCR7 morphants. Injected amounts of morpholino were kept constant by addition of control morpholino. Error bars represent SEM, n signifies the number of cells examined. (C) Reduction of CXCL12a expression suppresses the CXCR7 knockdown phenotype. Wild-type embryos were injected with CXCR7 morpholino, low levels of CXCL12a morpholino, and GFP-*nanos* mRNA to label PGCs. PGC migration defects were scored 24 hpf. The migration phenotype of embryos injected with CXCR7 morpholino (left panel, 66.4±2.8% ectopic cells per embryo, n=30 embryos) is suppressed by coinjection of low levels (0.02 pmol) of CXCL12a morpholino (middle panel: CXCL12a-MO, 29.4±2.6% ectopic cells per embryo, n=22 embryos; right panel: CXCR7-MO and CXCL12a-MO, 36.0±2.0% ectopic cells per embryo, n=63 embryos). Injected amounts of morpholino were kept constant by addition of control morpholino.

### 3.1.6. CXCR7 function is required for the establishment of PGC polarity

Dynamic relocation of the *cxcl12a* expression domain forms the basis for the step-wise attraction of PGCs towards the gonads, but continuous and global reduction of the ligand might be required in order to prevent accumulation of the chemokine. Removal of extracellular CXCL12a by CXCR7 might facilitate the generation of a chemotactic gradient of CXCL12a, whose accumulation in the extracellular space would otherwise

prevent the generation of an instructive chemotactic gradient. In other words, CXCR7 function could be envisioned as a mechanism to erase previous sites of *cxcl12a* expression from a developing embryo. As instructive chemotactic gradients cause a polarization of migrating cells towards the source of the gradient, we analyzed the polarity of PGCs in control and CXCR7-depleted environments (Figure 13). In control morpholino-treated embryos, PGCs migrated directionally and formed protrusions in the direction of their migration (Figure 13A, top panel). In CXCR7 morphants, the ability of the cells to form protrusions in a single direction was largely diminished. These cells moved back and forth, with protrusions pointing into opposite directions (Figure 13A, lower panel). The polarization defects in CXCR7 morphants manifested in a drastic reduction of PGC motility and shortened migratory tracks (Figure 13B) that were partially phenocopied by uniform overexpression of CXCL12a in wild-type embryos. In line with the previous findings, concomitant removal of CXCR7 and CXCL12 or CXCR4 restored PGC motility to basal levels, as observed in the absence of any CXCR4/CXCL12 signaling.

Migration defects observed in CXCR7 morphants thus were likely to be caused by excessive CXCL12a/CXCR4b signaling that impaired establishment of polarity and directional migration. We therefore reasoned that partial reduction of CXCL12a would alleviate the effects of CXCR7 knockdown on PGC migration, while still allowing them to migrate directionally. Indeed, whereas injection of low levels of CXCL12a morpholino alone caused only a mild reduction of PGC migration efficiency, it largely rescued the effect of loss of CXCR7 function (Figure 13C). This confirmed that continuous removal of CXCL12a by CXCR7 was required for the formation of an instructive chemokine gradient and subsequent PGC polarization.

### **3.1.7. CXCR7 function does not require the activation of major secondary signaling pathways**

Despite the described effect of CXCR7 knockdown on extracellular CXCL12a levels, we reasoned that CXCR7 could also control PGC migration by creating a secondary signal to the PGCs. Specifically, being expressed on the migratory route of PGCs, CXCR7 activation could cause somatic cells to produce additional signals that allow PGCs to migrate. We therefore checked whether main secondary messenger pathways of chemokine signaling (PI3K signaling and the release of calcium from intracellular stores, see section 1.2.2) were required in somatic cells expressing CXCR7 to allow PGC migration (Figure 14). Using calcium-sensitive dyes, we measured the effect of CXCR7 knockdown on free intracellular calcium levels in cells lining the migratory path of PGCs. We were not able to detect any significant change in intracellular calcium levels (Figure 14A), suggesting that CXCR7 function does not depend on calcium as a second messenger.

Furthermore, we tested the dependency of CXCR7 function on PI3K signaling by incubating embryos in medium containing the selective PI3K inhibitors Wortmannin or LY-294002. To assess the efficacy of PI3K inhibition, we expressed the PIP<sub>3</sub>-binding



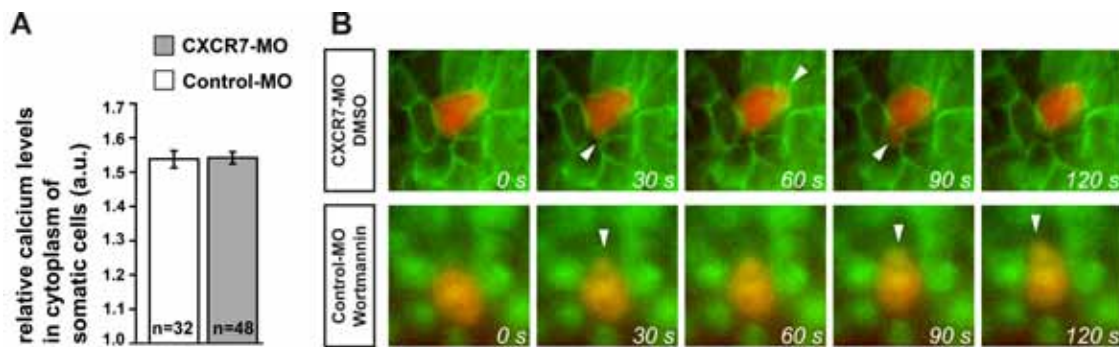


**Figure 14. CXCR7 does not activate major secondary pathways downstream to chemokine signaling.**

(A) CXCR7-depletion does not alter cytosolic calcium levels in somatic cells. Wild-type embryos were injected with CXCR7 or control morpholino, the calcium sensitive dye Dextran Oregon Green BAPTA-1, and *Vasa-DsRedEx-nanos* mRNA. The graph shows the relative calcium levels of somatic cells in the vicinity of migrating PGCs in control and CXCR7-depleted embryos (calculated as described in Experimental Procedures,  $p > 0.1$ , t-test).  $n$  signifies the number of cells examined. Error bars represent SEM. a.u. – arbitrary units.

(B) The effect of CXCR7 knockdown is not caused by absence of PI3K function. Transgenic embryos with *DsRedExpress* expressing PGCs were injected with CXCR7 or control morpholino and *AktPH-EGFP-globin* mRNA. PGC migration between 7 and 10 hpf was followed by high magnification time-lapse microscopy in embryos treated with the PI3K inhibitor Wortmannin (25  $\mu$ M) or DMSO as control. In CXCR7-depleted embryos treated with DMSO PGCs display multiple protrusions in opposing directions (upper panel, arrowheads), typical of CXCR7 inhibition. By contrast, PGCs in control morpholino-injected embryos treated with Wortmannin are polarized, and migrate with protrusions forming in the direction of migration (lower panel, arrowheads). Effective inhibition of PI3K function was monitored by localization of Akt-PH-EGFP. In DMSO-treated embryos (upper panel) the PH-domain localizes to the plasma membrane, whereas PI3K inhibition by Wortmannin induces cytosolic and nuclear translocation of the PH domain (lower panel).

PH-domain of Akt fused to EGFP. Normally, PI3K converts  $PIP_2$  in the plasma membrane to  $PIP_3$  and thereby localizes Akt-PH-EGFP to the plasma membrane (Figure 14B, top panel). Upon loss of PI3K activity the endogenous  $PIP_3$  pool is rapidly dephosphorylated, leading to a translocation of Akt-PH-EGFP to cytosol and nucleus (Figure 14B, lower panel). Both drugs were able to induce the translocation of the Akt-PH domain to the cytosol, but prolonged incubation of embryos in LY-294002 induced disintegration of the embryos. By contrast, Wortmannin-treated embryos were stable enough for prolonged microscopy.

Inhibition of PI3K had been previously been reported to affect PGC migration, specifically speed of migration<sup>238</sup>. However, we did not observe any of the above-mentioned phenotypes generated by CXCR7 knockdown, namely, the inability of PGCs to polarize (Figure 14 B, top panel) did not occur in Wortmannin-treated embryos (Figure 14B, lower panel). Thus, CXCR7 did not require the tested secondary signaling pathways to control PGC migration, suggesting that the receptor's main function in this context was the removal of extracellular CXCL12a ligand.

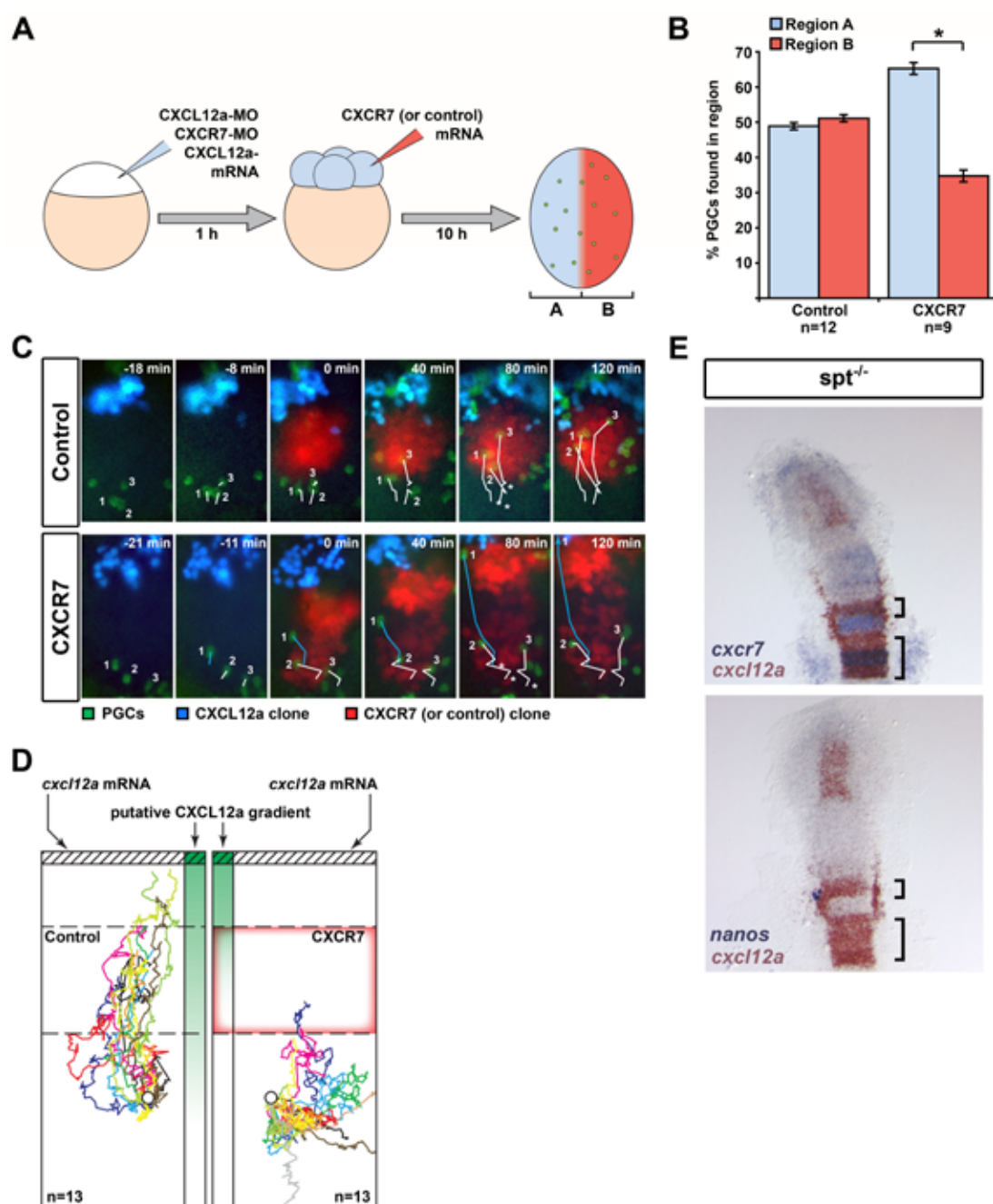


**Figure 15. CXCR7 affects directionality of germ cell migration *in vivo*.**

(A-B) PGCs vacate CXCR7-expressing tissues in embryos expressing CXCL12a uniformly. (A) A schematic representation of the experimental manipulations, generating a CXCR7 expression domain (red) superimposed on uniform CXCL12a expression (blue). Refer to the text for a detailed description. Germ cells were identified by EGFP-F expression and assigned to either the blue expression domain (devoid of CXCR7) or the red expression domain (expressing CXCR7 or control). (B) While in control experiments, PGCs did not display a preference for either domain, germ cells vacated the CXCR7-expressing tissue (p-value < 0.001, t-test). n signifies the number of embryos examined and error bars represent SEM.

(C-D) CXCR7-expressing tissues alter the path of directional PGC migration. Cells from 4 hpf wild-type embryos injected with CXCL12a-*globin* mRNA were transplanted into 6 hpf transgenic embryos with EGFP-F expressing germ cells, injected with CXCL12a and CXCL12b morpholinos. After initiation of PGC migration towards CXCL12a, cells from wild-type embryos injected with CXCR7-*globin* and mCherry-F-*globin*, or mCherry-F-*globin* mRNA alone, were transplanted into the path of migrating PGCs. (C) Snapshots of representative time-lapse movies with germ cells (green) migrating towards a transplanted source of CXCL12a (blue) in CXCL12-deficient

### 3.1.8. Localized CXCR7 expression shapes chemotactic CXCL12a gradients

Uniform expression of *cxcr7* in the first hours of development created the basis for the formation of an instructive chemotactic gradient. Constant removal of CXCL12a from the extracellular environment ensured that the chemokine concentration was highest in tissues actually expressing it. However, *cxcr7* expression adopted more specific expression patterns in later stages, which could imply a role of CXCR7 in shaping of CXCL12a gradients by creating local barriers for CXCL12a diffusion.

To test this idea, we first assessed whether *cxcr7* expression alone was capable of creating a gradient of CXCL12a in a uniform *cxcl12a* expression domain. For this purpose we engineered embryos that uniformly expressed CXCL12a and forced CXCR7 expression in only one half of the embryo. As shown in Figure 15A, we injected transgenic embryos with PGCs expressing EGFP-F with CXCR7 and CXCL12a morpholino. Additional coinjection of H1M-EGFP-*globin* and morpholino-resistant CXCL12a-*globin* mRNA created uniform CXCL12a expression, which was controlled by uniform nuclear labeling. At the 4-cell stage, CXCR7-*globin* and mCherry-F-*globin* mRNA (or mCherry-F-*globin* alone in control experiments) were injected into one of the four blastomers. This forced expression of CXCR7 in one half of the embryo, as visualized by red fluorescence of mCherry. The position of PGCs after 11 hpf served as readout of the CXCL12a gradient across an embryo. While control embryos displayed an equal distribution of PGCs to both halves of an embryo, this distribution was skewed in embryos expressing CXCR7 (Figure 15B). This indicated that CXCR7 is able to impose an instructive CXCL12a gradient on a uniform field of CXCL12a expression.

In addition to creating local gradients, CXCR7 function might also completely separate CXCL12a expression domains from each other, thereby forcing cells to change their migratory route to another source of CXCL12a. We tested this hypothesis by closely

---

embryos. A transplant of cells (red) expressing either CXCR7 or control protein was placed at the migration path. In control experiments (upper panel), germ cells (labelled with numbers 1 to 3) readily traverse the transplant towards the source of CXCL12a (white tracks, asterisks denote the starting points). When encountering a CXCR7-expressing transplant (lower panel), the migration towards the CXCL12a source is inhibited (cells 2 and 3, white tracks). Cells that do not encounter CXCR7-expressing cells on their migration path (cell 1) are not affected and arrive at the CXCL12a expression site (blue track). (D) Multiple migration tracks of germ cells encountering a control transplant (dashed box) or a transplant expressing CXCR7 (red box outline). Tracks have been corrected for morphogenetic movements and were given a common starting coordinate (circle). The CXCL12a transplant was positioned to the upper (hatched box), with the putative gradient of CXCL12a protein (green shadow) pointing upwards. *n* signifies the number of cells examined. Tracks represent 150 minutes of PGC migration.

(E) Regions expressing *cxcl12a* fail to attract PGCs if the expression overlaps with that of *cxcr7*. Two-color *in situ* hybridization on 13hpf *spt<sup>-/-</sup>* embryos using *cxcr7* (blue) and *cxcl12a* (red) probes (upper panel), and *nanos1* (blue) and *cxcl12a* (red) probes (lower panel).

following the migration of PGCs towards a transplant of cells expressing CXCL12a in otherwise CXCL12-deficient embryos (Figure 15C). Shortly after transplantation, PGCs polarized and migrated towards this source of CXCL12a. We reasoned that a group of cells expressing CXCR7 might be able to interfere with the existing chemotactic gradient. When placed in between PGCs and the CXCL12a source, these cells should force the PGCs to change their migratory route towards the source of CXCL12a. When transplanting control cells, PGCs were not distracted from their original course and migrated through the interfering transplant towards the CXCL12a source (Figure 15C, top panel, and D). However, when transplanting cells expressing CXCR7 into the migration path, PGCs were no longer able to migrate towards CXCL12a-expressing cells (Figure 15C, lower panel, and D). Mostly, PGCs initiated a random migration or even retracted from the CXCR7-expressing transplant. In cases where CXCR7-expressing cells did not completely block the route towards CXCL12a-expressing cells, PGCs were still able to reach their target (Figure 15C, blue cell track lower panel).

The previous finding suggested that local expression of CXCR7 could regulate migration of CXCL12a responsive cells in a complex environment with several *cxcl12a* expression domains. To test this idea *in vivo*, we turned our attention to PGC migration in the mutant *spadetail*. In this mutant, PGC clusters were found in ectopic positions at anterior *cxcl12a* expression domains at 24 hpf (Figure 15C, and <sup>156</sup>). Interestingly, this domain consisted of two stripes of *cxcl12a* expression, a small anterior stripe (Figure 15C, small brackets) followed by a much larger posterior stripe at the head-trunk border (Figure 15C, large brackets). Interestingly, PGCs were more often associated with the smaller expression domain than with the larger posterior domain (Figure 15C, upper panel). Strikingly, the posterior domain was shielded by lateral *cxcr7* expression domains and also contained a region of high *cxcr7* expression in the middle of the posterior *cxcl12a* expression site (Figure 15C, lower panel). Thus, CXCR7 could possibly have prevented the migration of PGCs towards the more posterior CXCL12a source and rerouted them towards the more anterior domain.

### 3.1.9. Summary

In this section we investigated the function of the second CXCL12-receptor, CXCR7, in PGC migration. In contrast to the previously characterized CXCR4, CXCR7 lacked PGC-specific expression, but displayed uniform expression during early embryonic development. Nevertheless, loss of CXCR7 function led to a pronounced PGC migration defect. We found that CXCR7 function was not required within PGCs but instead, mediated CXCL12a uptake and degradation by somatic cells. Upon CXCR7 absence, CXCL12 accumulated in the extracellular space and thereby prevented proper PGC polarization and migration towards the gonads. Our results furthermore suggested that CXCR7 could specifically direct migration of cells by creating local chemokine sinks, thereby shaping the instructing gradient.

### 3.2. Differential recognition of two chemokine ligands in zebrafish PGC migration

#### 3.2.1. Zebrafish PGCs are responsive to two CXCL12 ligands

Zebrafish PGCs are guided by the chemokine CXCL12a, but the zebrafish genome also encodes for a paralog, CXCL12b, which shares 85% sequence identity with CXCL12a (excluding the signal peptide, Figure 16A). Although expression pattern analysis did not allow the conclusion that CXCL12b would be required for PGC migration<sup>156</sup>, it had later been suggested to be important for this process<sup>157</sup>. We assessed the effect of CXCL12b knockdown on PGC migration once more, and found that CXCL12b knockdown affected PGC targeting towards the gonads, yet to a much lesser extent than CXCL12a knockdown (Figure 16C-E). This finding suggested that, although PGCs are responsive to both CXCL12 paralog, CXCL12a played a more dominant role in guiding these cells towards their target.

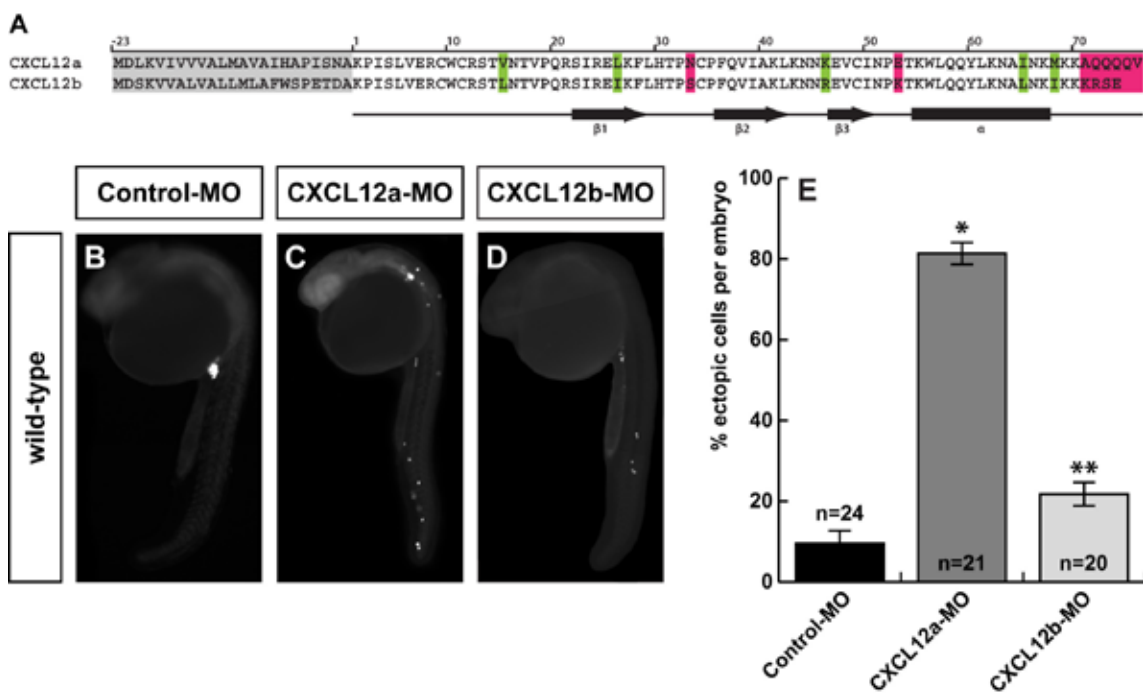


**Figure 16. CXCL12b can function as a guidance cue for PGCs, but is not essential for normal PGC migration.**

(A) SWISSPlot alignment and secondary structure prediction of CXCL12a and CXCL12b. The secretion peptide sequences are marked in grey and are not considered for designation of the amino acid numbers of the actual chemokines. Conservative mutations are marked in green. Non-conservative mutations are marked in magenta. Boxes and arrows mark the predicted sites of  $\alpha$ -helices and  $\beta$ -strands, respectively. Secondary structure prediction was performed using PredictProtein<sup>239</sup>.

(B-E) Reduction of CXCL12b causes mild PGC migration defects. Images of 24 hpf wild-type embryos injected with control (B), CXCL12a (C), or CXCL12b (D) morpholino and GFP-*nanos* mRNA. (E) Graph showing average numbers of ectopic PGCs per embryo in control, CXCL12a, and CXCL12b morpholino-treated embryos. n signifies the number of embryos examined, error bars represent SEM, asterisks denote significance compared to control ( $p < 0.05$ , t-test).

### 3.2.2. Comparative expression analysis of CXCL12 paralogs during early zebrafish development

To determine how *cxcl12b* and *cxcl12a* differed in guiding PGCs towards the gonads, we compared the expression levels and patterns of these genes. We performed comparative *in situ* hybridization, in which probe length and staining procedures were kept identical for both genes in order to minimize variations in signal intensities (Figure 17). During the early phase of PGC migration at 6 hpf, *cxcl12a* expression was found in the germring. At this stage, *cxcl12b* was not expressed at a level detectable by *in situ* hybridization, although it could be detected by RT-PCR<sup>233</sup>. At 8 hpf, *cxcl12b* expression resembled that of *cxcl12a*, with the exception that *cxcl12b* mRNA was not excluded from the dorsal shield. At 9 hpf, both genes were expressed in two lobes projecting away from the midline that reached all around the embryo perimeter. Again, *cxcl12b* transcript was not excluded from the midline, and its two lobes displayed a broader spread compared to *cxcl12a* expression.

With the beginning of segmentation and formation of smites at 10 hpf, the *cxcl12b* expression pattern rapidly separated from *cxcl12a* expression ((Figure 17, middle panels). While the latter concentrated into the lateral plate mesoderm, *cxcl12b* expression was now found along the midline at a slightly lower level, and only weakly in the lateral plate mesoderm. From this point onwards, PGCs were strictly following *cxcl12a* expression in wild-type embryos<sup>36,156</sup>. Consequently, the *cxcl12b* expression pattern of the following stages drastically differed from that of *cxcl12a* expression. Specifically, *cxcl12b* expression at the midline ceased, and very strong expression domains in the head-trunk border and in the forming tail developed ((Figure 17, middle and right panels). Interestingly, throughout segmentation, the lateral plate mesoderm was expressing *cxcl12a* and *cxcl12b*, thus CXCL12b might have taken part in the guidance of trailing clusters towards the gonads. However, the actual region of the developing gonad exhibited reduced *cxcl12b* expression compared to *cxcl12a* ((Figure 17, insets in 18 hpf and 21 hpf).

### 3.2.3. CXCL12a is a more potent ligand than CXCL12b

Until the beginning of somitogenesis, both chemokine genes would be capable to direct PGCs to the lateral plate mesoderm. It was at the beginning of somitogenesis that PGCs obviously followed *cxcl12a* expression rather than *cxcl12b*<sup>156</sup>. At this timepoint, transcript levels of *cxcl12a* in the lateral plate mesoderm increased relative to *cxcl12b* at the midline, which could serve as a simple explanation for the importance of CXCL12a for PGC migration. Despite the fact that staining times of the *in situ* hybridizations were tightly controlled, the signal intensities might not have given an accurate representation of the actual protein expression by these cells. Theoretically, it was thus possible that while both chemokines were expressed at similar levels, their activity on PGC migration still was not equal. To directly compare the effect of expression levels on the ability of the chemokines to attract PGCs, we transplanted cells from embryos injected with various amounts of *in vitro* transcribed CXCL12a-*globin* or CXCL12b-*globin* mRNA into embryos

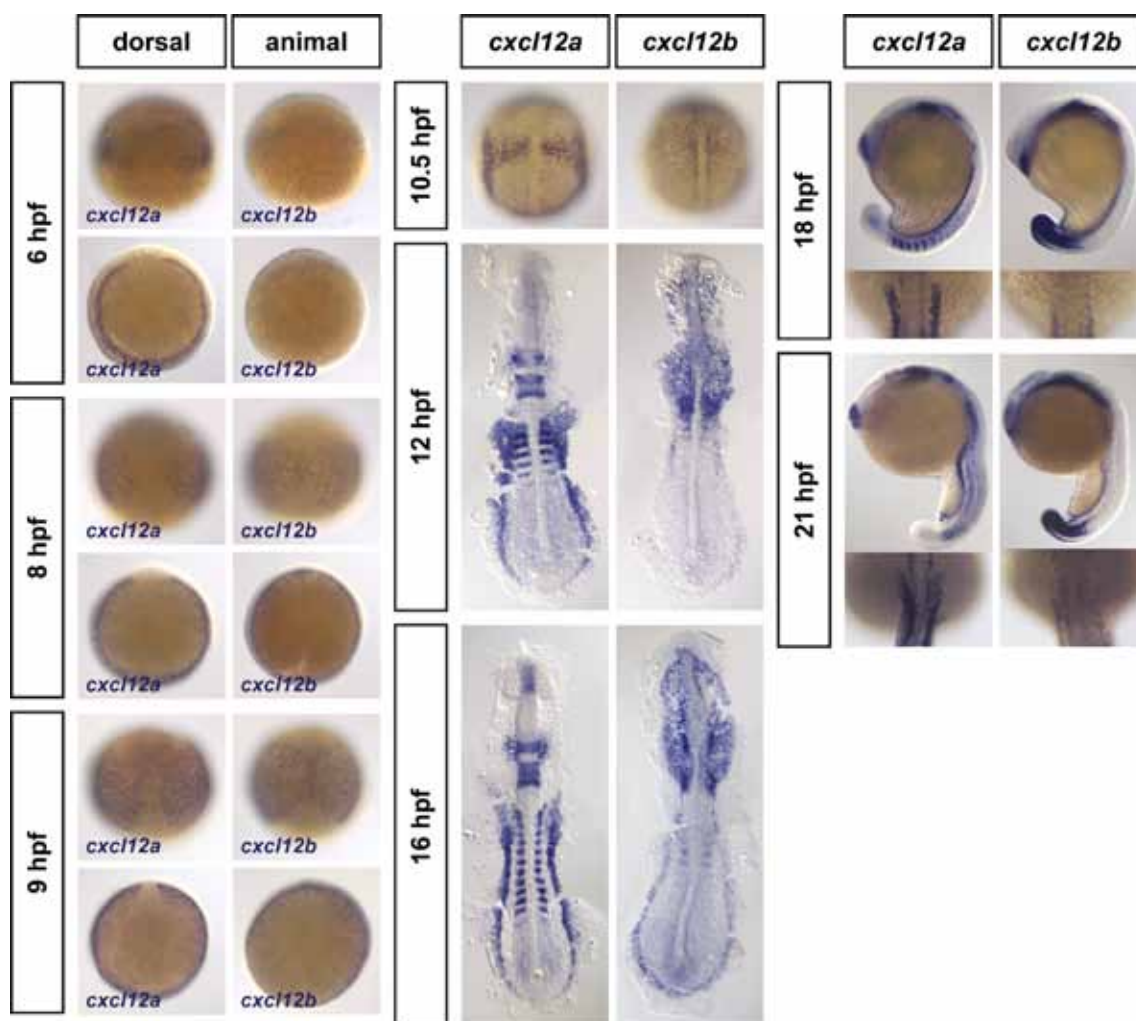


**Figure 17. Comparative expression analysis of the zebrafish *cxcl12* paralogs.**

*In situ* hybridization of wild-type embryos using probes of equal lengths for *cxcl12a* and *cxcl12b*. Left panels: dorsal and animal views of *cxcl12* expression during the first hours of PGC migration. Middle panels: the beginning of embryonic segmentation is accompanied by rapid separation of *cxcl12a* and *cxcl12b* expression. Right panels: Both chemokines are expressed in the lateral mesoderm, leading PGCs towards the developing gonads, with *cxcl12b* being expressed at lower levels (insets).

injected with CXCL12a and CXCL12b morpholinos. Three hours after transplantation, we determined the position of PGCs relative to the transplant by *in situ* hybridization, and found that both chemokine ligands attracted PGCs, with reduced CXCL12b activity at lower amounts of injected mRNA (Figure 18A). Interestingly, this result inferred that CXCL12b is a less potent chemoattractant for PGCs. To confirm this hypothesis, we simultaneously transplanted clusters of cells from embryos injected with equal amounts of either CXCL12a-*globin* or CXCL12b-*globin* mRNA into CXCL12-depleted embryos, and followed the migration of EGFP-labelled PGCs towards these transplants by time-lapse microscopy. In all cases, PGCs preferred to migrate towards cells expressing CXCL12a, traversing cell clusters expressing CXCL12b on their way (Figure 18B). Therefore, when presented to both chemokine ligands at the same time, PGCs distinguished between the two ligands and preferred CXCL12a to CXCL12b.

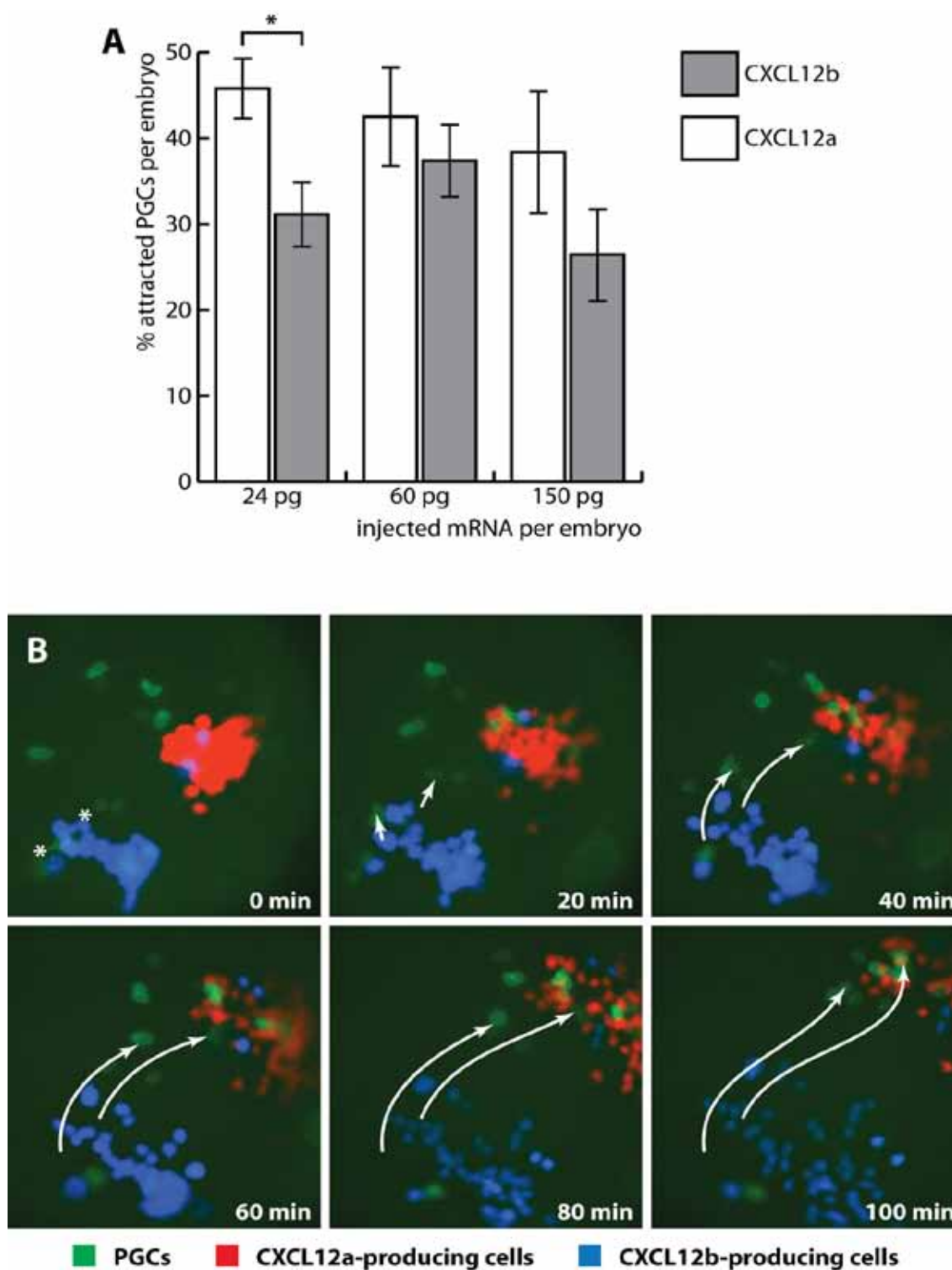


**Figure 18. CXCL12a is a more potent chemoattractant for PGCs compared to CXCL12b.**

(A) Cells expressing different levels of CXCL12a or CXCL12b were tested for their ability to attract PGCs. Cells were transplanted from embryos injected with various amounts of CXCL12a-*globin* or CXCL12b-*globin* mRNA into CXCL12 morphant embryos. The amount of injected mRNA was kept constant by addition of EGFP-F-*globin* mRNA to 300 pg. 3 hours after transplantation, embryos were fixed and stained by two-color *in situ* hybridization for PGCs (*nanos1* probe) and the transplant (*egfp* probe). PGCs in immediate proximity (2 cell diameters) of a transplanted cell were counted as attracted. For CXCL12a, 42, 10, and 11 embryos were examined (24, 60, 150 pg, respectively). For CXCL12b, 13, 15, and 11 embryos were examined (24, 60, 150 pg,



### 3.2.4. A single amino acid determines the chemotactic activity of the zebrafish CXCL12 paralogs

The observation that CXCL12a seemed more potent in attracting CXCL12b was peculiar, as the canonical site for receptor activation, the unstructured N-terminus of the ligand domain, is identical in both chemokine ligands (Figure 18). Thus, the reduced activity of CXCL12b might have been mediated by other biochemical parameters, such as secretion, free ligand diffusion, or receptor activation. To identify the part of the molecule that is responsible for the increased chemotactic activity in CXCL12a, we sought for an *in vivo* test to measure the effect of the few non-homologous amino acids found in CXCL12a and CXCL12b. PGC-specific production of CXCL12a creates a local field of attraction that competes with the normal CXCL12a gradient within the embryo, and was found to cause clustering of PGCs in ectopic locations in the embryos<sup>156</sup> (Figure 28B). We repeated this experiment and found that CXCL12a expression led to a more pronounced migration defect of PGCs compared to CXCL12b or control, thus the effect of a mutation on the activity of CXCL12a could be quickly assessed by counting ectopic PGCs at 24 hpf (Figure 28C). We created chimeric versions of both chemokines, in which we exchanged non-homologous domains or single amino acids, and expressed these specifically in PGCs of wild-type embryos (Figure 19B).

At first, we exchanged the ten most C-terminal amino acids, as this domain exhibits the least homology between the two ligands. However, this C-terminal domain swap was not responsible for the different ligand activity (Figure 19A and C, mutants Cterm 1). We then exchanged the C-terminal half of the ligand domains between CXCL12a and CXCL12b (beginning with leucine 29), and found that this mutation reduced CXCL12a activity to a level of wildtype CXCL12b, and vice versa (Figure 19A and C, mutants Cterm 2). The different activity of the CXCL12 paralogs thus must have been caused by three amino acids differing between CXCL12a and CXCL12b in this region (positions 33, 46, and 53). To exclude the possibility that the differing two amino acids in the N-terminal half of the proteins were involved in chemotactic activity, we exchanged the complete chemokine ligand sequences, leaving only the original secretion peptide (Figure 19A and C, mutants Ligand). These mutants exhibited identical chemotactic activity as the corresponding wild-type proteins and the Cterm 2 mutants, eliminating these two ami-

---

respectively). Error bars represent SEM. The asterisk signifies  $p < 0.01$  (pairwise t-test, comparing activity of CXCL12a versus CXCL12b at the indicated concentration).

(B) In competition with CXCL12a, CXCL12b is not able to attract PGCs. Cells from wild-type embryos injected with equal amounts of either CXCL12a-*globin* or CXCL12b-*globin* mRNA were transplanted into Tol-*kop-egfp-f-nanos* transgenic embryos, injected with CXCL12a and CXCL12b morpholinos. CXCL12a-expressing embryos were labelled by coinjection of Dextran-Alexa568 (red), CXCL12b-expressing embryos were labelled by coinjection of ECFP-*globin* mRNA (blue). Snapshots of low magnification time-lapse movies are shown. The starting position of two representative PGCs (green) are labelled with an asterisk, arrows indicate tracks of migration.

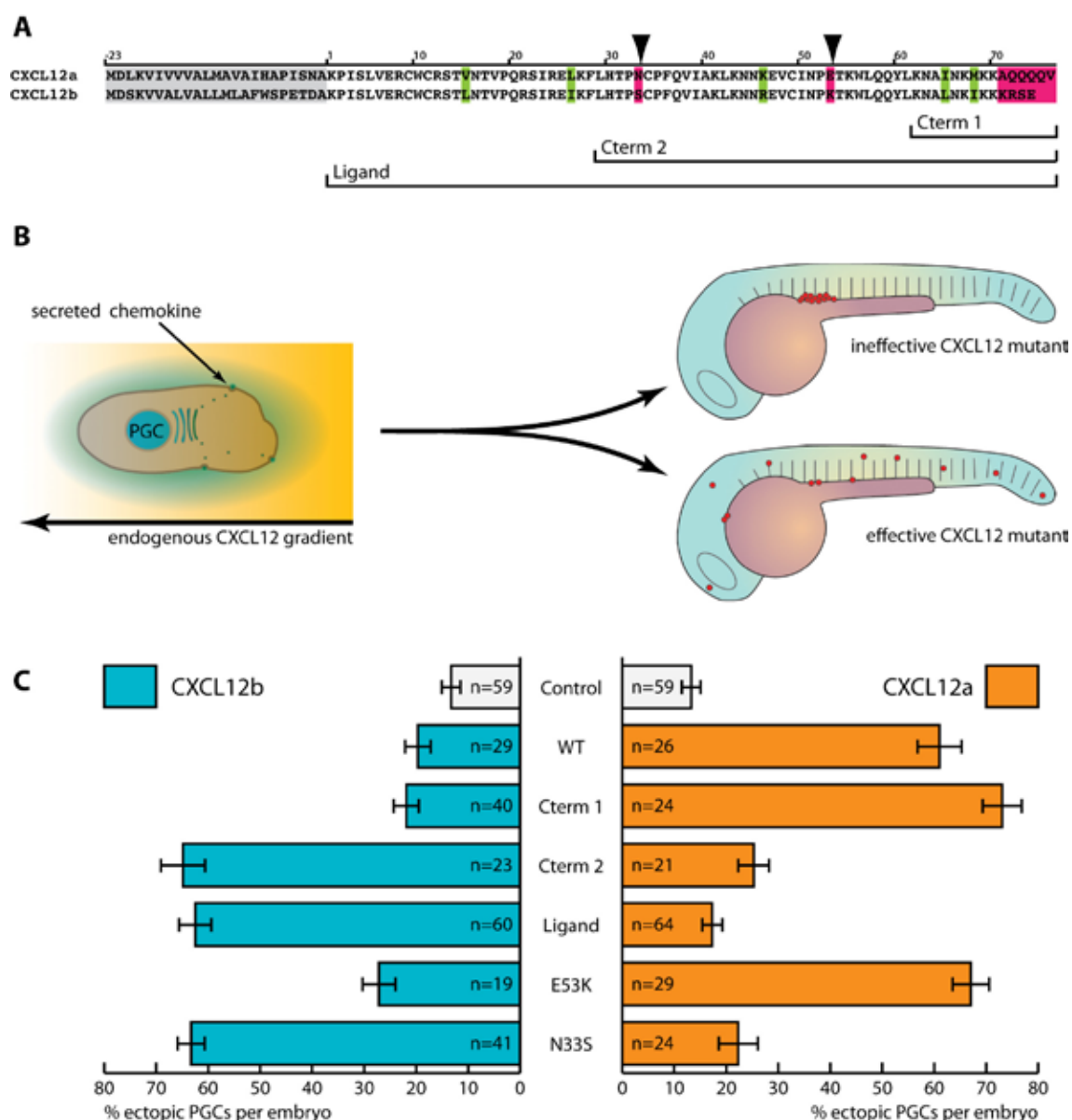


**Figure 19. The chemotactic activity of zebrafish CXCL12 is defined by amino acid position 33.**

(A) Alignment of the amino acid sequence of CXCL12a and CXCL12b, and indication of the domain exchanges (bars below the sequence) and point mutations (arrowheads above the sequence) investigated. The secretion peptide sequences are marked in grey and are not considered for designation of the amino acid numbers of the actual chemokines. Conservative mutations are marked in green. Non-conservative mutations are marked in magenta.

(B) Schematic representation of the experiment. Wild-type embryos were injected with GFP-*nanos* and the mutated CXCL12-*nanos* mRNA of interest. PGCs expressing the CXCL12 mutant formed a local chemotactic field that interfered with the endogenous CXCL12a gradient. At 24 hpf, ectopic PGCs were counted by fluorescence or by *in situ* hybridization, using a *gfp* probe.

(C) Mutagenesis of zebrafish CXCL12 paralogs and expression in PGCs identified amino acid position 33 as crucial for higher chemotactic activity of CXCL12a. The graphs shows average numbers of ectopic PGCs per embryo for control (grey), CXCL12a (orange), and CXCL12b (blue) versions tested. The position of the domains and amino acids mutated are shown in (A), N33S and E53K denote the single-point mutations. n signifies embryos examined, error bars represent SEM.

noacids as effectors on differential chemotactic activity. Additionally, this experiment also excluded the possibility of differential secretion of the chemokines. Next, we investigated those mutations that changed the charge of the aminoacid (serine to asparagine at position 33, and glutamate to lysine at position 53), and found that mutating position 33, but not position 53, reduced the chemotactic activity of CXCL12a to that of CXCL12b and vice versa (Figure 19A and C, mutants N33S and E53K). As the mutant K46R contains a conservative mutation, and the obtained activities for N33S were identical to the corresponding wild-type and Cterm 2 chimeras, we did not investigate this mutation.

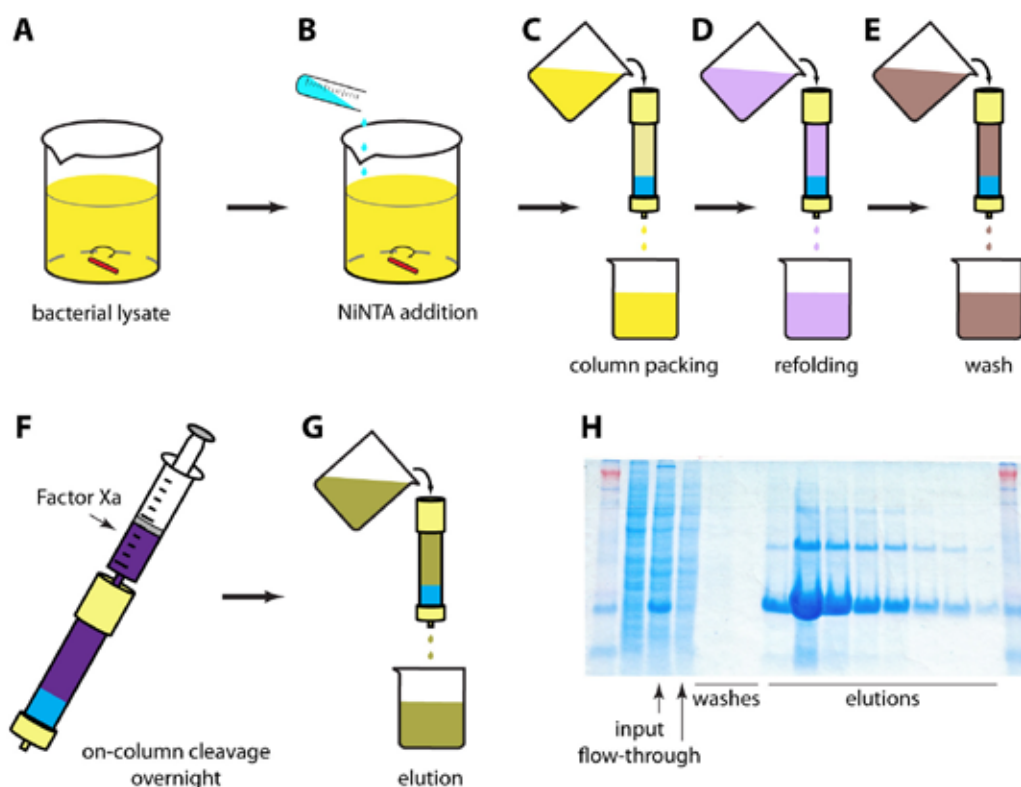
Aminoacid position 33 is located immediately adjacent to the second cystine bridge, in the 30's loop connecting the first and second strand of the antiparallel beta-sheet. In most chemokines this loop is marked by a high degree of flexibility, and a mathematical model had suggested that coordinated movement of this loop and the unstructured N-terminus may be required for activation of human CXCR4<sup>240</sup>. However, this model had not been validated experimentally, thus, we decided to acquire structural information of the CXCL12 paralogs in order to understand the effect of this mutation. Furthermore, we decided to additionally investigate ECM/GAG interactions as these could have influenced chemokine activity.

### 3.2.5. Expression and purification of recombinant zebrafish chemokines

To determine the structure of zebrafish CXCL12 proteins, we expressed and purified wild-type CXCL12a and CXCL12b, and the mutants CXCL12a N33S and CXCL12b S33N from *E. coli*. The *E. coli* BL21 expression host allows high-level expression of chemokines into inclusion bodies<sup>241</sup>, from which the chemokines can be refolded into their native state.

In a first attempt, we followed published procedures in which the chemokines were tagged with an N-terminal hexahistidine tag, which was separated from the chemokine by a Factor Xa cleavage site. Purification of this chemokine from cell lysates was facilitated by metal chelate chromatography under denaturing conditions<sup>242</sup> (Figure 20A-H). The proteins were refolded while bound to the column using a redox buffer system, and release of the chemokine was achieved by on-column cleavage of the protein from the hexahistidine tag. The Factor Xa enzyme used in this step generated a native N-terminus of the chemokine, which is pivotal for proper chemokine function. This method produced large amounts of recombinant protein with some contaminations detectable by Coomassie staining (Figure 20H).

To test the functionality of recombinant CXCL12a and CXCL12b chemokines *in vivo*, we made use of the high affinity of chemokines to glycosaminoglycans. We incubated heparin-coated microspheres with recombinant CXCL12a and CXCL12b protein, and implanted the chemokine-loaded spheres into CXCL12-depleted embryos with fluorescently labelled PGCs (Figure 21). We observed a rapid migration of PGCs towards these beads, indicating that refolding of the proteins was successful. Microspheres incubated



### strategy 1

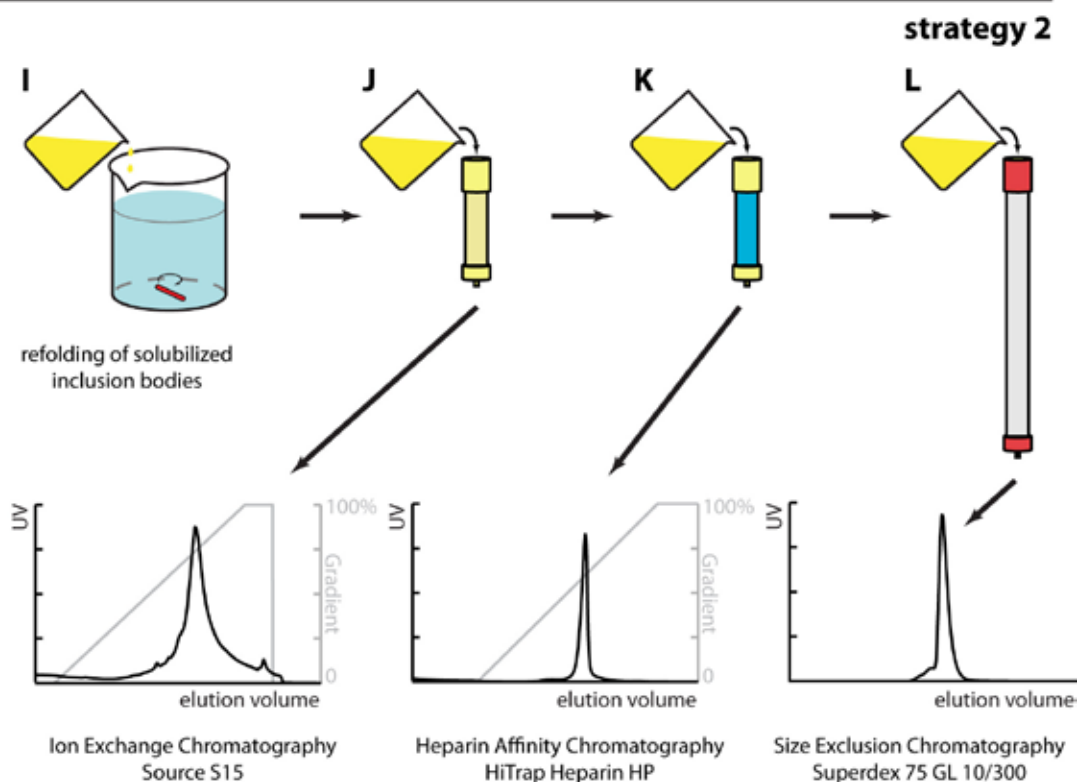


### Figure 20. Chemokine purification strategies.

(A-H) On-column refolding of chemokines from denatured whole-cell lysates using NiNTA batch purification. A representative SDS-PAGE gel is shown. (I-J) 4-step purification of refolded inclusion bodies using FPLC. Representative chromatograms of production steps are shown. Consult text for further details.

in buffer without chemokine did not attract PGCs (data not shown). To further verify this production method, we determined molecular weight, aminoacid sequence, and proper formation of the disulfide bridges using mass spectrometry. Unfortunately, unspecific N- and C-terminal cleavages, improper formation of disulfide bridges, and intermolecular crosslinking was observed in all protein samples (data not shown).

As the observed mix of proteins from the first strategy was unsuitable to perform structural and biochemical studies, we sought for a different purification strategy. In a second attempt, we produced the chemokines without any N-terminal modifications in *E.coli*, and refolded the protein from inclusion bodies using rapid dilution and overnight air oxidation<sup>241</sup> (Figure 20, strategy 2). Following refolding, the positively charged chemokines were purified from contaminants and improperly folded protein using cation exchange and heparin affinity chromatography. Sequence and formation of both disulfide bridges was confirmed using mass spectrometry (data not shown). The proteins were separated from remaining contaminants by size exclusion chromatography. We successfully produced CXCL12a, CXCL12b, and the “CXCL12b-to-CXCL12a” mutant

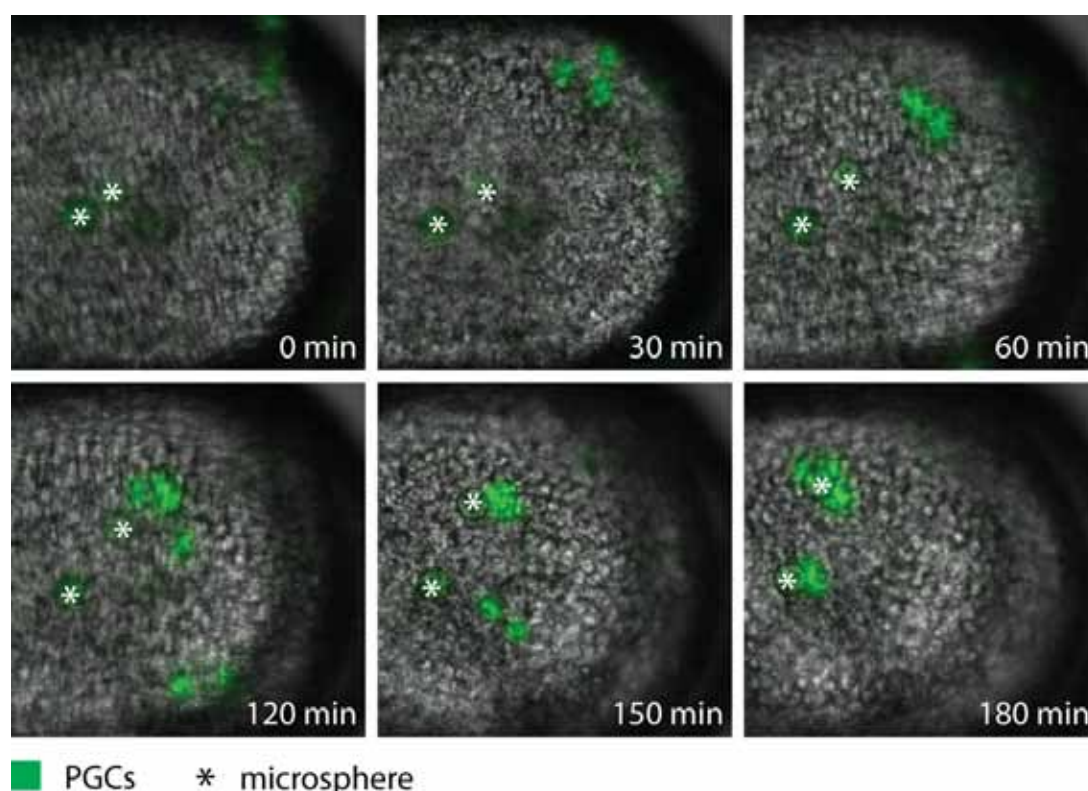


**Figure 21. Delivery of recombinant CXCL12 into zebrafish embryos by implantation of heparin-coated microspheres.**

Representative snapshots of time-lapse movies showing migration of PGCs (green) towards CXCL12-loaded microspheres (marked by asterisks). Heparin-coated microspheres were incubated with 5  $\mu\text{g/ml}$  recombinant CXCL12a or CXCL12b (purification strategy 1) in PBS for 1 h on ice prior to implantation into 6 hpf transgenic embryos with PGC-specific EGFP-F expression, injected with CXCL12a and CXCL12b morpholinos. PGC migration was followed by epifluorescence and brightfield time-lapse microscopy.

protein CXCL12b S33N using this method. The reverse mutant CXCL12a N33S did not fold properly under the conditions used (as determined by mass spectrometry), thus we only used CXCL12b N33S for further experiments. All proteins contained an N-terminal methionine that needs to be removed for chemotaxis experiments. We are currently determining optimal conditions for enzymatic processing of the chemokines. Since NMR spectroscopy and ECM binding studies did not depend on the native N-terminus, these experiments were performed on protein still containing the N-terminal methionine.

### 3.2.6. Structure determination of CXCL12a and CXCL12b indicates oligomerization of the chemokine

In order to identify the structural basis for the reduced chemotactic activity of CXCL12b *in vivo*, we established collaboration with Cedric Laguri and Hugues Lortat-Jacob (Institut de Biologie Structurale Jean-Pierre Ebel, Grenoble, France). Our collaborators investigated the structures of CXCL12a and CXCL12b in solution using NMR spectroscopy. As of today, backbone and side-chain assignment of CXCL12b are in progress, whereas NMR spectra derived from CXCL12a were very difficult to interpret. The difficulties in the assignment of CXCL12a spectra were probably caused by an exchange of monomeric and oligomeric forms of CXCL12a, whereas CXCL12b appeared as a uniform population. This was in line with the observation that in size exclusion chromatography CXCL12a eluted at an earlier timepoint than CXCL12b (Figure 22). Interestingly, CXCL12b S33N eluted at a timepoint that was slightly shifted towards that of CXCL12a, indicating that the decrease in chemotactic activity of CXCL12b could be linked to a change in oligomeriza-

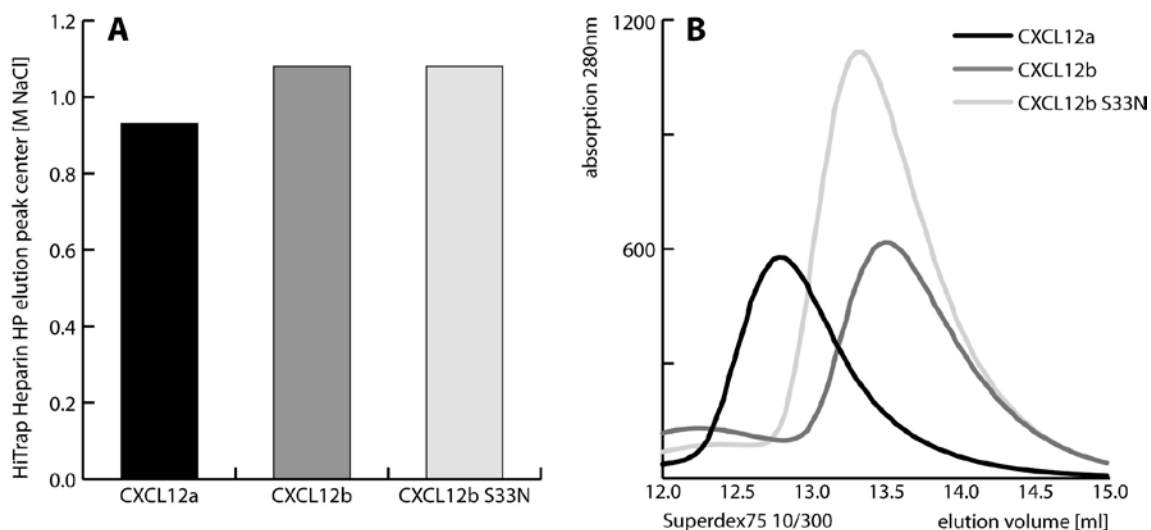


**Figure 22. Properties of recombinant zebrafish CXCL12 protein.**

(A) Comparison of buffer conditions for elution of CXCL12a (black), CXCL12b (dark grey), and CXCL12b S33N (light grey) from heparin affinity columns indicates that CXCL12b and CXCL12b S33N have a higher affinity to heparin compared to CXCL12a. (B) Comparison of elution peak centers of CXCL12a (black line), CXCL12b (dark grey), and CXCL12b S33N (light grey) in size exclusion chromatography indicates a higher apparent molecular weight of CXCL12a, compared to CXCL12b and CXCL12b S33N.

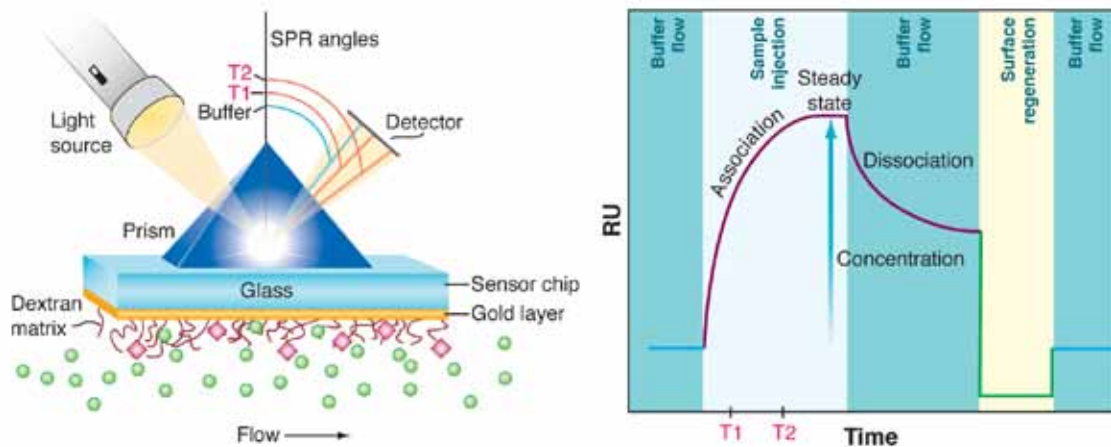


**Figure 23. Illustration of the SPR principle.**

At the left, the optical unit on the sensor chip is shown. A light beam is reflected by the sensor chip, and the angle of deflection is dependent on the mass the molecules bound to the gold layer surface. Binding of the analyte (green spheres) to immobilized ligand (pink diamonds) increases the mass of the sensor chip surface and changes the deflection angle, which is measured in response units (RU) in the SPR sensorgrams to the right. As the concentration of bound analyte increases, the RU reaches a saturation level, whereas upon ligand removal the complexes dissociate and the RU values approach the baseline with time. From these two phases of the sensorgram association and dissociation rates can be derived, the steady state allows the calculation of the dissociation constants by non-linear fitting or Scatchard Plot analysis. Adapted from<sup>243</sup>.

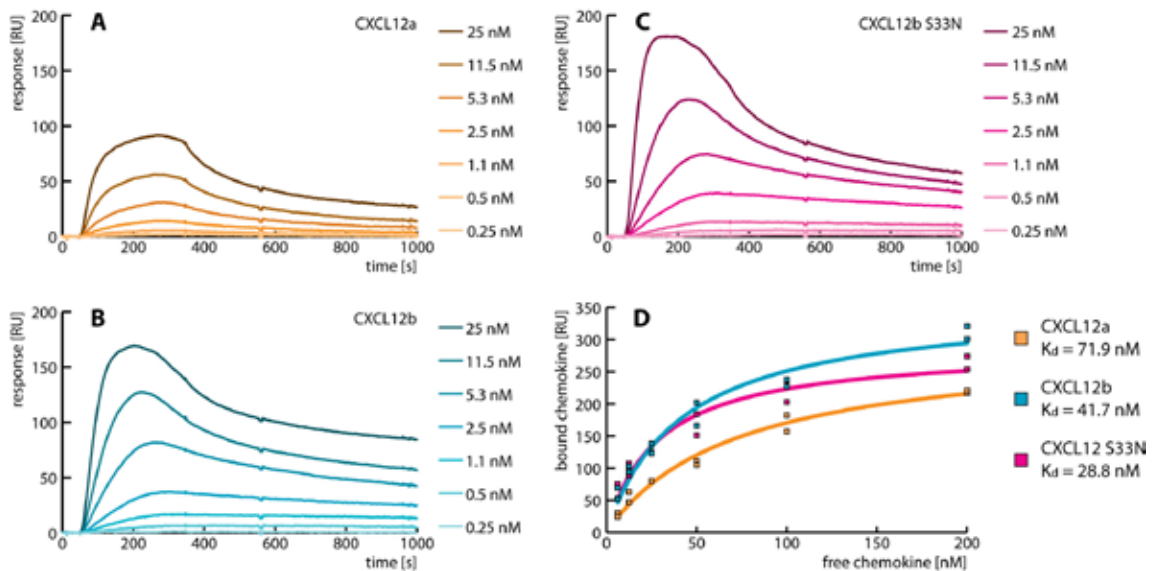


**Figure 24. Increased chemotactic activity of CXCL12b S33N does not depend on GAG affinity.**

Serial dilutions of CXCL12a (A), CXCL12b (B), and CXCL12b S33N (C) were injected at low concentrations into flow cells coated with heparan sulfate. All chromatograms were corrected for unspecific binding by on-line subtraction of the response of untreated reference cells. (D) Numerical fitting of steady state binding values of a wide range of chemokine concentrations injected into flow cells coated with heparan sulfate.  $K_d$  values are indicated in the legend.

tion. To determine the dimer dissociation constants for the zebrafish chemokines, our collaborators performed analytical ultracentrifugation. Although further experiments are required to obtain precise numerical values, preliminary data suggested that CXCL12a and CXCL12b S33N exhibit a higher tendency to form oligomers compared to CXCL12b (data not shown).

### 3.2.7. Zebrafish CXCL12 exhibits very high affinity to GAGs

Chemokine function is highly dependent on the interaction with GAGs *in vivo*<sup>102</sup>. Drastic differences in binding to GAGs might help creating very different diffusion patterns within the developing organism, and thereby render a chemokine as a short-distance or long-distance chemoattractant. Heparin affinity chromatography performed in the purification of all zebrafish chemokines indicated a high affinity to Heparin, yet CXCL12a eluted at lower salt concentration compared to CXCL12b (Figure 22). CXCL12b S33N eluted at the same conditions as CXCL12b, thus the point mutation at aminoacid position 33 was unlikely to affect GAG binding.

To confirm this notion, we used surface plasmon resonance (SPR) technology to investigate the binding parameters of the zebrafish chemokines to GAGs. In SPR the binding of a soluble analyte to a ligand immobilized on the sensor chip surface is measured, and knowledge of the analyte concentration allows the calculation of the dissociation constants, and kinetic association and dissociation rates (Figure 23). We immobilized size-defined heparan sulfate fragments on streptavidin-coated microchips, and injected CXCL12a, CXCL12b, and CXCL12b S33N at physiological concentrations (0.25 to 25 nM). We found high affinity of both wild-type proteins to the GAG surface (Figure 24). Remarkably, CXCL12b displayed extremely slow dissociation of the CXCL12b-GAG complex compared to CXCL12a, which was consistent with higher affinity observed in heparin affinity chromatography (Figure 24). In line with the previous observation, CXCL12b S33N did not display fundamentally altered characteristics in binding to these GAGs, with the exception of a slightly faster dissociation of the complex compared to the very stable CXCL12b-GAG complexes (Figure 24B-C).

Unfortunately, kinetic constants could not be derived from the sensorgrams, as the association curves did not follow standard binding models. We therefore derived the dissociation constants by nonlinear fitting of the steady states against a wide range of concentrations (6.25 to 200 nM, Figure 24D). Similar to heparin affinity chromatography, we found a higher affinity of CXCL12b and CXCL12b S33N to heparan sulfate, compared CXCL12a. We repeated the experiments above with immobilized heparin fragments, and found similar results (data not shown). These results suggested that although GAG interactions differ between CXCL12a and CXCL12b, this might not be required for the enhanced activity of CXCL12a on PGC migration.



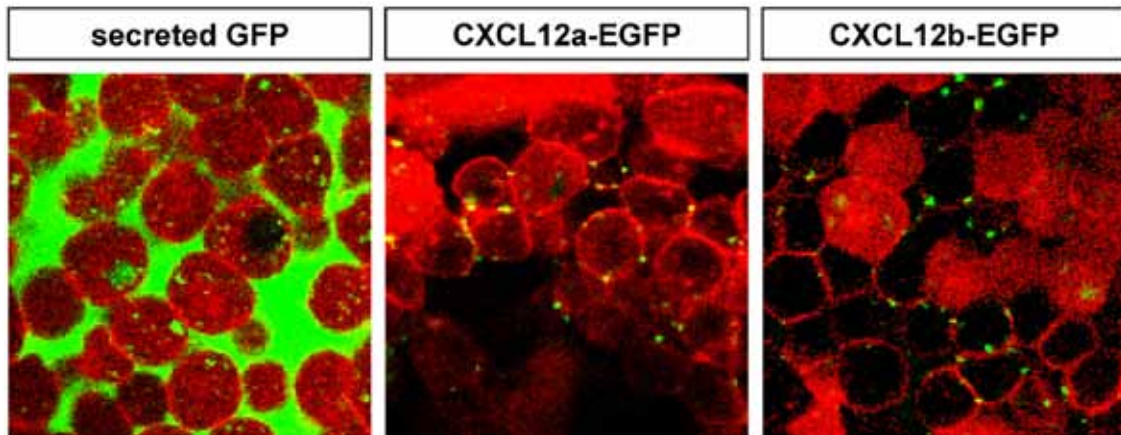


**Figure 25. Accumulation of CXCL12-EGFP protein on cell membranes.**

Confocal sections of gastrulating embryos uniformly expressing GFP secreted by the CXCL12a secretion peptide (left panel), CXCL12a-EGFP (middle panel), or CXCL12b-EGFP (right panel). Wild-type embryos were injected with mCherry-F-*globin* and CXCL12aSP-EGFP-*globin*, CXCL12a-EGFP-*globin*, or CXCL12b-EGFP-*globin* mRNA and observed at 6 hpf.

### 3.2.8. Diffusion of the zebrafish CXCL12 paralogs *in vivo*

In addition to tested GAGs above, the ECM contains many other GAGs and glycoproteins that may bind CXCL12<sup>244</sup>, and the sum of all these interactions might translate into a prominent effect *in vivo*. To test whether the interaction with ECM/GAGs resulted in different diffusion of CXCL12a and CXCL12b, we used the previously described CXCL12a-EGFP and an identically designed CXCL12b-EGFP fusion protein. We injected wild-type embryos with CXCL12a-EGFP-*globin* or CXCL12b-EGFP-*globin* mRNA at levels equimolar to the previously shown attraction experiments (see sections 3.1.8 and 3.2.3), and observed the accumulation of the proteins in 6 hpf embryos. In order to observe diffusion of EGFP alone, we deleted the CXCL12 ligand sequence from the CXCL12a-EGFP-*globin* construct. The resulting construct forces secretion of EGFP by the CXCL12a signal peptide. In line with the high affinity to GAGs measured before, we observed patterns of brightly fluorescent spots on cell membranes in embryos expressing these chemokine-EGFP fusion proteins (Figure 25, middle and right panel). By contrast, in embryos that were producing freely diffusible EGFP protein, EGFP fluorescence uniformly filled the extracellular space. This suggested that both CXCL12 paralogs were primarily bound to ECM components, but not freely diffusing. (Figure 25, left panel). Since CXCL12a and CXCL12b were able to attract PGCs from distant locations in the embryo (Figure 18 and Figure 26), some degree of diffusion of the protein must have occurred. The different affinity of the paralogs to GAGs could have retarded the diffusion of CXCL12b in comparison to CXCL12a, manifesting in a reduced chemotactic activity. To investigate how the proteins diffused from the site of production, we transplanted cells from embryos uniformly expressing CXCL12a-EGFP into transgenic embryos with PGC-specific expression of EGFP-F that were depleted of endogenous CXCL12. We found that, although germ cells were migrating towards the cells expressing CXCL12a-EGFP, we were not able to detect diffusion of CXCL12a-EGFP fusion proteins from these cells

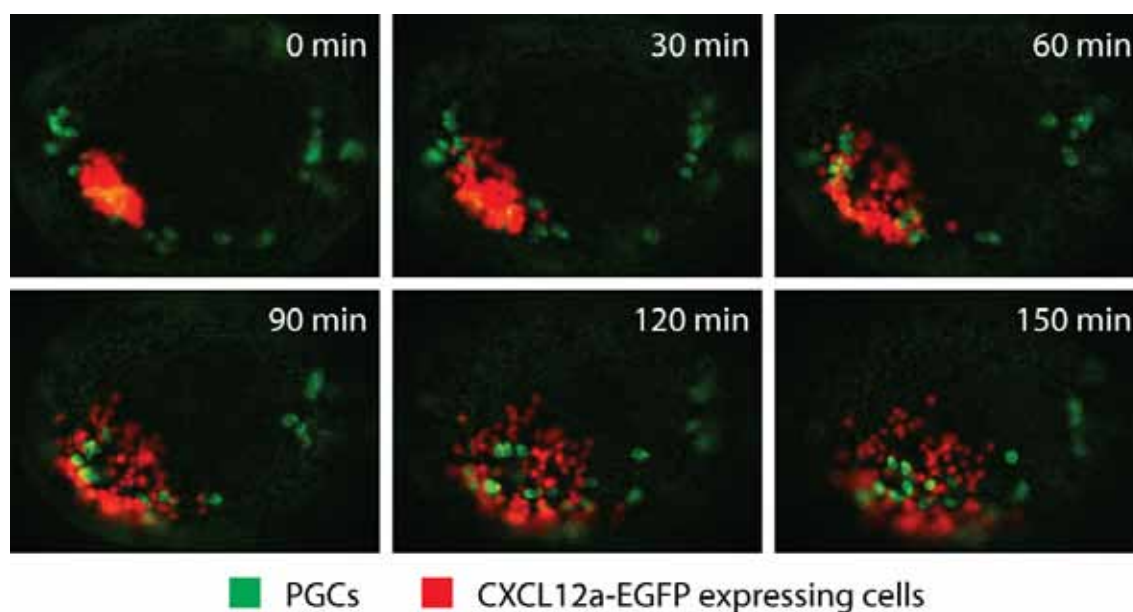


**Figure 26. Diffusion of CXCL12a-EGFP is not detectable by *in vivo* microscopy.** Snapshots of a time-lapse movie showing migration of EGFP-F-labelled PGCs (green) towards transplanted cells (red) expressing CXCL12a-EGFP (green). Cells from 4 hpf wild-type embryos injected with CXCL12a-EGFP-*globin* and mCherry-F-*globin* mRNA were transplanted into 6 hpf transgenic embryos with PGC-specific EGFP-F expression, injected with CXCL12a and CXCL12b morpholino. Migration of PGCs and diffusion of CXCL12a-EGFP was followed by epifluorescence time-lapse microscopy. Although cells migrated towards the transplant, a gradient of CXCL12a-EGFP was not detectable.

(Figure 26, and data not shown). Only accumulations of CXCL12a-EGFP on somatic cell membranes were detected hours after transplantation (data not shown), but at this time PGCs had already arrived at the CXCL12a-EGFP expressing cells. Thus, the concentration of diffusing CXCL12a and CXCL12b protein was below detection limits of *in vivo* microscopy, and only protein accumulations on ECM could be detected.

We also attempted visualization of CXCL12 by immunofluorescence labeling. We implanted cells from embryos expressing CXCL12 proteins fused to C-terminal epitopes (e.g. HA, FLAG) in embryos and stained the proteins using commercially available anti-HA and anti-FLAG antibodies. We also acquired a monoclonal antibody directed against the N-terminus of mammalian CXCL12 (generous gift by F. Arenzana-Seisdedos, Institut Pasteur, Paris, France). All antibodies were able to recognize either epitope-tagged CXCL12a in conditioned medium, or untagged recombinant protein in immunoblots (data not shown). We are currently optimizing procedures to visualize the extracellular protein pool *in vivo*.

### 3.2.9. Measuring CXCR4 binding and activation

Since mathematical modeling on human CXCL12 suggested that the 30's loop harboring the single point mutation was involved in receptor binding and activation, we sought for an experimental system to quantitatively compare receptor affinity and activation potential of the zebrafish chemokines. As previous attempts of our laboratory to establish *in*

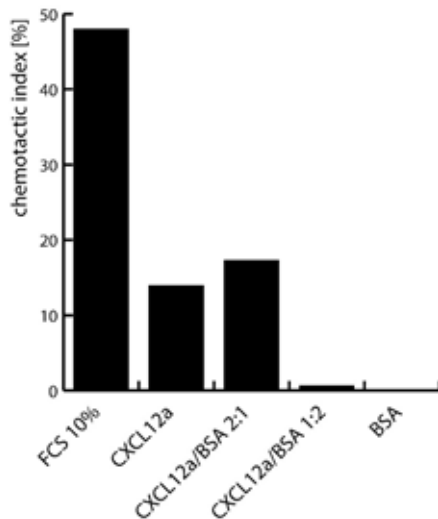


**Figure 27. Migration of NIH/3T3-CXCR4b cells towards CXCL12a-conditioned medium *in vitro*.**

Transiently transfected NIH/3T3 fibroblasts expressing CXCR4b were seeded in transwell filters placed in wells containing DMEM with 10% FCS, dilutions of serum-free medium conditioned by HEK293T cells transiently expressing CXCL12a, and medium containing BSA as control. Migrated cells were counted the next day after plating. The chemotactic index is defined as the number of migrated cells divided by the total number of cells plated. Values of CXCL12a-conditioned medium were corrected for basal conditioning by HEK293T cells expressing EGFP.

*in vitro* cultures of zebrafish PGCs were not successful, and recent data suggested that PGC migration requires cell-cell contacts for migration (Kardash *et al.*, submitted), we tested whether expression of zebrafish CXCR4b in murine fibroblasts would render these cells responsive to zebrafish CXCL12a. We transiently expressed CXCR4b in NIH/3T3 cells (NIH/3T3-CXCR4b) and tested their ability to migrate towards medium conditioned by HEK293T cells expressing zebrafish CXCL12a using transwell filter assays. We observed a dose-dependent migratory response of NIH/3T3-CXCR4b cells to CXCL12a-conditioned medium (Figure 27), but no response to medium containing BSA. These findings indicated that this heterologous expression system was suitable for further studies. As variations in transfection efficiency would influence the results, we decided to create cell lines stably expressing epitope-tagged versions of CXCR4b. We are currently validating the cell lines for stable expression of the transgenes.

### 3.2.10. Enhanced internalization of CXCL12a by CXCR7 *in vivo*

A difference in receptor affinity might also affect CXCR7-mediated removal of CXCL12b compared to CXCL12a (see section 3.1). In order to test this possibility, we transferred somatic cells overexpressing CXCR7 and farnesylated mCherry into embryos uniformly expressing CXCL12b-EGFP or CXCL12a-EGFP and investigated CXCL12 internalization by the transplanted cells. We observed that internalization of CXCL12b-EGFP fusion protein was reduced, compared to that of CXCL12a-EGFP (Figure 28). Thus, CXCL12b binding to CXCR7 could be impaired in a similar manner as proposed for CXCR4b. Therefore, we decided to investigate the internalization of CXCL12 by mammalian cell lines stably expressing zebrafish CXCR7. Currently, we are preparing these cell lines.

### 3.2.11. Summary

In this part we investigated the function of the second CXCL12 paralog, CXCL12b, in PGC migration. We observed that, although not important for PGC guidance towards the gonads, CXCL12b was a functional guidance cue for PGCs. We compared expression

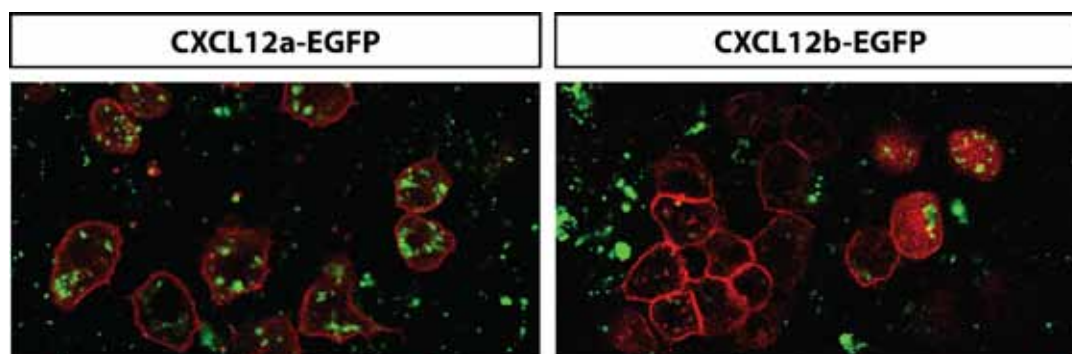


**Figure 28. Reduced internalization of CXCL12b by CXCR7 *in vivo*.**

Confocal sections comparing CXCL12a (green, left panel) and CXCL12b (green, right panel) internalization by CXCR7-expressing cells (red). Cells from 4hpf embryos injected with CXCR7-*globin* and mCherry-F-*globin* mRNA were transplanted into 6 hpf embryos injected with either CXCL12a-EGFP-*globin* or CXCL12b-EGFP-*globin* mRNA. Embryos were analyzed 30 minutes after transplantation.

patterns of both paralogs and found, that until the beginning of segmentation both genes may have functioned together in guiding PGCs towards the lateral plate mesoderm. However, from this point on PGCs followed *cxcl12a* expression towards somatic gonadal precursor cells, and ignored *cxcl12b*. Similarly, when exposed to two ectopic clusters with identical expression levels of either CXCL12a or CXCL12b, PGCs only migrated towards CXCL12a.

We sought for the molecular basis of the differential chemotactic activity of these proteins and identified that amino acid position 33 was responsible for this phenomenon *in vivo*. This amino acid is located in a flexible loop that had been identified to be necessary for receptor binding and activation in mathematical models. To allow *in vitro* biochemical studies on the paralogs and their mutants, we established recombinant production and purification of CXCL12a, CXCL12b, and the “CXCL12a-to-CXCL12b” mutant CXCL12b S33N. We initiated structure determination using NMR spectroscopy of CXCL12a and CXCL12b. While NMR assignment is in progress for CXCL12b, CXCL12a could not be analyzed due to a monomer-oligomer equilibrium of CXCL12a. In agreement with this, CXCL12a exhibited a higher apparent mass compared to that of CXCL12b in size exclusion chromatography. Interestingly, the apparent mass of CXCL12b S33N mutant protein appeared to be only slightly higher than that of CXCL12. This was in conflict with preliminary data from analytical ultracentrifugation experiments, in which CXCL12a and CXCL12b S33N exhibited a higher tendency to oligomerize than CXCL12b.

We also investigated whether differential binding of zebrafish CXCL12 to components of the extracellular matrix might attribute to the decreased chemotactic activity of CXCL12b. *In vitro*, we observed pronounced differences between CXCL12a and CXCL12b in their affinity to glycosaminoglycans, but only marginal differences between CXCL12b S33N and CXCL12b. *In vivo*, we found accumulations of both, CXCL12a and CXCL12b, on cell membranes of somatic cells, but were not able to detect freely diffusing ligand in the extracellular space.

In order to measure the binding and activation of CXCR4b by the CXCL12 paralog *in vitro*, we tested whether transwell filter migration assays using mammalian cell lines expressing zebrafish CXCR4b would be suitable for this purpose. We found that CXCR4b directed NIH/3T3 towards CXCL12a-conditioned medium. We also addressed CXCR7-mediated internalization of CXCL12a-EGFP and CXCL12b-EGFP *in vivo*, and observed a reduction of CXCL12b-EGFP internalization compared to that of CXCL12a-EGFP. To quantify these interactions *in vitro*, we are currently creating and verifying cell lines stably expressing CXCR4b and CXCR7 receptors. Although experiments are still in progress, we believe that the molecular basis for the differential activity of CXCL12a and CXCL12b was caused by a difference in receptor binding and activation, possibly accompanied by a change of oligomerization rate of the ligand.

## 4. Discussion

### 4.1. *CXCR7* functions as a decoy receptor in cell migration

#### 4.1.1. *CXCR7* controls PGC migration by CXCL12a sequestration

Dynamic alterations in the expression pattern of *cxc/12a* guide germ cells towards the developing gonads and PGCs always maintain their position in close proximity to tissues that produce the chemokine<sup>36</sup> (Figure 29, left panels). Two processes could account for the observed tight association of PGCs with *cxc/12a*-transcribing cells. First, the responding cells could be capable of detecting minute differences in the level of the attractant and would therefore continuously migrate to remain within domains of *cxc/12a* transcription, where slightly higher levels of the secreted CXCL12a would be found. In addition to the sensitivity and effective response of PGCs to the signal, processes in the environment could cooperate by controlling the shape of the CXCL12a gradient. For example, continuous clearing of the ligand from somatic tissues would constitute a useful mechanism for achieving migration precision.

In this study, we found that CXCR7, a recently identified receptor for CXCL12, is required for proper PGC migration. Specifically, CXCR7 exerts its effect on PGC guidance by scavenging free CXCL12a ligand from the extracellular space and directing it towards degradation in lysosomes (Figure 10 and Figure 12). This facilitates a continuous reduction of CXCL12a levels, essential for attaining a distribution of CXCL12a that is capable of polarizing PGCs and directing their migration towards cells expressing the mRNA of the attractant (Figure 13). In contrast to CXCR4b, whose internalization regulates the signaling level of the receptor by removing it from the membrane<sup>166</sup>, CXCR7 regulates the signaling level of CXCR4b by reducing the level of CXCL12a in the extracellular environment. In the absence of CXCR7 activity, an increase in the absolute level of CXCL12a and a decrease in gradient steepness would thus interfere with proper directed migration, despite the correct RNA expression pattern (Figure 29, right panels). Whereas anti-CXCL12 staining procedures in zebrafish embryos are currently not yet efficient enough, such a reagent would provide interesting insights into the precise effect of CXCR7 loss of function on the distribution of the chemoattractant in the embryo.

Our hypothesis on CXCR7 function is supported by a recent study of PGC migration in another teleost fish, *medaka*. The authors found that CXCR7 is also not expressed within migrating PGCs, but in tissues surrounding the PGCs, specifically the somites<sup>245</sup>. Similar to PGC migration in zebrafish, *medaka* PGCs cluster in an intermediate position before they move posterior towards the somatic part of the gonads (compare Figure 6D). Interestingly, in *medaka*, this is accompanied by posterior expansion of the *cxc7* expression domain, and the authors have described this process, as if cells expressing CXCR7 pushed PGCs towards the gonads<sup>245</sup>. Local removal of CXCL12a by CXCR7

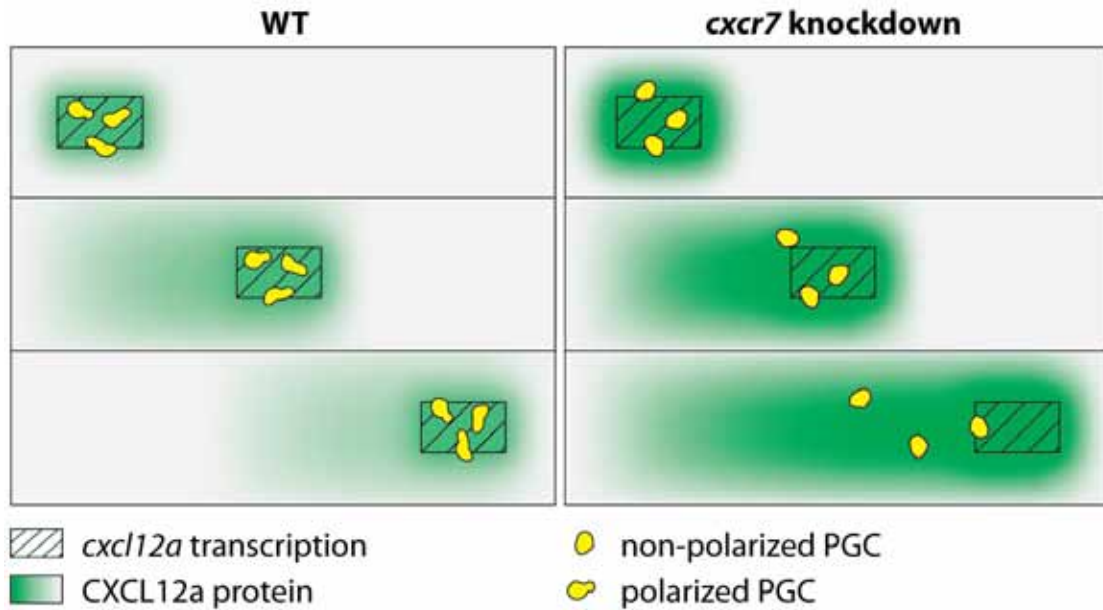


**Figure 29. A model for the role of CXCR7 in PGC migration.**

Morphogenetic movements and changes in expression pattern cause dynamic shifts of *cxcl12a* expression sites (hatched box). Under normal conditions (left panel), CXCR7-mediated removal of CXCL12a facilitates the generation of a sharp gradient (green) allowing the germ cells (yellow) to polarize and migrate towards the site of *cxcl12a* transcription. In the absence of CXCR7 function (right panel), CXCL12a is not cleared efficiently (extended green gradient) resulting in abnormally high CXCL12a levels and inability of germ cells to establish polarity. Consequently, germ cells lose their close association with *cxcl12a* transcription domains.

could account for this observation. Finally, *medaka* PGCs were able to migrate in the direction of the gonad in *cxcr7* mutant embryos, yet a large proportion of cells stopped on their way. This finding is similar as it is depicted in Figure 29, where loss of CXCR7 function creates an extended gradient of CXCL12a, which prevents germ cells to remain in close association with the *cxcl12a* transcription domain.

While the molecular details differ, the suggested mechanism for controlling cell migration by ligand removal is reminiscent to early guidance mechanisms proposed for *Drosophila* and mouse PGC migration to exit the gut (see section 1.3). In both cases, the removal of a survival factor from the surrounding tissues renders these regions repulsive, thereby directing PGCs towards another guidance cue that ultimately guides PGCs towards the gonads. Differing to mouse and *Drosophila*, in which these mechanisms also affect PGC numbers, zebrafish PGC survival and proliferation is not regulated by CXCL12a<sup>156</sup>.

#### 4.1.2. CXCR7 function in the regulation of inflammatory responses

We like to describe CXCR7 function as an effective mechanism to remove “old” CXCL12a, deposited for transient attraction of PGCs during embryonic development. The generation of such a “short-termed memory” for attracting landmarks in the surrounding

of PGCs is reminiscent of the mechanisms observed in the resolution of an inflammatory response. In this case, lymphocytes that were initially attracted towards sites of infections need to be sent back into the blood stream after the pathogens have been cleared from the tissues. Different mechanisms that promote clearing of the attractive signal were identified, and these allow efficient resolution of inflammation and reduction of tissue damage (reviewed in <sup>92,167,246</sup>).

Of particular relevance for this work is chemokine depletion by incompetent-incompetent receptors, which was proposed to account for the function of the anti-inflammatory cytokine IL-10<sup>247</sup>. At the end of inflammation, apoptotic lymphocytes induce the production of IL-10 by macrophages, thereby increasing the expression of chemokine receptors CCR1, CCR2 and CCR5 on mature dendritic cells (DCs). These function exclusively in sequestering the pro-inflammatory chemokines CCL3 and CCL5, and do not induce signaling or chemotaxis. As CXCL12 has been implicated in rheumatoid arthritis and in acute lung injury inflammatory responses (e.g.<sup>248-251</sup>, it would be interesting to examine whether CXCR7 is involved in regulation of inflammation in these tissues. Furthermore, since the CXCL12/CXCR4 pair is involved in other pathological conditions (in particular cancer, e.g. <sup>147,148</sup>) and controls a wide range of developmental and homeostatic activities (e.g. <sup>88,252,253</sup>), examining the role of CXCR7 in these processes would be an important avenue for future research.

#### 4.1.3. CXCR7 – professional decoy or signaling receptor?

Our results provide strong evidence that CXCR7 is a non-signaling receptor that functions as a sink for CXCL12a in the case of PGC migration. This is conflicting with the very first report of CXCR7 that reported CXCR7 alone being able to induce cell migration towards CXCL12 *in vitro*<sup>158</sup>. The idea that CXCR7 is a silent receptor is also pressed by another report, in which CXCR7 was not found to induce calcium mobilization, or migration<sup>159</sup>. However, the authors found that CXCR7 expression increased cell adhesion, which hints towards activation of signaling pathways not required for directional signaling.

Interestingly, CXCR7 and CXCR4b expression is also required for guidance of the zebrafish lateral line primordium<sup>231,254</sup>. The lateral line primordium is a migratory tissue that deposits neuromasts along the zebrafish body axis, while migrating along a stripe of *cxcl12a* expression<sup>254</sup>. Whereas in PGC migration *cxcl12a* expression levels gradually increase towards the target site, this is not the case for the lateral line primordium, and it has been unclear how this uniform expression could polarize the migrating organ. Two recent reports found, that while *cxcr4b* expression is prominent at the migratory front of the organ, *cxcr7* expression is predominantly found in the trailing cells<sup>231,254</sup>. However, both studies have come to different interpretations of the phenotypes observed in embryos knocked down for *cxcl12a*, *cxcr4b*, and *cxcr7b*. Dambly-Chaudière *et al.* suggested that CXCR7 and CXCR4b mutually inhibit their transcription to enforce a gradient of CXCR4b activity on the lateral line. Additionally, CXCR7 and CXCR4b compete for the



same ligand, reducing CXCR4 activity in the back of the organ even further<sup>254</sup>. Valentin *et al.*<sup>231</sup> instead proposed that both receptors are used to sense the gradient of CXCL12a, with different downstream signaling pathways that define front and back of the organ. The growing lists of reports showing that CXCR7 alone is not able to induce signaling<sup>114,159</sup>, reduces the likelihood of Valentin's proposal. Furthermore, the data presented in this work favors the hypothesis of Dambly-Chaudière, in which graded CXCR7 activity establishes the polarity of the lateral line. Yet, according to our model, CXCR7 expression in the trailing cells would impose polarity on the organ by a creating a directional gradient of CXCL12a.

Recently, heterodimerization of CXCR4 and CXCR7, occurring in cells expressing both receptors, has been shown to modulate CXCR4 activity *in vitro*<sup>114</sup>. Again, CXCR7 alone was not found to be able to induce calcium mobilization or G-protein activation. Interestingly, when incorporated into a functional heterodimer with CXCR4, CXCR7 reduced the sensitivity of CXCR4 towards CXCL12, but did not abolish signaling completely. For PGC migration *per se*, this finding does not seem to be of relevance, as *cxcr7* mRNA was not detected in migrating PGCs, and CXCR7-deficient PGCs migrate normally to the gonads (Figure 8). However, we did not assess whether CXCR4 was required for CXCR7 function in somatic tissues. In these tissues, both receptors might be expressed by the same cells (this work and <sup>156</sup>), offering the possibility of heterodimer formation. Nevertheless, we did not detect a requirement for chemokine signaling in somatic cells for PGC migration (Figure 14), and CXCR7-expressing cells in culture did not require CXCR4 in order to remove CXCL12a from conditioned medium. Together, this argues against the necessity of somatic CXCR4/CXCR7 heterodimerization for PGC migration. In case of the lateral line primordium however, the formation of heterodimers in trailing cells could serve as an additional mechanism to keep CXCR4 activity at minimum. Hence, the question whether CXCR7 regulates CXCL12-directed cell migration by acting as a professional decoy, or by reducing CXCR4 activity in functional heterodimers, requires detailed examination of biochemical and cellular responses in the different settings, in which this receptor functions.

## **4.2. Differential recognition of two CXCL12 paralogs in PGC migration**

### **4.2.1. PGCs distinguish between two CXCL12 paralogs**

As previously established<sup>156</sup>, PGCs are guided by the expression of *cxc12a* towards the developing gonad, and *cxc12a* gene knockdown gives rise to a strong migration defect (Figure 16). The zebrafish genome also encodes for another CXCL12 paralog, *cxc12b*. Despite high sequence homology between these ligands, *cxc12b* knockdown causes only mild defects in PGC migration (Figure 16). Primarily, this can be explained by higher expression of *cxc12a* during development (Figure 17). Interestingly, we found that when expressed at equal levels, CXCL12b appears less effective in guiding PGC migration than CXCL12a (Figure 18). This implies that the few amino acids differing between CXCL12a and CXCL12b are important for proper function of CXCL12, and possibly chemokines in general.

### **4.2.2. Structural implications of the 30's loop for the function of CXCL12**

Using chimeric mutants, we identified aminoacid position 33 to be responsible for the increased chemotactic activity of CXCL12a. Located within the flexible 30's loop that connects the first and second  $\beta$ -strand of the CXCL12 chemokine fold, the importance of this amino acid and the 30's loop have not fully been addressed so far. A mathematical model of intramolecular motions of CXCL12 proposes that the 30's loop is important for the activation of CXCR4 by CXCL12<sup>240</sup>. After docking of the N-loop to CXCR4, the 30's loop assists the N-terminus in binding to a deeper binding groove in close proximity to the transmembrane helices of CXCR4. This second binding step induces receptor rearrangement and G protein activation<sup>255</sup>. In line with the idea of differential receptor interaction, we observed reduced levels of CXCR7-mediated internalization for CXCL12b *in vivo*, compared to those of CXCL12a (Figure 28). Making the assumption that CXCR7 and CXCR4 bind CXCL12 in a similar manner, this observation could hint to an impaired binding of the chemokine to the receptor, or a reduced level of receptor activation.

Interestingly, the first crystal structure of human CXCL12 $\alpha$  was based on synthetic CXCL12 $\alpha$  N33A, whose activity was found to be indistinguishable from wildtype CXCL12 $\alpha$  *in vitro*<sup>256,257</sup>. Additionally, zebrafish CXCL12 paralogs lack the RFFESH motif that is required to mediate the first docking of the N-loop to the receptor. Thus, zebrafish CXCL12 may employ a very different mechanism to bind and activate the receptor. Of interest in this aspect could be the viral chemokine-like protein vMIP-II. This viral "chemokine" acts as an unspecific antagonist to many chemokine receptors, amongst them CXCR4<sup>258</sup>. Interestingly, vMIP-II does not require the RFFESH motif to bind CXCR4. Instead, the 30s loop is believed to interact with the N-terminus and not the N-loop to overcome the lack of sequence-specific interactions<sup>240</sup>.

Structure determination of zebrafish CXCL12 is still in progress, yet comparison of the paralogs will be difficult using NMR spectroscopy as prominent oligomerization of CXCL12a prevents proper assignment of the obtained spectra. Thus, inducing mutations that disrupt oligomerization might allow the generation of solution structures for CXCL12a. However, CXCL12a and CXCL12b S33N seem to have a different tendency to form oligomers, compared to that of CXCL12b, thus changing the oligomerization state of CXCL12a may affect receptor activation. Similarly, a recent study on human CXCL12 $\alpha$  has shown that monomeric and dimeric CXCL12 activate CXCR4 to a different extent<sup>107</sup>. Specifically, constitutively dimeric CXCL12 was not able to direct cell migration, despite its ability to induce calcium release. Consequently, a constitutively monomeric form of CXCL12 displayed a much wider range of chemotactic activity than wild-type CXCL12, as it would not oligomerize at higher protein concentrations. Therefore, mutations affecting oligomerization should be used carefully in order to prevent misinterpretation of the results.

As an alternative to NMR spectroscopy, X-ray crystallography may be more successful in gaining insight into structural differences, as the method is not affected by oligomerization. However, the crystal structures might not be able to resolve molecule dynamics, such as the flexibility of the 30's loop, which could be of importance for future research.

#### **4.2.3. CXCL12-GAG interactions in PGC guidance**

In this work, we also investigated the interaction of zebrafish CXCL12 with glycosaminoglycans. These sugar chains in the extracellular matrix are essential for the function of chemokines *in vivo*<sup>102</sup> and GAGs are powerful modulators of the chemokine activity<sup>103</sup>. Both, heparin affinity chromatography and surface plasmon resonance have shown higher affinity of zebrafish CXCL12b and CXCL12b S33N, than observed for CXCL12a to heparan sulfate and the related heparin. Although CXCL12b S33N exhibited less stable chemokine-GAG complexes compared to CXCL12b in SPR measurements, this did not translate to a noticeable difference in heparin affinity chromatography. In line with this finding, the affinity of CXCL12b S33N towards heparan sulfate was more similar to CXCL12b, rather than CXCL12a. Problematic to the SPR measurements is the apparent competition of different oligomeric forms for GAG binding sites. In conjunction with dimerization constants derived by analytical ultracentrifugation, it should be possible to improve the fitting of the experimental data to carefully chosen datasets. Although a more thorough investigation of the GAG interaction using SPR is required to fully characterize the chemokine-GAG interaction, it seems at this point unlikely that GAG interactions are the underlying cause for the increased chemotactic activity of CXCL12a.

#### **4.2.4. Zebrafish embryonic development is an accessible system to study chemokine ligand-receptor networks**

As for CXCL12a and CXCL12b, the zebrafish genome also contains two paralogs for CXCR4, both of which have been found to play a role in cell migration. The paralog CXCR4a controls, for example, the migration of endodermal cells during gastrulation<sup>13,150</sup>. Specifically, CXCL12b expressed by mesodermal cells activates CXCR4a on endodermal cells, which then increases the expression of integrins in these cells. In turn, increased expression of integrins mediates tethering of endodermal cells to the mesoderm. Interestingly, PGCs migrate at the same time through these tissues, yet they are guided by CXCR4b, and follow CXCL12a. Although the expression patterns of both chemokines do not differ drastically at this stage (Figure 17 and <sup>150</sup>), these two cell populations take different actions in response to these similar stimuli. Consequently, CXCL12a knockdown does not affect endoderm migration<sup>13,150</sup>, and CXCL12b knockdown does not disrupt PGC migration (this work). It is thus possible that CXCL12a and CXCL12b also show differential binding and activation of CXCR4a. It would be of interest, whether the same amino acid position is responsible for this phenomenon, as it would imply that the 30's loop is an essential regulator of receptor specificity for chemokines in general.

## 5. Summary and Conclusions

In this work, we have studied the chemokine network guiding primordial germ cells to the developing gonads during zebrafish embryonic development. We showed that, although two similar CXCL12 chemokine ligands are present, the cells are able to distinguish between these signals and prioritize CXCL12a over the conflicting information of CXCL12b. We identified the 30's loop as responsible for this differential chemotactic activity and established the recombinant production of zebrafish CXCL12 paralogs for biochemical characterization. Although the precise mechanisms remain unclear, it appeared that a single amino acid in the 30's loop of the chemokine could define the receptor specificity of the ligand, and thereby allowed precise migration of these cells through a field of conflicting chemotactic gradients.

The formation of these gradients has been another focus of this work. We found that germ cells require a second receptor, CXCR7, for proper migration towards their target. Interestingly, this receptor was not required within the migrating cells themselves, but instead was indispensable in the surrounding cells. In these cells, CXCR7 served as a high affinity decoy for the chemotactic cue, facilitating removal of free CXCL12a from the extracellular space. Thereby, the receptor limited the lifetime of the protein, and allowed formation of an instructive chemokine gradient. Furthermore, we showed that locally restricted expression of this receptor could define chemotactic paths, and created local CXCL12 diffusion boundaries, thereby allowing the separation of different cell types that use the same chemotactic cue.

Chemokine signaling plays numerous roles in many migratory processes, and is especially important in guidance of the immune system to sites of infection. Our findings thus serve as a general model for more complicated migratory mechanisms in higher vertebrates. Future research will focus on the final elucidation of the structural and biochemical differences between the CXCL12 paralogs, and how these are transmitted into distinct cell behavior.

## 6. Bibliography

1. Keller and Danilchik. Regional expression, pattern and timing of convergence and extension during gastrulation of *Xenopus laevis*. *Development* **103**, 193-209 (1988).
2. Warga and Kimmel. Cell movements during epiboly and gastrulation in zebrafish. *Development* **108**, 569-580 (1990).
3. Zhang, Talbot, and Schier. Positional cloning identifies zebrafish one-eyed pinhead as a permissive EGF-related ligand required during gastrulation. *Cell* **92**, 241-251 (1998).
4. Peyri ras, Str hle, and Rosa. Conversion of zebrafish blastomeres to an endodermal fate by TGF-beta-related signaling. *Curr Biol* **8**, 783-786 (1998).
5. Hammerschmidt, Pelegri, Mullins, Kane, Brand, Eeden, Furutani-Seiki, Granato, Haffter, Heisenberg, Jiang, Kelsh, Odenthal, Warga, and Nusslein-Volhard. Mutations affecting morphogenesis during gastrulation and tail formation in the zebrafish, *Danio rerio*. *Development* **123**, 143-151 (1996).
6. Topczewski, Sepich, Myers, Walker, Amores, Lele, Hammerschmidt, Postlethwait, and Solnica-Krezel. The zebrafish glypican knypek controls cell polarity during gastrulation movements of convergent extension. *Developmental Cell* **1**, 251-264 (2001).
7. Myers, Sepich, and Solnica-Krezel. Bmp activity gradient regulates convergent extension during zebrafish gastrulation. *Dev Biol* **243**, 81-98. (2002).
8. Es and Devreotes. Molecular basis of localized responses during chemotaxis in amoebae and leukocytes. *Cell Mol Life Sci* **55**, 1341-1351 (1999).
9. Dormann and Weijer. Chemotactic cell movement during development. *Curr Opin Genet Dev* **13**, 358-364 (2003).
10. Chisholm and Firtel. Insights into morphogenesis from a simple developmental system. *Nat Rev Mol Cell Biol* **5**, 531-541, doi:10.1038/nrm1427 (2004).
11. Haas and Gilmour. Chemokine signaling mediates self-organizing tissue migration in the zebrafish lateral line. *Dev Cell* **10**, 673-680 (2006).
12. P zeron, Mourrain, Courty, Ghislain, Becker, Rosa, and David. Live analysis of endodermal layer formation identifies random walk as a novel gastrulation movement. *Curr Biol* **18**, 276-281, doi:10.1016/j.cub.2008.01.028 (2008).
13. Nair and Schilling. Chemokine signaling controls endodermal migration during zebrafish gastrulation. *Science* **322**, 89-92, doi:10.1126/science.1160038 (2008).
14. Montell. Border-cell migration: the race is on. *Nat Rev Mol Cell Biol* **4**, 13-24, doi:10.1038/nrm1006 (2003).
15. Brabletz, Jung, Spaderna, Hlubek, and Kirchner. Opinion: Migrating cancer stem cells — an integrated concept of malignant tumour progression. *Nature Reviews Cancer* **5**, 744-749, doi:10.1038/nrc1694 (2005).
16. O'Hayre, Salanga, Handel, and Allen. Chemokines and cancer: migration, intracellular signalling and intercellular communication in the microenvironment. *Biochem J* **409**, 635-649 (2008).
17. Mantovani, Allavena, Sica, and Balkwill. Cancer-related inflammation. *Nature* **454**, 436-444 (2008).
18. Viola and Luster. Chemokines and their receptors: drug targets in immunity and inflammation. *Annu Rev Pharmacol Toxicol* **48**, 171-197 (2008).
19. Gaggioli, Hooper, Hidalgo-Carcedo, Grosse, Marshall, Harrington, and Sahai. Fibroblast-led collective invasion of carcinoma cells with differing roles for RhoGTPases in leading and following cells. *Nat Cell Biol* **9**, 1392-1400 (2007).

20. Kucia, Reza, Miekus, Wanzeck, Wojakowski, Janowska-Wieczorek, Ratajczak, and Ratajczak. Trafficking of normal stem cells and metastasis of cancer stem cells involve similar mechanisms: pivotal role of the SDF-1-CXCR4 axis. *Stem Cells* **23**, 879-894 (2005).
21. Naora and Montell. Ovarian cancer metastasis: integrating insights from disparate model organisms. *Nat Rev Cancer* **5**, 355-366 (2005).
22. Balkwill. Cancer and the chemokine network. *Nat Rev Cancer* **4**, 540-550, doi:10.1038/nrc1388 [pii] (2004).
23. Friedl and Wolf. Tumour-cell invasion and migration: diversity and escape mechanisms. *Nature Reviews Cancer* **3**, 362-374, doi:10.1038/nrc1075 (2003).
24. Lukacs. Role of chemokines in the pathogenesis of asthma. *Nat Rev Immunol* **1**, 108-116, doi:10.1038/35100503 (2001).
25. Adler. Chemotaxis in bacteria. *Annu. Rev. Biochem.* (1975).
26. Berg and Brown. Chemotaxis in *Escherichia coli* analyzed by three-dimensional tracking. *Antibiotics and chemotherapy* **19**, 55-78 (1974).
27. Blair. How bacteria sense and swim. *Annu Rev Microbiol* **49**, 489-522, doi:10.1146/annurev.mi.49.100195.002421 (1995).
28. Wadhams and Armitage. Making sense of it all: bacterial chemotaxis. *Nat Rev Mol Cell Biol* **5**, 1024-1037, doi:10.1038/nrm1524 (2004).
29. Rubik and Koshland. Potentiation, desensitization, and inversion of response in bacterial sensing of chemical stimuli. *Proc Natl Acad Sci U S A* **75**, 2820-2824 (1978).
30. Berg and Brown. Chemotaxis in *Escherichia coli* analysed by three-dimensional tracking. *Nature* **239**, 500-504 (1972).
31. Kollmann, Løvdok, Bartholomé, Timmer, and Sourjik. Design principles of a bacterial signalling network. *Nature* **438**, 504-507, doi:10.1038/nature04228 (2005).
32. Falke, Bass, Butler, Chervitz, and Danielson. The two-component signaling pathway of bacterial chemotaxis: a molecular view of signal transduction by receptors, kinases, and adaptation enzymes. *Annual Review of Cell and Developmental Biology* **13**, 457-512, doi:10.1146/annurev.cellbio.13.1.457 (1997).
33. Webre, Wolanin, and Stock. Bacterial chemotaxis. *Curr Biol* **13**, R47-49 (2003).
34. Levit, Grebe, and Stock. Organization of the receptor-kinase signaling array that regulates *Escherichia coli* chemotaxis. *Journal of Biological Chemistry* **277**, 36748-36754 (2002).
35. Parent and Devreotes. A cell's sense of direction. *Science* **284**, 765-770 (1999).
36. Reichman-Fried, Minina, and Raz. Autonomous Modes of Behavior in Primordial Germ Cell Migration. *Developmental Cell* **6**, 589-596 (2004).
37. Gerisch. CyclicAMP and other signals controlling cell development and differentiation in *Dictyostelium*. *Annu. Rev. Biochem.* **56**, 853-879, doi:10.1146/annurev.bi.56.070187.004225 (1987).
38. Parent and Devreotes. Molecular genetics of signal transduction in *Dictyostelium*. *Annu Rev Biochem* **65**, 411-440 (1996).
39. Affolter and Weijer. Signaling to cytoskeletal dynamics during chemotaxis. *Dev Cell* **9**, 19-34 (2005).
40. Devreotes and Janetopoulos. Eukaryotic chemotaxis: distinctions between directional sensing and polarization. *J Biol Chem* **278**, 20445-20448 (2003).
41. Keijzer, Serge, Hemert, and Lommerse. A spatially restricted increase in receptor mobility is involved in directional sensing during .... *Journal of Cell Science* (2008).

42. Endres and Wingreen. Accuracy of direct gradient sensing by single cells. *Proceedings of the National Academy of Sciences* (2008).
43. Xiao, Zhang, Murphy, and Devreotes. Dynamic distribution of chemoattractant receptors in living cells during chemotaxis and persistent stimulation. *J Cell Biol* **139**, 365-374 (1997).
44. Huang, Iijima, Parent, Funamoto, Firtel, and Devreotes. Receptor-mediated regulation of PI3Ks confines PI(3,4,5)P3 to the leading edge of chemotaxing cells. *Mol Biol Cell* **14**, 1913-1922, doi:10.1091/mbc.E02-10-0703 (2003).
45. Franca-Koh, Kamimura, and Devreotes. Navigating signaling networks: chemotaxis in Dictyostelium discoideum. *Curr Opin Genet Dev* **16**, 333-338 (2006).
46. Dormann, Weijer, Parent, Devreotes, and Weijer. Visualizing PI3 Kinase-Mediated Cell-Cell Signaling during Dictyostelium Development. *Curr Biol* **12**, 1178 (2002).
47. Merlot and Firtel. Leading the way: Directional sensing through phosphatidylinositol 3-kinase and other signaling pathways. *J Cell Sci* **116**, 3471-3478 (2003).
48. Haastert and Devreotes. Chemotaxis: signalling the way forward. *Nat Rev Mol Cell Biol* **5**, 626-634, doi:10.1038/nrm1435 (2004).
49. Thelen and Stein. How chemokines invite leukocytes to dance. *Nat Immunol* **9**, 953-959 (2008).
50. Rorth. Collective guidance of collective cell migration. *Trends Cell Biol* **17**, 575-579 (2007).
51. Thiery. Cell adhesion in development: a complex signaling network. *Curr Opin Genet Dev* **13**, 365-371 (2003).
52. Burridge and Chrzanowska-Wodnicka. Focal adhesions, contractility, and signaling. *Annu Rev Cell Dev Biol* **12**, 463-518 (1996).
53. Perris and Perissinotto. Role of the extracellular matrix during neural crest cell migration. *Mech Dev* **95**, 3-21 (2000).
54. Bülow and Hobert. The Molecular Diversity of Glycosaminoglycans Shapes Animal Development. *Annual Review of Cell and Developmental Biology* **22**, 375-407, doi:10.1146/cellbio.2006.22.issue-1 (2006).
55. Handel, Johnson, Crown, Lau, and Proudfoot. Regulation of protein function by glycosaminoglycans--as exemplified by chemokines. *Annu Rev Biochem* **74**, 385-410 (2005).
56. Bateman, Boot-Handford, and Lamandé. Genetic diseases of connective tissues: cellular and extracellular effects of ECM mutations. *Nature Reviews Genetics* **10**, 173-183, doi:10.1038/nrg2520 (2009).
57. Cukierman, Pankov, Stevens, and Yamada. Taking cell-matrix adhesions to the third dimension. *Science* **294**, 1708-1712, doi:10.1126/science.1064829 (2001).
58. Wolf. Compensation mechanism in tumor cell migration: mesenchymal-amoeboid transition after blocking of pericellular proteolysis. *The Journal of Cell Biology* **160**, 267-277, doi:10.1083/jcb.200209006 (2003).
59. Sahai and Marshall. Differing modes of tumour cell invasion have distinct requirements for Rho/ROCK signalling and extracellular proteolysis. *Nat. Cell Biol.* **5**, 711-719, doi:10.1038/ncb1019 (2003).
60. Yang, Tanaka, Jang, Bai, Hayasaka, and Miyasaka. Binding of lymphoid chemokines to collagen IV that accumulates in the basal lamina of high endothelial venules: its implications in lymphocyte trafficking. *J Immunol* **179**, 4376-4382 (2007).
61. Pelletier, Laan, and Hildbrand. Presentation of chemokine SDF-1alpha by fibronectin mediates directed migration of T cells. *Blood* (2000).
62. Patel, Koopmann, Imai, and Whichard. Chemokines have diverse abilities to form solid phase gradients. *Clinical Immunology* (2001).



63. Lint and Libert. Chemokine and cytokine processing by matrix metalloproteinases and its effect on leukocyte migration .... *Journal of Leukocyte Biology* (2007).
64. Struyf, Noppen, Loos, Mortier, Gouwy, Verbeke, Huskens, Luangsay, Parmentier, Geboes, Schols, Damme, and Proost. Citrullination of CXCL12 differentially reduces CXCR4 and CXCR7 binding with loss of inflammatory and anti-HIV-1 activity via CXCR4. *J Immunol* **182**, 666-674 (2009).
65. Proost, Mortier, Loos, Vandercappellen, Gouwy, Ronsse, Schutyser, Put, Parmentier, Struyf, and Damme. Proteolytic processing of CXCL11 by CD13/aminopeptidase N impairs CXCR3 and CXCR7 binding and signaling and reduces lymphocyte and endothelial cell migration. *Blood* **110**, 37-44 (2007).
66. Cox, Dean, Roberts, and Overall. Matrix Metalloproteinase Processing of CXCL11/I-TAC Results in Loss of Chemoattractant Activity and Altered Glycosaminoglycan Binding. *J Biol Chem* **283**, 19389-19399, doi:10.1074/jbc.M800266200 (2008).
67. Sadir. Heparan Sulfate/Heparin Oligosaccharides Protect Stromal Cell-derived Factor-1 (SDF-1)/CXCL12 against Proteolysis Induced by CD26/Dipeptidyl Peptidase IV. *Journal of Biological Chemistry* **279**, 43854-43860, doi:10.1074/jbc.M405392200 (2004).
68. Woolf, Grigorova, Sagiv, Grabovsky, Feigelson, Shulman, Hartmann, Sixt, Cyster, and Alon. Lymph node chemokines promote sustained T lymphocyte motility without triggering stable integrin adhesiveness in the absence of shear forces. *Nat. Immunol.* **8**, 1076-1085, doi:10.1038/ni1499 (2007).
69. Herzmark, Campbell, Wang, Wong, and .... Bound attractant at the leading vs. the trailing edge determines chemotactic prowess. *Proceedings of the National Academy of Sciences* (2007).
70. Wang, Ding, Wang, Jacobs, and Qian. Profiling signaling polarity in chemotactic cells. *Proceedings of the National Academy of Sciences* (2007).
71. Olson and Sahai. The actin cytoskeleton in cancer cell motility. *Clin Exp Metastasis*, **15**, doi:10.1007/s10585-008-9174-2 (2008).
72. Bromley, Mempel, and Luster. Orchestrating the orchestrators: chemokines in control of T cell traffic. *Nat. Immunol.* **9**, 970-980, doi:10.1038/ni.f.213 (2008).
73. Kimmel. Genetics and early development of zebrafish. *Trends in Genetics* **5**, 283-288 (1989).
74. Postlethwait, Yan, Gates, Horne, Amores, Brownlie, Donovan, Egan, Force, Gong, Goutel, Fritz, Kelsh, Knapik, Liao, Paw, Ransom, Singer, Thomson, Abduljabbar, Yelick, Beier, Joly, Larhammar, Rosa, and al. Vertebrate genome evolution and the zebrafish gene map. *Nat Genet* **18**, 345-349 (1998).
75. Zlotnik, Yoshie, and Nomiya. The chemokine and chemokine receptor superfamilies and their molecular evolution. *Genome Biol* **7**, 243 (2006).
76. DeVries, Kelvin, Xu, Ran, Robinson, and Kelvin. Defining the origins and evolution of the chemokine/chemokine receptor system. *J Immunol* **176**, 401-415 (2006).
77. Nomiya, Hieshima, Osada, Kato-Unoki, Otsuka-Ono, Takegawa, Izawa, Yoshizawa, Kikuchi, Tanase, Miura, Kusuda, Nakao, and Yoshie. Extensive expansion and diversification of the chemokine gene family in zebrafish: identification of a novel chemokine subfamily CX. *BMC Genomics* **9**, 222, doi:10.1186/1471-2164-9-222 (2008).
78. Stuart, McMurray, and Westerfield. Replication, integration and stable germ-line transmission of foreign sequences injected into early zebrafish embryos. *Development* **103**, 403-412 (1988).
79. Kawakami, Takeda, Kawakami, Kobayashi, Matsuda, and Mishina. A transposon-mediated gene trap approach identifies developmentally regulated genes in zebrafish. *Dev Cell* **7**, 133-144 (2004).

80. Linney, Hardison, Lonze, Lyons, and DiNapoli. Transgene expression in zebrafish: A comparison of retroviral-vector and DNA-injection approaches. *Dev Biol* **213**, 207-216. (1999).
81. Higashijima, Okamoto, Ueno, Hotta, and Eguchi. High-frequency generation of transgenic zebrafish which reliably express GFP in whole muscles or the whole body by using promoters of zebrafish origin. *Developmental biology* **192**, 289-299 (1997).
82. Heasman. Morpholino oligos: making sense of antisense? *Dev Biol* **243**, 209-214. (2002).
83. Nasevicius and Ekker. Effective targeted gene 'knockdown' in zebrafish. *Nat Genet* **26**, 216-220. (2000).
84. Horuk. Chemokine receptors. *Cytokine & Growth Factor Reviews* **12**, 313-335 (2001).
85. Rossi and Zlotnik. The biology of chemokines and their receptors. *Annu Rev Immunol* **18**, 217-242 (2000).
86. Rollins. Chemokines. *Blood* **90**, 909-928 (1997).
87. Zhu, Yu, Zhang, Nagasawa, Wu, and Rao. Role of the chemokine SDF-1 as the meningeal attractant for embryonic cerebellar neurons. *Nat Neurosci* **5**, 719-720 (2002).
88. Zou, Kottmann, Kuroda, Taniuchi, and Littman. Function of the chemokine receptor CXCR4 in haematopoiesis and in cerebellar development. *Nature* **393**, 595-599, doi:10.1038/31269 (1998).
89. Tachibana, Hirota, Iizasa, Yoshida, Kawabata, Kataoka, Kitamura, Matsushima, Yoshida, Nishikawa, Kishimoto, and Nagasawa. The chemokine receptor CXCR4 is essential for vascularization of the gastrointestinal tract. *Nature* **393**, 591-594, doi:10.1038/31261 (1998).
90. Suratt, Petty, Young, Malcolm, Lieber, Nick, Gonzalo, Henson, and Worthen. Role of the CXCR4/SDF-1 chemokine axis in circulating neutrophil homeostasis. *Blood* **104**, 565-571 (2004).
91. Zlotnik. Chemokines and cancer. *Int J Cancer* **119**, 2026-2029 (2006).
92. Mantovani, Bonecchi, and Locati. Tuning inflammation and immunity by chemokine sequestration: decoys and more. *Nat Rev Immunol* **6**, 907-918, doi:10.1038/nri1964 (2006).
93. Allen, Crown, and Handel. Chemokine: receptor structure, interactions, and antagonism. (2007).
94. Crump, Elisseeva, Gong, Clark-Lewis, and Sykes. Structure/function of human herpesvirus-8 MIP-II (1-71) and the antagonist N-terminal segment (1-10). *FEBS Letters* **489**, 171-175 (2001).
95. Moser, Dewald, Barella, Schumacher, Baggiolini, and Clark-Lewis. Interleukin-8 antagonists generated by N-terminal modification. *J Biol Chem* **268**, 7125-7128 (1993).
96. Elisseeva, Slupsky, Crump, Clark-Lewis, and Sykes. NMR studies of active N-terminal peptides of stromal cell-derived factor-1. Structural basis for receptor binding. *J Biol Chem* **275**, 26799-26805, doi:10.1074/jbc.M003386200 (2000).
97. Amara, Lorthioir, Valenzuela, Magerus, Thelen, Montes, Virelizier, Delepierre, Baleux, Lortat-Jacob, and Arenzana-Seisdedos. Stromal cell-derived factor-1alpha associates with heparan sulfates through the first beta-strand of the chemokine. *J Biol Chem* **274**, 23916-23925 (1999).
98. Johnson, Kosco-Vilbois, Herren, Cirillo, Muzio, Zaratin, Carbonatto, Mack, Smailbegovic, Rose, Lever, Page, Wells, and Proudfoot. Interference with heparin binding and oligomerization creates a novel anti-inflammatory strategy targeting the chemokine system. *J Immunol* **173**, 5776-5785 (2004).
99. Laguri, Sadir, Rueda, Baleux, Gans, Arenzana-Seisdedos, and Lortat-Jacob. The novel CXCL12gamma isoform encodes an unstructured cationic domain which regulates bio-

- activity and interaction with both glycosaminoglycans and CXCR4. *PLoS ONE* **2**, e1110, doi:10.1371/journal.pone.0001110 (2007).
100. Laguri, Arenzana-Seisdedos, and Lortat-Jacob. Relationships between glycosaminoglycan and receptor binding sites in chemokines—the CXCL12 example. *Carbohydr Res* **343**, 2018-2023, doi:10.1016/j.carres.2008.01.047 (2008).
  101. Murphy, Cho, Sachpatzidis, Fan, Hodsdon, and Lolis. Structural and functional basis of CXCL12 (stromal cell-derived factor-1 alpha) binding to heparin. *J Biol Chem* **282**, 10018-10027, doi:10.1074/jbc.M608796200 (2007).
  102. Proudfoot, Handel, Johnson, Lau, LiWang, Clark-Lewis, Borlat, Wells, and Kosco-Vilbois. Glycosaminoglycan binding and oligomerization are essential for the in vivo activity of certain chemokines. *Proc Natl Acad Sci U S A* **100**, 1885-1890 (2003).
  103. Handel, Johnson, Crown, Lau, Sweeney, and Proudfoot. REGULATION OF PROTEIN FUNCTION BY GLYCOSAMINOGLYCANS AS EXEMPLIFIED BY CHEMOKINES. *Annu. Rev. Biochem.* **74**, 385-410, doi:10.1146/biochem.2005.74.issue-1 (2005).
  104. Veldkamp, Peterson, Pelzek, and Volkman. The monomer-dimer equilibrium of stromal cell-derived factor-1 (CXCL 12) is altered by pH, phosphate, sulfate, and heparin. *Protein Sci* **14**, 1071-1081, doi:10.1110/ps.041219505 (2005).
  105. Hoogewerf, Kuschert, Proudfoot, Borlat, Clark-Lewis, Power, and Wells. Glycosaminoglycans mediate cell surface oligomerization of chemokines. *Biochemistry* **36**, 13570-13578, doi:10.1021/bi971125s (1997).
  106. Uchimura, Morimoto-Tomita, Bistrup, Li, Lyon, Gallagher, Werb, and Rosen. HSulf-2, an extracellular endoglucosamine-6-sulfatase, selectively mobilizes heparin-bound growth factors and chemokines: effects on VEGF, FGF-1, and SDF-1. *BMC Biochem* **7**, 2, doi:10.1186/1471-2091-7-2 (2006).
  107. Veldkamp, Seibert, Peterson, Cruz, Haugner, Basnet, Sakmar, and Volkman. Structural basis of CXCR4 sulfotyrosine recognition by the chemokine SDF-1/CXCL12. *Science Signaling* **1**, ra4, doi:10.1126/scisignal.1160755 (2008).
  108. Fermas, Gonnet, Sutton, Charnaux, Mulloy, Du, Baleux, and Daniel. Sulfated oligosaccharides (heparin and fucoidan) binding and dimerization of stromal cell-derived factor-1 (SDF-1/CXCL 12) are coupled as evidenced by affinity CE-MS analysis. *Glycobiology* **18**, 1054-1064, doi:10.1093/glycob/cwn088 (2008).
  109. Crown, Yu, Sweeney, Leary, and Handel. Heterodimerization of CCR2 chemokines and regulation by glycosaminoglycan binding. *J Biol Chem* **281**, 25438-25446, doi:10.1074/jbc.M601518200 (2006).
  110. Nesmelova, Sham, Gao, and Mayo. CXC and CC-chemokines form mixed heterodimers: Association free energies from MD simulations and experimental correlations. *J Biol Chem*, doi:10.1074/jbc.M803308200 (2008).
  111. D'Ambrosio, Panina-Bordignon, and Sinigaglia. Chemokine receptors in inflammation: an overview. *J Immunol Methods* **273**, 3-13 (2003).
  112. Milligan, Ramsay, Pascal, and Carrillo. GPCR dimerisation. *Life Sci* **74**, 181-188 (2003).
  113. Breitwieser. G protein-coupled receptor oligomerization: implications for G protein activation and cell signaling. *Circulation Research* **94**, 17-27, doi:10.1161/01.RES.0000110420.68526.19 (2004).
  114. Levoe, Balabanian, Baleux, Bachelier, and Lagane. CXCR7 heterodimerizes with CXCR4 and regulates CXCL12-mediated G protein signalling. *Blood*, doi:10.1182/blood-2008-12-196618 (2009).
  115. Mellado, Rodríguez-Frade, Vila-Coro, Fernández, Ana, Jones, Torán, and Martínez-A. Chemokine receptor homo- or heterodimerization activates distinct signaling pathways. *Embo J* **20**, 2497-2507, doi:10.1093/emboj/20.10.2497 (2001).

116. Isik, Hereld, and Jin. Fluorescence Resonance Energy Transfer Imaging Reveals that Chemokine-Binding Modulates Heterodimers .... *PLoS ONE* (2008).
117. Rot and Andrian. Chemokines in innate and adaptive host defense: basic chemokines grammar for immune cells. *Annual review of immunology* **22**, 891-928, doi:10.1146/annurev.immunol.22.012703.104543 (2004).
118. Sodhi, Montaner, and Gutkind. Viral hijacking of G-protein-coupled-receptor signalling networks. *Nature Reviews Molecular Cell Biology* **5**, 998-1012, doi:10.1038/nrm1529 (2004).
119. Tian, Lee, Yung, Allen, Slocombe, Twomey, and Wong. Differential involvement of Gα16 in CC chemokine-induced stimulation of phospholipase Cβ, ERK, and chemotaxis. *Cell Signal* **20**, 1179-1189, doi:10.1016/j.cellsig.2008.02.014 (2008).
120. Jones, Peak, Brader, Eccles, and Katan. PLCγ1 is essential for early events in integrin signalling required for cell motility. *J Cell Sci* **118**, 2695-2706 (2005).
121. Busillo and Benovic. Regulation of CXCR4 signaling. *Biochimica et Biophysica Acta (BBA) - Biomembranes* **1768**, 952-963, doi:10.1016/j.bbamem.2006.11.002 (2007).
122. Wei, Wang, Chen, Ouyang, Song, and Cheng. Calcium flickers steer cell migration. *Nature* **457**, 901-905, doi:10.1038/nature07577 (2009).
123. Franco and Huttenlocher. Regulating cell migration: calpains make the cut. *J Cell Sci* **118**, 3829-3838 (2005).
124. Blaser, Reichmanfried, Castanon, Dumstrei, Marlow, Kawakami, Solnicakrezel, Heisenberg, and Raz. Migration of Zebrafish Primordial Germ Cells: A Role for Myosin Contraction and Cytoplasmic Flow. *Developmental Cell* **11**, 613-627, doi:10.1016/j.devcel.2006.09.023 (2006).
125. Deane and Fruman. Phosphoinositide 3-kinase: diverse roles in immune cell activation. *Annual review of immunology* **22**, 563-598, doi:10.1146/annurev.immunol.22.012703.104721 (2004).
126. Litman, Amieva, and Furthmayr. Imaging of dynamic changes of the actin cytoskeleton in microextensions of live NIH3T3 cells with a GFP fusion of the F-actin binding domain of moesin. *BMC Cell Biol* **1**, 1 (2000).
127. Kay, Langridge, Traynor, and Hoeller. Changing directions in the study of chemotaxis. *Nature Reviews Molecular Cell Biology* (2008).
128. Heit, Robbins, Downey, Guan, Colarusso, Miller, Jirik, and Kubes. PTEN functions to 'prioritize' chemotactic cues and prevent 'distraction' in migrating neutrophils. *Nat. Immunol.* **9**, 743-752, doi:10.1038/ni.1623 (2008).
129. Iijima and Devreotes. Tumor suppressor PTEN mediates sensing of chemoattractant gradients. *Cell* **109**, 599-610 (2002).
130. Comer and Parent. PI 3-kinases and PTEN: how opposites chemoattract. *Cell* **109**, 541-544 (2002).
131. Samuels, Diaz, Schmidt-Kittler, Cummins, Delong, Cheong, Rago, Huso, Lengauer, Kinzler, Vogelstein, and Velculescu. Mutant PIK3CA promotes cell growth and invasion of human cancer cells. *Cancer Cell* **7**, 561-573, doi:10.1016/j.ccr.2005.05.014 (2005).
132. Phillips, Mestas, Gharaee-Kermani, Burdick, Sica, Belperio, Keane, and Strieter. Epidermal growth factor and hypoxia-induced expression of CXC chemokine receptor 4 on non-small cell lung cancer cells is regulated by the phosphatidylinositol 3-kinase/PTEN/AKT/mammalian target of rapamycin signaling pathway and activation of hypoxia inducible factor-1α. *J Biol Chem* **280**, 22473-22481, doi:10.1074/jbc.M500963200 (2005).
133. Fukata. Roles of Rho-family GTPases in cell polarisation and directional migration. *Current Opinion in Cell Biology* **15**, 590-597, doi:10.1016/S0955-0674(03)00097-8 (2003).

134. Ridley, Schwartz, Burridge, Firtel, Ginsberg, Borisy, Parsons, and Horwitz. Cell migration: integrating signals from front to back. *Science* **302**, 1704-1709, doi:10.1126/science.1092053 (2003).
135. Allen, Zicha, Ridley, and Jones. A role for Cdc42 in macrophage chemotaxis. *The Journal of Cell Biology* **141**, 1147-1157 (1998).
136. Allen, Jones, Pollard, and Ridley. Rho, Rac and Cdc42 regulate actin organization and cell adhesion in macrophages. *Journal of Cell Science* **110 ( Pt 6)**, 707-720 (1997).
137. Nobes and Hall. Rho, rac, and cdc42 GTPases regulate the assembly of multimolecular focal complexes associated with actin stress fibers, lamellipodia, and filopodia. *Cell* **81**, 53-62. (1995).
138. Bartolomé, Molina-Ortiz, Samaniego, Sánchez-Mateos, Bustelo, and Teixidó. Activation of Vav/Rho GTPase signaling by CXCL12 controls membrane-type matrix metalloproteinase-dependent melanoma cell invasion. *Cancer Research* **66**, 248-258, doi:10.1158/0008-5472.CAN-05-2489 (2006).
139. Nagasawa, Kikutani, and Kishimoto. Molecular cloning and structure of a pre-B-cell growth-stimulating factor. *Proc Natl Acad Sci U S A* **91**, 2305-2309 (1994).
140. Tashiro, Tada, Heilker, Shirozu, Nakano, and Honjo. Signal sequence trap: a cloning strategy for secreted proteins and type I membrane proteins. *Science* **261**, 600-603 (1993).
141. Nagasawa, Hirota, Tachibana, Takakura, Nishikawa, Kitamura, Yoshida, Kikutani, and Kishimoto. Defects of B-cell lymphopoiesis and bone-marrow myelopoiesis in mice lacking the CXC chemokine PBSF/SDF-1. *Nature* **382**, 635-638. (1996).
142. Bleul, Farzan, Choe, Parolin, Clark-Lewis, Sodroski, and Springer. The lymphocyte chemoattractant SDF-1 is a ligand for LESTR/fusin and blocks HIV-1 entry. *Nature* **382**, 829-833, doi:10.1038/382829a0 (1996).
143. Bleul, Fuhlbrigge, Casasnovas, Aiuti, and Springer. A highly efficacious lymphocyte chemoattractant, stromal cell-derived factor 1 (SDF-1). *J Exp Med* **184**, 1101-1109 (1996).
144. Diaz. CXCR4 mutations in WHIM syndrome: a misguided immune system? *Immunol Rev* **203**, 235-243 (2005).
145. Hernandez, Gorlin, Lukens, Taniuchi, Bohinjec, Francois, Klotman, and Diaz. Mutations in the chemokine receptor gene CXCR4 are associated with WHIM syndrome, a combined immunodeficiency disease. *Nat Genet* **34**, 70-74, doi:10.1038/ng1149 (2003).
146. Staller, Sulitkova, Lisztwan, Moch, Oakeley, and Krek. Chemokine receptor CXCR4 downregulated by von Hippel-Lindau tumour suppressor pVHL. *Nature* **425**, 307-311 (2003).
147. Müller, Homey, Soto, Ge, Catron, Buchanan, McClanahan, Murphy, Yuan, Wagner, Barrera, Mohar, Verástegui, and Zlotnik. Involvement of chemokine receptors in breast cancer metastasis. *Nature* **410**, 50-56, doi:10.1038/35065016 (2001).
148. Orimo, Gupta, Sgroi, Arenzana-Seisdedos, Delaunay, Naeem, Carey, Richardson, and Weinberg. Stromal Fibroblasts Present in Invasive Human Breast Carcinomas Promote Tumor Growth and Angiogenesis through Elevated SDF-1/CXCL12 Secretion. *Cell* **121**, 335-348, doi:10.1016/j.cell.2005.02.034 (2005).
149. Burger and Kipps. CXCR4: a key receptor in the crosstalk between tumor cells and their microenvironment. *Blood* **107**, 1761-1767 (2006).
150. Mizoguchi, Verkade, Heath, Kuroiwa, and Kikuchi. Sdf1/Cxcr4 signaling controls the dorsal migration of endodermal cells during zebrafish gastrulation. *Development*, doi:10.1242/dev.020107 (2008).
151. Ara, Tokoyoda, Okamoto, Koni, and Nagasawa. The role of CXCL12 in the organ-specific process of artery formation. *Blood* **105**, 3155-3161 (2005).

152. Ghysen and Dambly-Chaudiere. The lateral line microcosmos. *Genes Dev* **21**, 2118-2130 (2007).
153. Tiveron and Cremer. CXCL12/CXCR4 signalling in neuronal cell migration. *Curr Opin Neurobiol* (2008).
154. Molyneaux, Zinszner, Kunwar, Schaible, Stebler, Sunshine, O'Brien, Raz, Littman, Wylie, and Lehmann. The chemokine SDF1/CXCL12 and its receptor CXCR4 regulate mouse germ cell migration and survival. *Development* **130**, 4279-4286 (2003).
155. Ara, Nakamura, Egawa, Sugiyama, Abe, Kishimoto, Matsui, and Nagasawa. Impaired colonization of the gonads by primordial germ cells in mice lacking a chemokine, stromal cell-derived factor-1 (SDF-1). *Proc Natl Acad Sci U S A* **100**, 5319-5323, doi:10.1073/pnas.0730719100 (2003).
156. Doitsidou, Reichman-Fried, Stebler, Köprunner, Dörries, Meyer, Esguerra, Leung, and Raz. Guidance of primordial germ cell migration by the chemokine SDF-1. *Cell* **111**, 647-659 (2002).
157. Knaut, Werz, Geisler, Consortium, and Nüsslein-Volhard. A zebrafish homologue of the chemokine receptor Cxcr4 is a germ-cell guidance receptor. *Nature* **421**, 279-282, doi:10.1038/nature01338 (2003).
158. Balabanian, Lagane, Infantino, Chow, Harriague, Moepps, Arenzana-Seisdedos, Thelen, and Bachelier. The chemokine SDF-1/CXCL12 binds to and signals through the orphan receptor RDC1 in T lymphocytes. *J Biol Chem* **280**, 35760-35766 (2005).
159. Burns. A novel chemokine receptor for SDF-1 and I-TAC involved in cell survival, cell adhesion, and tumor development. *Journal of Experimental Medicine* **203**, 2201-2213, doi:10.1084/jem.20052144 (2006).
160. Sierro, Biben, Martinez-Munoz, Mellado, Ransohoff, Li, Woehl, Leung, Groom, Batten, Harvey, Martinez, Mackay, and Mackay. Disrupted cardiac development but normal hematopoiesis in mice deficient in the second CXCL12/SDF-1 receptor, CXCR7. *Proc Natl Acad Sci U S A* **104**, 14759-14764 (2007).
161. Loos, Mortier, Gouwy, Ronsse, Put, Lenaerts, Damme, and Proost. Citrullination of CXCL10 and CXCL11 by peptidylarginine deiminase: a naturally occurring posttranslational modification of chemokines and new dimension of immunoregulation. *Blood* **112**, 2648-2656, doi:10.1182/blood-2008-04-149039 (2008).
162. Premont and Gainetdinov. Physiological roles of G protein-coupled receptor kinases and arrestins. *Annu Rev Physiol* **69**, 511-534, doi:10.1146/annurev.physiol.69.022405.154731 (2007).
163. Krupnick and Benovic. The role of receptor kinases and arrestins in G protein-coupled receptor regulation. *Annu Rev Pharmacol Toxicol* **38**, 289-319 (1998).
164. Kawai, Choi, Whiting-Theobald, Linton, Brenner, Sechler, Murphy, and Malech. Enhanced function with decreased internalization of carboxy-terminus truncated CXCR4 responsible for WHIM syndrome. *Exp Hematol* **33**, 460-468 (2005).
165. Lagane, Chow, Balabanian, Levoye, Harriague, Planchenault, Baleux, Gunera-Saad, Arenzana-Seisdedos, and Bachelier. CXCR4 dimerization and beta-arrestin-mediated signaling account for the enhanced chemotaxis to CXCL12 in WHIM syndrome. *Blood* **112**, 34-44, doi:10.1182/blood-2007-07-102103 (2008).
166. Minina, Reichmanfried, and Raz. Control of Receptor Internalization, Signaling Level, and Precise Arrival at the Target in Guided Cell Migration. *Current Biology* **17**, 1164-1172, doi:10.1016/j.cub.2007.05.073 (2007).
167. Hansell and Nibbs. Professional and Part-Time Chemokine Decoys in the Resolution of Inflammation. *Science Signaling* **2007** (2007).
168. Locati, Torre, Galliera, Bonecchi, Bodduluri, Vago, Vecchi, and Mantovani. Silent chemoattractant receptors: D6 as a decoy and scavenger receptor for inflammatory CC chemo-

- kines. *Cytokine & Growth Factor Reviews* **16**, 679-686, doi:10.1016/j.cytogfr.2005.05.003 (2005).
169. Di Liberto, Locati, Caccamo, Vecchi, Meraviglia, Salerno, Sireci, Nebuloni, Caceres, Cardona, Dieli, and Mantovani. Role of the chemokine decoy receptor D6 in balancing inflammation, immune activation, and antimicrobial resistance in Mycobacterium tuberculosis infection. *J Exp Med* **205**, 2075-2084, doi:10.1084/jem.20070608 (2008).
170. Martinez de la Torre, Locati, Buracchi, Dupor, Cook, Bonecchi, Nebuloni, Rukavina, Vago, Vecchi, Lira, and Mantovani. Increased inflammation in mice deficient for the chemokine decoy receptor D6. *Eur. J. Immunol.* **35**, 1342-1346, doi:10.1002/eji.200526114 (2005).
171. Pruenster, Mudde, Bombosi, Dimitrova, Zsak, Middleton, Richmond, Graham, Segerer, Nibbs, and Rot. The Duffy antigen receptor for chemokines transports chemokines and supports their promigratory activity. *Nat. Immunol.*, doi:10.1038/ni.1675 (2008).
172. Lee, Wurfel, Matute-Bello, Frevert, Rosengart, Ranganathan, Wong, Holden, Sutlief, Richmond, Peiper, and Martin. The Duffy antigen modifies systemic and local tissue chemokine responses following lipopolysaccharide stimulation. *J Immunol* **177**, 8086-8094 (2006).
173. Foxman, Campbell, and Butcher. Multistep navigation and the combinatorial control of leukocyte chemotaxis. *The Journal of Cell Biology* **139**, 1349-1360 (1997).
174. Foxman, Kunkel, and Butcher. Integrating conflicting chemotactic signals. The role of memory in leukocyte navigation. *The Journal of Cell Biology* **147**, 577-588 (1999).
175. Oelz, Schmeiser, and Soreff. Multistep navigation of leukocytes: a stochastic model with memory effects. *Mathematical medicine and biology : a journal of the IMA* **22**, 291-303, doi:10.1093/imammb/dqi009 (2005).
176. Baggiolini, Dewald, and Moser. Interleukin-8 and related chemotactic cytokines--CXC and CC chemokines. *Adv Immunol* **55**, 97-179 (1994).
177. Heit, Tavener, Raharjo, and Kubes. An intracellular signaling hierarchy determines direction of migration in opposing chemotactic gradients. *The Journal of Cell Biology* **159**, 91-102, doi:10.1083/jcb.200202114 (2002).
178. Campbell, Foxman, and Butcher. Chemoattractant receptor cross talk as a regulatory mechanism in leukocyte adhesion and migration. *Eur. J. Immunol.* **27**, 2571-2578 (1997).
179. Salanga, O'Hayre, and Handel. Modulation of chemokine receptor activity through dimerization and crosstalk. *Cell Mol Life Sci*, doi:10.1007/s00018-008-8666-1 (2008).
180. Bai, Hayasaka, Kobayashi, Li, Guo, Jang, Kondo, Choi, Iwakura, and Miyasaka. CXC chemokine ligand 12 promotes CCR7-dependent naive T cell trafficking to lymph nodes and Peyer's patches. *J Immunol* **182**, 1287-1295 (2009).
181. Vichalkovski, Baltensperger, Thomann, and Porzig. Two different pathways link G-protein-coupled receptors with tyrosine kinases for the modulation of growth and survival in human hematopoietic progenitor cells. *Cell Signal* **17**, 447-459, doi:10.1016/j.cellsig.2004.09.010 (2005).
182. Schneider, Weiss, and Miller. Pertussis toxin signals through the TCR to initiate cross-desensitization of the chemokine receptor CXCR4. *J Immunol* **182**, 5730-5739, doi:10.4049/jimmunol.0803114 (2009).
183. Kumar, Humphreys, Kremer, Bramati, Bradfield, Edgar, and Hedin. CXCR4 physically associates with the T cell receptor to signal in T cells. *Immunity* **25**, 213-224, doi:10.1016/j.immuni.2006.06.015 (2006).
184. Peacock and Jirik. TCR activation inhibits chemotaxis toward stromal cell-derived factor-1: evidence for reciprocal regulation between CXCR4 and the TCR. *J Immunol* **162**, 215-223 (1999).

185. Kunwar, Siekhaus, and Lehmann. In vivo migration: a germ cell perspective. *Annual Review of Cell and Developmental Biology* **22**, 237-265, doi:10.1146/annurev.cell-bio.22.010305.103337 (2006).
186. Wylie. Germ cells. *Cell* **96**, 165-174 (1999).
187. Wylie. Germ cells. *Current Opinion in Genetics & Development* **10**, 410-413 (2000).
188. Wolke, Weidinger, Köprunner, and Raz. Multiple levels of posttranscriptional control lead to germ line-specific gene expression in the zebrafish. *Curr Biol* **12**, 289-294 (2002).
189. Houston and King. Germ plasm and molecular determinants of germ cell fate. *Curr Top Dev Biol* **50**, 155-181 (2000).
190. Martinho, Kunwar, Casanova, and Lehmann. A noncoding RNA is required for the repression of RNAPolIII-dependent transcription in primordial germ cells. *Curr Biol* **14**, 159-165 (2004).
191. Kedde, Strasser, Boldajipour, Vrielink, Slanchev, Sage, Nagel, Voorhoeve, Duijse, Ørom, Lund, Perrakis, Raz, and Agami. RNA-binding protein Dnd1 inhibits microRNA access to target mRNA. *Cell* **131**, 1273-1286, doi:10.1016/j.cell.2007.11.034 (2007).
192. Santos and Lehmann. Germ cell specification and migration in Drosophila and beyond. *Curr Biol* **14**, R578-589 (2004).
193. Starz-Gaiano and Lehmann. Moving towards the next generation. *Mechanisms of Development* **105**, 5-18 (2001).
194. Kunwar, Sano, Renault, Barbosa, Fuse, and Lehmann. Tre1 GPCR initiates germ cell transepithelial migration by regulating Drosophila melanogaster E-cadherin. *The Journal of Cell Biology* **183**, 157-168, doi:10.1083/jcb.200807049 (2008).
195. Kunwar, Starz-Gaiano, Bainton, Heberlein, and Lehmann. Tre1, a G Protein-Coupled Receptor, Directs Transepithelial Migration of Drosophila Germ Cells. *PLoS Biol* **1**, e80, doi:10.1371/journal.pbio.0000080 (2003).
196. Starz-Gaiano, Cho, Forbes, and Lehmann. Spatially restricted activity of a Drosophila lipid phosphatase guides migrating germ cells. *Development* **128**, 983-991 (2001).
197. Zhang, Zhang, Purcell, Cheng, and Howard. The Drosophila protein Wunen repels migrating germ cells. *Nature* **385**, 64-67, doi:10.1038/385064a0 (1997).
198. Zhang, Zhang, Cheng, and Howard. Identification and genetic analysis of wunen, a gene guiding Drosophila melanogaster germ cell migration. *Genetics* **143**, 1231-1241 (1996).
199. Sano, Renault, and Lehmann. Control of lateral migration and germ cell elimination by the Drosophila melanogaster lipid phosphate phosphatases Wunen and Wunen 2. *The Journal of Cell Biology* **171**, 675-683, doi:10.1083/jcb.200506038 (2005).
200. Renault, Sigal, Morris, and Lehmann. Soma-germ line competition for lipid phosphate uptake regulates germ cell migration and survival. *Science* **305**, 1963-1966, doi:10.1126/science.1102421 (2004).
201. Burnett, Makridou, Hewlett, and Howard. Lipid phosphate phosphatases dimerise, but this interaction is not required for in vivo activity. *BMC Biochem* **5**, 2, doi:10.1186/1471-2091-5-2 (2004).
202. Burnett and Howard. Fly and mammalian lipid phosphate phosphatase isoforms differ in activity both in vitro and in vivo. *EMBO Rep* **4**, 793-799, doi:10.1038/sj.embor.embor900 (2003).
203. Hanyu-Nakamura, Kobayashi, and Nakamura. Germ cell-autonomous Wunen2 is required for germline development in Drosophila embryos. *Development* **131**, 4545-4553, doi:10.1242/dev.01321 (2004).
204. Doren, Broihier, Moore, and Lehmann. HMG-CoA reductase guides migrating primordial germ cells. *Nature* **396**, 466-469, doi:10.1038/24871 (1998).



205. Jaglarz and Howard. The active migration of *Drosophila* primordial germ cells. *Development* **121**, 3495-3503 (1995).
206. Tsunekawa, Naito, Sakai, Nishida, and Noce. Isolation of chicken vasa homolog gene and tracing the origin of primordial germ cells. *Development* **127**, 2741-2750 (2000).
207. Extavour. Mechanisms of germ cell specification across the metazoans: epigenesis and preformation. *Development* **130**, 5869-5884, doi:10.1242/dev.00804 (2003).
208. Stebler. Primordial germ cell migration in the chick and mouse embryo: the role of the chemokine SDF-1/CXCL12\*1. *Developmental biology* **272**, 351-361, doi:10.1016/j.ydbio.2004.05.009 (2004).
209. Peled, Grabovsky, Habler, Sandbank, Arenzana-Seisdedos, Petit, Ben-Hur, Lapidot, and Alon. The chemokine SDF-1 stimulates integrin-mediated arrest of CD34(+) cells on vascular endothelium under shear flow. *J Clin Invest* **104**, 1199-1211. (1999).
210. Phillips and Ager. Activation of pertussis toxin-sensitive CXCL12 (SDF-1) receptors mediates transendothelial migration of T lymphocytes across lymph node high endothelial cells. *Eur J Immunol* **32**, 837-847 (2002).
211. Hamburger and Hamilton. A series of normal stages in the development of the chick embryo. 1951. *Dev Dyn* **195**, 231-272, doi:10.1002/aja.1001950404 (1992).
212. Molyneaux and Wylie. Primordial germ cell migration. *Int J Dev Biol* **48**, 537-544, doi:10.1387/ijdb.041833km (2004).
213. Bendel-Stenzel, Anderson, Heasman, and Wylie. The origin and migration of primordial germ cells in the mouse. *Semin Cell Dev Biol* **9**, 393-400, doi:10.1006/scdb.1998.0204 (1998).
214. Runyan, Schaible, Molyneaux, Wang, Levin, and Wylie. Steel factor controls midline cell death of primordial germ cells and is essential for their normal proliferation and migration. *Development* **133**, 4861-4869, doi:10.1242/dev.02688 (2006).
215. Matsui, Toksoz, Nishikawa, Williams, Zsebo, and Hogan. Effect of Steel factor and leukaemia inhibitory factor on murine primordial germ cells in culture. *Nature* **353**, 750-752, doi:10.1038/353750a0 (1991).
216. Dolci, Williams, Ernst, Resnick, Brannan, Lock, Lyman, Boswell, and Donovan. Requirement for mast cell growth factor for primordial germ cell survival in culture. *Nature* **352**, 809-811, doi:10.1038/352809a0 (1991).
217. Godin, Deed, Cooke, Zsebo, Dexter, and Wylie. Effects of the steel gene product on mouse primordial germ cells in culture. *Nature* **352**, 807-809, doi:10.1038/352807a0 (1991).
218. Boldajipour and Raz. What is left behind—quality control in germ cell migration. *Sci STKE* **2007**, pe16, doi:10.1126/stke.3832007pe16 (2007).
219. Weidinger, Wolke, Köprunner, Klinger, and Raz. Identification of tissues and patterning events required for distinct steps in early migration of zebrafish primordial germ cells. *Development* **126**, 5295-5307 (1999).
220. Blaser, Eisenbeiss, Neumann, Reichman-Fried, Thisse, Thisse, and Raz. Transition from non-motile behaviour to directed migration during early PGC development in zebrafish. *Journal of Cell Science* **118**, 4027-4038, doi:10.1242/jcs.02522 (2005).
221. Weidinger, Wolke, Köprunner, Thisse, Thisse, and Raz. Regulation of zebrafish primordial germ cell migration by attraction towards an intermediate target. *Development* **129**, 25-36 (2002).
222. Raz. Guidance of primordial germ cell migration. *Curr Opin Cell Biol* **16**, 169-173 (2004).
223. Raz. Primordial germ-cell development: the zebrafish perspective. *Nature Reviews Genetics* **4**, 690-700, doi:10.1038/nrg1154 (2003).

224. Amores, Force, Yan, Joly, Amemiya, Fritz, Ho, Langeland, Prince, Wang, Westerfield, Ekker, and Postlethwait. Zebrafish hox clusters and vertebrate genome evolution. *Science* **282**, 1711-1714 (1998).
225. Gates, Kim, Egan, Cardozo, Sirotkin, Dougan, Lashkari, Abagyan, Schier, and Talbot. A genetic linkage map for zebrafish: comparative analysis and localization of genes and expressed sequences. *Genome Res* **9**, 334-347 (1999).
226. Kassahn, Dang, Wilkins, Perkins, and Ragan. Evolution of gene function and regulatory control after whole-genome duplication: Comparative analyses in vertebrates. *Genome Res*, doi:10.1101/gr.086827.108 (2009).
227. Chong, Emelyanov, Gong, and Korzh. Expression pattern of two zebrafish genes, cxcr4a and cxcr4b. *Mechanisms of Development* **109**, 347-354 (2001).
228. David, Sapede, Saint-Etienne, Thisse, Thisse, Dambly-Chaudiere, Rosa, and Ghysen. Molecular basis of cell migration in the fish lateral line: Role of the chemokine receptor CXCR4 and of its ligand, SDF1. *Proc Natl Acad Sci U S A* (2002).
229. Tachibana, Hirota, Iizasa, and Yoshida. The chemokine receptor CXCR4 is essential for vascularization of the gastrointestinal tract. *Nature* (1998).
230. Ma, Jones, Borghesani, Segal, Nagasawa, Kishimoto, Bronson, and Springer. Impaired B-lymphopoiesis, myelopoiesis, and derailed cerebellar neuron migration in CXCR4- and SDF-1-deficient mice. *Proc Natl Acad Sci U S A* **95**, 9448-9453 (1998).
231. Valentin, Haas, and Gilmour. The Chemokine SDF1a Coordinates Tissue Migration through the Spatially Restricted Activation of Cxcr7 and Cxcr4b. *Current Biology* (2007).
232. Dufourcq and Vríz. The chemokine SDF-1 regulates blastema formation during zebrafish fin regeneration. *Development Genes and Evolution* **216**, 635-639, doi:10.1007/s00427-006-0066-7 (2006).
233. Chong, Nguyet, Jiang, and Korzh. The chemokine Sdf-1 and its receptor Cxcr4 are required for formation of muscle in zebrafish. *BMC Dev Biol* **7**, 54 (2007).
234. Kimmel, Kane, Walker, Warga, and Rothman. A mutation that changes cell movement and cell fate in the zebrafish embryo. *Nature* **337**, 358-362 (1989).
235. Summerton and Weller. Morpholino antisense oligomers: design, preparation, and properties. *Antisense Nucleic Acid Drug Dev* **7**, 187-195. (1997).
236. Thisse and Thisse. High-resolution in situ hybridization to whole-mount zebrafish embryos. *Nat Protoc* **3**, 59-69, doi:10.1038/nprot.2007.514 (2008).
237. Middleton, Neil, Wintle, Clark-Lewis, Moore, Lam, Auer, Hub, and Rot. Transcytosis and surface presentation of IL-8 by venular endothelial cells. *Cell* **91**, 385-395 (1997).
238. Dumstrei, Mennecke, and Raz. Signaling Pathways Controlling Primordial Germ Cell Migration in Zebrafish. *Journal of Cell Science* **117**, 4787-4795 (2004).
239. Rost, Yachdav, and Liu. The predictprotein server. *Nucleic Acids Research* **32**, W321 (2004).
240. Baysal and Atilgan. Elucidating the structural mechanisms for biological activity of the chemokine family. *Proteins* **43**, 150-160 (2001).
241. Proudfoot and Borlat. Purification of recombinant chemokines from E. coli. *Methods Mol Biol* **138**, 75-87 (2000).
242. Veldkamp, Peterson, Hayes, Mattmiller, Haugner, Cruz, and Volkman. On-column refolding of recombinant chemokines for NMR studies and biological assays. *Protein Expr Purif* **52**, 202-209, doi:10.1016/j.pep.2006.09.009 (2007).
243. Wilson. Tech.Sight. Analyzing biomolecular interactions. *Science* **295**, 2103-2105, doi:10.1126/science.295.5562.2103 (2002).

244. Pelletier, Laan, Hildbrand, Siani, Thompson, Dawson, Torbett, and Salomon. Presentation of chemokine SDF-1 alpha by fibronectin mediates directed migration of T cells. *Blood* **96**, 2682-2690 (2000).
245. Sasado, Yasuoka, Abe, Mitani, Furutani-Seiki, Tanaka, and Kondoh. Distinct contributions of CXCR4b and CXCR7/RDC1 receptor systems in regulation of PGC migration revealed by medaka mutants *kazura* and *yanagi*. *Developmental biology* **320**, 328-339, doi:10.1016/j.ydbio.2008.05.544 (2008).
246. Serhan and Savill. Resolution of inflammation: the beginning programs the end. *Nat Immunol* **6**, 1191-1197, doi:10.1038/ni1276 (2005).
247. D'Amico, Frascaroli, Bianchi, Transidico, Doni, Vecchi, Sozzani, Allavena, and Mantovani. Uncoupling of inflammatory chemokine receptors by IL-10: generation of functional decoys. *Nat. Immunol.* **1**, 387-391, doi:10.1038/80819 (2000).
248. Petty, Sueblinvong, Lenox, Jones, Cosgrove, Cool, Rai, Brown, Weiss, Poynter, and Surratt. Pulmonary stromal-derived factor-1 expression and effect on neutrophil recruitment during acute lung injury. *J Immunol* **178**, 8148-8157 (2007).
249. Klerck, Geboes, Hatse, Kelchtermans, Meyvis, Vermeire, Bridger, Billiau, Schols, and Matthys. Pro-inflammatory properties of stromal cell-derived factor-1 (CXCL12) in collagen-induced arthritis. *Arthritis Res Ther* **7**, R1208-1220 (2005).
250. Matthys, Hatse, Vermeire, Wuyts, Bridger, Henson, Clercq, Billiau, and Schols. AMD3100, a potent and specific antagonist of the stromal cell-derived factor-1 chemokine receptor CXCR4, inhibits autoimmune joint inflammation in IFN-gamma receptor-deficient mice. *J Immunol* **167**, 4686-4692 (2001).
251. Nanki, Hayashida, El-Gabalawy, Suson, Shi, Girschick, Yavuz, and Lipsky. Stromal cell-derived factor-1-CXC chemokine receptor 4 interactions play a central role in CD4+ T cell accumulation in rheumatoid arthritis synovium. *J Immunol* **165**, 6590-6598. (2000).
252. Aiuti, Webb, Bleul, Springer, and Gutierrez-Ramos. The chemokine SDF-1 is a chemoattractant for human CD34+ hematopoietic progenitor cells and provides a new mechanism to explain the mobilization of CD34+ progenitors to peripheral blood. *J Exp Med* **185**, 111-120 (1997).
253. Peled, Petit, Kollet, Magid, Ponomaryov, Byk, Nagler, Ben-Hur, Many, Shultz, Lider, Alon, Zipori, and Lapidot. Dependence of human stem cell engraftment and repopulation of NOD/SCID mice on CXCR4. *Science* **283**, 845-848 (1999).
254. Dambly-Chaudière, Cubedo, and Ghysen. Control of cell migration in the development of the posterior lateral line: antagonistic interactions between the chemokine receptors CXCR4 and CXCR7/RDC1. *BMC Developmental Biology* **7**, 23, doi:10.1186/1471-213X-7-23 (2007).
255. Crump, Gong, Loetscher, Rajarathnam, Amara, Arenzana-Seisdedos, Virelizier, Baggiolini, Sykes, and Clark-Lewis. Solution structure and basis for functional activity of stromal cell-derived factor-1; dissociation of CXCR4 activation from binding and inhibition of HIV-1. *Embo J* **16**, 6996-7007 (1997).
256. Dealwis, Fernandez, Thompson, Simon, Siani, and Lolis. Crystal structure of chemically synthesized [N33A] stromal cell-derived factor 1alpha, a potent ligand for the HIV-1 "fusin" coreceptor. *Proc Natl Acad Sci U S A* **95**, 6941-6946 (1998).
257. Ueda, Siani, Gong, Thompson, Brown, and Wang. Chemically synthesized SDF-1alpha analogue, N33A, is a potent chemotactic agent for CXCR4/Fusin/LESTR-expressing human leukocytes. *J Biol Chem* **272**, 24966-24970 (1997).
258. Kledal, Rosenkilde, Coulin, Simmons, Johnsen, Alouani, Power, Lüttichau, Gerstoff, Clapham, Clark-Lewis, Wells, and Schwartz. A broad-spectrum chemokine antagonist encoded by Kaposi's sarcoma-associated herpesvirus. *Science* **277**, 1656-1659 (1997).

259. Köprunner, Thisse, Thisse, and Raz. A zebrafish nanos-related gene is essential for the development of primordial germ cells. *Genes & Development* **15**, 2877-2885, doi:10.1101/gad.212401 (2001).

## 7. Appendix

### 7.1. Declaration of author contributions

Some of the data presented in this thesis was generated in a collaborative effort with other researchers. In order to present my work within the logic of the full project I had to include foreign data into this thesis. These were as such:

- Harsha Mahabaleshwar performed the experiments in Figure 7, Figure 8A-L, Figure 9B, Figure 12B, Figure 13A, Figure 15E.
- Elena Kardash performed the experiments in Figure 9A, Figure 12A, Figure 13C.
- Michal Reichman-Fried performed the experiments in Figure 13B.
- Sofia Minina performed the experiments in Figure 15A.
- Heiko Blaser performed the experiments in Figure 14A.
- Maria Doitsidou set the basis for the work of section 3.2, cloned CXCL12a, CXCL12b, generated the chimeric mutants and the fluorescent fusion protein constructs.
- Cedric Laguri performed NMR structure determination and analytical ultracentrifugation of the zebrafish CXCL12 paralogs.

### 7.2. List of constructs

#### Table 3. List and description of constructs used in this work.

Listed are the names used in this work, laboratory stock numbers, and description of the constructs. For *in vitro* translation constructs, the amount of injected mRNA per embryo is indicated. All mRNA constructs were designed as morpholino-resistant constructs by mutating the morpholino-binding site, unless stated otherwise. For *in situ* hybridization probes, the gene targeted, laboratory stock number, and publication of first appearance is given.

Bacterial expression constructs		
pET-28a-Xa-CX-CL12a	A501	IPTG-inducible expression of hexahistidine-tagged CXCL12a in prokaryotic cells. Contains a FactorXa-cleavage site to remove the His-tag
pET-28a-Xa-CX-CL12b	A502	IPTG-inducible expression of hexahistidine-tagged CXCL12b in prokaryotic cells. Contains a FactorXa-cleavage site to remove the His-tag
pET-CXCL12a	B203	IPTG-inducible expression of untagged CXCL12a in prokaryotic cells.
pET-CXCL12b	B204	IPTG-inducible expression of untagged CXCL12b in prokaryotic cells.
pET-CXCL12a-N33S	B209	IPTG-inducible expression of untagged CXCL12a N33S in prokaryotic cells.
pET-CXCL12b-S33N	B295	IPTG-inducible expression of untagged CXCL12b S33N in prokaryotic cells.

<b>Mammalian expression constructs</b>		
pcDNA-CXCR4b-YPet	A637	Constitutive expression of CXCR4b-YPet in mammalian cells
pcDNA-CXCR7-YPet	A639	Constitutive expression of CXCR7-YPet in mammalian cells
pcDNA-SDF1a	A492	Constitutive expression of CXCL12a in mammalian cells
<b><i>In vitro</i> mRNA translation constructs</b>		
AktPH-GFP- <i>globin</i>	A870	Uniform expression of GFP-tagged Akt PH-domain to label PIP3
CXCL12a-EGFP- <i>globin</i>	905	Uniform expression of EGFP-tagged CXCL12a morpholino-resistant, 150 pg
CXCL12a- <i>globin</i>	624	Uniform expression of CXCL12a, morpholino-resistant 24-150 pg
CXCL12a-SP-EGFP- <i>globin</i>	A774	Uniform expression of secreted EGFP, 37.5 pg
CXCL12b-EGFP- <i>globin</i>	907	Uniform expression of EGFP-tagged CXCL12b, morpholino-resistant, 150 pg
CXCL12b- <i>globin</i>	927	Uniform expression of CXCL12b, morpholino-resistant, 24-150 pg
CXCR4b-EGFP- <i>globin</i>	934	Uniform expression of EGFP-tagged CXCR4b, morpholino-resistant
CXCR4b-EGFP- <i>nanos</i>	760	Germ cell-specific expression of EGFP-tagged CXCR4b
CXCR7-EGFP- <i>globin</i>	A724	Uniform expression of EGFP-tagged CXCR7, morpholino-sensitive
CXCR7-mDsRed- <i>globin</i>	A817	Uniform expression of mDsRed-tagged CXCR7
ECFP- <i>globin</i>	802	Uniform expression of ECFP, 60 pg
EGFP-F- <i>nanos</i>	493	Germ cell-specific expression of farnesylated EGFP to label cell membranes 90 – 225 pg
GFP- <i>nanos</i>	355	Germ cell-specific expression of GFP, 90-225 pg
H1M-GFP- <i>globin</i>	345	Uniform expression of GFP-tagged histone H1M to label nuclei
LAMP1-mDsRed- <i>globin</i>	A804	Uniform expression of monomeric DsRed-tagged LAMP1 to label lysosomes
mCherry-F- <i>globin</i>	A709	Uniform expression of farnesylated mCherry to label cell membranes, 150 pg
mutCXCR7- <i>globin</i>	A537	Uniform expression of CXCR7
mutCXCR7- <i>nanos</i>	A536	Germ cell-specific expression of CXCR7
various	790-797	Germ cell-specific expression of chimeric CXCL12 mutants
various	A084-A089	Germ cell-specific expression of CXCL12 single point mutants

Vasa-dsRedEx- <i>globin</i>	A135	Germ cell-specific expression of DsRed-tagged Vasa to label perinuclear granules
Vasa-GFP- <i>nanos</i>	179	Germ cell-specific expression of GFP-tagged Vasa to label perinuclear granules
<b><i>In situ</i> hybridization probes</b>		
<i>cxcl12a</i> probe	A253	This work
<i>cxcl12b</i> probe	A253	This work
<i>cxcr7</i> probe	A489	This work
<i>egfp</i>	763	Reference 220
<i>gfp</i>	172	Reference 259
<i>nanos</i>	213	Reference 259

### 7.3. List of morpholinos and primers

**Table 4. List of morpholinos and primers used in this work.**

For morpholinos, the targeted gene, lab stock number, sequence, and injected amount per embryo is given here, unless stated otherwise in the text. Primers used to generate novel probes and expression constructs of CXCR7 and CXCL12 are given. Indicated are the targeted gene, purpose of experiment, and primer sequence.

<b>Morpholinos</b>		
Control	1	CCTCTTACCTCAgTTACAATTTATA, various amounts
CXCL12a	12	TTGAGATCCATGTTTGCAGTGTGAA, 0.4 pmol
CXCL12b	14	TTGCTATCCATGCCAAGAGCGAGTG, 0.4 pmol
CXCR4b	7	AAATGATGCTATCGTAAAATTCCAT, 0.4 pmol
CXCR7	42	ATCATTACGTTCCACTCATCTTG, 1.2 pmol
<b>Primer</b>		
<i>cxcl12a</i>	<i>in situ</i> probe	5'-ACTGCAAACATGGATCTCAAA-3' (forward) 5'-ATTAACAAAACAGATGATTTAATGC-3' (reverse)
<i>cxcl12b</i>	<i>in situ</i> probe	5'-GCTCTTGGCATGGATAGCA-3' (forward) 5'-TGTGTGTGTGTGGTGAGCTG-3' (reverse)
<i>cxcr7</i>	<i>in situ</i> probe and RT-PCR	5'-GATGCACTGGGTGAACTGAA-3' (forward) 5'-GTGCAGTGCTGCGTAGAGAG-3' (reverse)
<i>cxcr7</i>	<i>n a n o s</i> construct	5'-CGGGATCCACCATGAGCGTCAATGTCAACGATTTCAAT-3' (forward) 5'-CCGCTCGAGTCATAATGGTCCCTGGTTTT-3' (reverse)
<i>cxcr7</i>	<i>g l o b i n</i> construct	5'-GCACTAGTACCATGAGCGTCAATGTCAACGATTTCAAT-3' (forward); 5'-CCGCTCGAGTCATAATGGTCCCTGGTTTT-3' (reverse)
<i>odc1</i>	RT-PCR	5'-GTTTGCAGGCTGAGTGTGAA-3' (forward) 5'-CGCATGATCATAACAGGATGC-3' (reverse)

## 8. Curriculum Vitae

Full name: Bijan Andre Boldajipour  
Nationality: Germany  
Place and date of birth: Bremen (Germany), May 30 1982  
Laboratory address: Institute of Cell Biology  
Center of the Molecular Biology of Inflammation  
Westphalian Wilhelms-University Münster  
Von-Esmarch-Str. 56  
48149 Münster  
Germany  
Phone: +49 251 8358613  
FAX: +49 251 8358616  
email: [bijan.boldajipour@uni-muenster.de](mailto:bijan.boldajipour@uni-muenster.de)  
Private address: Kampstr. 26  
48147 Münster  
Germany  
Phone: +49 251 2101451  
Mobile: +49 178 3400211  
email: [bijan@boldajipour.de](mailto:bijan@boldajipour.de)

### UNIVERSITY ENTRANCE QUALIFICATION

**Gymnasium am Wall, Verden/Aller, Germany** **2001**  
Abitur

### UNIVERSITY EDUCATION

**Lübeck University, Lübeck, Germany** **2001 – 2004**  
B.Sc. Program Molecular Biotechnology

BSc Thesis "DNA Solid-State Sequencing" with Dr. Dmitry Tcherkassov, Genovoxx GmbH, Lübeck, Germany. University supervisor: Prof. Enno Hartmann (Institute of Biology, Lübeck University)

**Georg-August Universität Göttingen, Germany** **2004 - 2009**

MSc/PhD Program International Max-Planck Research School Molecular Biology

PhD Thesis "Molecular Mechanisms Controlling Guided Germ Cell Migration in Zebrafish" with Prof. Erez Raz, Institute of Cell Biology, Center for Molecular Biology of Inflammation, Münster University, Münster, Germany

(formerly Independent Research Group Germ Cell Development, Max-Planck-Institute for Biophysical Chemistry, Göttingen, Germany)



**CONFERENCE TALKS**

**Georg-August Universität, Göttingen, Germany** **2008**  
Symposium Horizons in Molecular Biology

**Gordon Research Conference, Aussois, France** **2008**  
Conference Chemotactic Cytokines

**Weizmann Institute of Science, Rehovot, Israel** **2009**  
Symposium Development Now!

**FELLOWSHIPS**

**Friedrich-Ebert-Stiftung** **2006**  
PhD Fellowship

**Boehringer Ingelheim Fonds** **2006 - 2008**  
PhD Fellowship